PSSFSS Theory Documentation

Peter S. Simon

July 14, 2020

Contents

Introduction

These notes constitute the theory documentation for the PSSFSS program. PSSFSS is a Julia [1] program for the analysis of polarization and frequency selective surfaces (PSSs and FSSs). The structure under consideration may contain any number of stratified dielectric *layers*, possibly including one or more zero-thickness conducting[1] *sheets* located at the dielectric interface layers. The metalization pattern on the sheets is assumed to exhibit a two-dimensional periodicity, which may vary from sheet to sheet. The structure is illuminated by a monochromatic plane wave incident at an arbitrary angle, and the goal of this analysis is to efficiently compute the complex scattering matrix whose entries are reflection and transmission coefficients for the scattered plane waves. Various performance parameters can be obtained from the scattering matrix, such as reflection and transmission coefficients, axial ratio, polarization purity, delta insertion phase delay, etc.

To calculate the fields scattered from the metallic sheets, we will use one of two approaches, depending on the sheet geometry:

1. If a sheet's unit cell of periodicity is mostly absent of metalization ("wire", "strip", or "capacitive" type FSSs are typical examples of this), it is more efficient to replace the metalization with unknown induced electric surface current, which will be solved for in the course of the analysis.

2. Alternatively, if the unit cell is mostly metalized (as in a "slot" or "inductive" type of FSS), then it is more efficient to solve for the tangential electric field in the non-metalized ("void") area. In practice this is done by filling in the void regions with metalization and impressing upon these regions induced (fictitious) magnetic surface current. Note that this technique can only be used when the metalization is assumed to be perfectly conducting. Lossy conducting metalization requires the use of electric surface currents.

The unknown electric or magnetic surface currents in the unit cell are approximately determined by solving a mixed-potential integral equation using the method of moments in conjunction with the so-called "RWG" triangle subdomain basis functions [2].

---

[1]imperfect conductors are also allowed

Each sheet in the structure is characterized by its generalized scattering matrix (GSM). "Generalized" refers to the fact that both propagating and evanescent modes are treated. The GSMs of the sheets and dielectric layers are cascaded to obtain the GSM of the entire structure. If the sheets do not all share the same periodic lattice, then the sheet interactions are approximated by accounting only for the dominant, propagating TE and TM modes during the cascading process. Also, if a sheet is surrounded by very thin dielectric layers, then it would require a very large number of evanescent modes to correctly model the effects of these layers. So in this case, the composite GSM of the sheet together with its surrounding thin layers is directly computed, by using a Green's function for multiply stratified dielectric layers.

This document is organized as follows:

Chapter 1 documents the basic assumptions and fundamental equations for the fields and potentials needed in the rest of the analysis.

Chapter 2 describes the type of periodic structures treated in this analysis, defines the direct and reciprocal lattices, and derives the form of Floquet modes used in subsequent chapters.

Chapter 3 defines the generalized scattering matrix (GSM), and derives formulas for the GSMs of canonical structures needed later in the analysis.

Chapter 4 derives an efficient, wide-band formula for the potential Green's functions for abutted half-spaces under quasi-periodic (Floquet) boundary conditions, as needed for FSS and PSS sheets that are surrounded by reasonably thick adjacent dielectric layers.

Chapter 5 extends this formulation to multiply stratified media on each side of the sheet, as is needed for a sheet immediately adjacent to one or more very thin dielectric layers.

Chapter 6 discusses how to calculate the incident fields and extract scattering matrix entries from computed currents.

Chapter 7 provides the details of the method of moments (MoM) solution of the mixed potential integral equations for the electric or magnetic currents flowing on the FSS/PSS sheets. Care is taken to exploit the wide-band nature of the Green's functions to minimize matrix fill time for multi-frequency analysis.

Chapter 1

Fundamentals

This chapter documents the definitions for fields, potentials, and Fourier transforms that are employed in remainder of this document.

We restrict consideration to time-harmonic sources in simple, linear media, assuming and suppressing a time dependence of $e^{j\omega t}$. RMS phasers are used throughout, employing rationalized MKS units. Thus, if V is a (complex) phaser voltage, then the corresponding function of time is $v(t) = \sqrt{2}\,\text{Re}\left\{V e^{j\omega t}\right\}$.

A right-handed Cartesian coordinate system is adopted, with x, y, and z axes, and unit vectors $\hat{x}$, $\hat{y}$, and $\hat{z}$. A point $P = (x, y, z)$ is typically identified by the vector $\boldsymbol{r} = x\hat{x} + y\hat{y} + z\hat{z}$ which measures the displacement of P from the origin.

The medium under consideration is characterized by its scalar, complex permittivity ϵ [F/m] and its scalar, complex permeability μ [H/m], both of which may be functions of position, $\epsilon = \epsilon(\boldsymbol{r})$, $\mu = \mu(\boldsymbol{r})$. Although these parameters are both positive for lossless media, in the presence of electric and/or magnetic losses the imaginary part of ϵ and/or μ, respectively, is negative. Thus, ϵ and μ both lie in the fourth quadrant (or positive real axis) of the complex plane.

For convenience we define the medium's intrinsic wavenumber

$$k = \omega\sqrt{\mu\epsilon} \qquad \text{(fourth quadrant)} \tag{1.1}$$

and intrinsic impedance

$$\eta = \sqrt{\mu/\epsilon} \qquad \left(|\arg \eta| < \frac{\pi}{4}\right), \tag{1.2}$$

which, of course, vary with position if ϵ or μ do.

1.1   Maxwell's Equations and Potentials for Electric Sources

Under the assumptions listed above, and postulating the existence of only electric sources, Maxwell's curl equations (Ampere's Law and Faraday's Law) take the form

$$\nabla \times \boldsymbol{H} = j\omega\epsilon\boldsymbol{E} + \boldsymbol{J} \tag{1.3a}$$

$$\nabla \times \boldsymbol{E} = -j\omega\mu\boldsymbol{H} \tag{1.3b}$$

where $\boldsymbol{E}$ is the electric field vector [V/m], $\boldsymbol{H}$ is the magnetic field vector [A/m], and $\boldsymbol{J}$ is the electric current density [A/m^2]. When combined with the equation of continuity

$$\nabla \cdot \boldsymbol{J} + j\omega q_{\text{e}} = 0 \tag{1.4}$$

we obtain the divergence relations

$$\nabla \cdot \epsilon\boldsymbol{E} = q_{\text{e}} \tag{1.5a}$$

$$\nabla \cdot \mu\boldsymbol{H} = 0, \tag{1.5b}$$

where q_{e} is the electric charge density, with units of [C/m^3]. The fact that $\mu\boldsymbol{H}$ is divergenceless leads to the introduction of the magnetic vector potential $\boldsymbol{A}$ having units of [Vs/m]:

$$\boxed{\mu\boldsymbol{H} = \nabla \times \boldsymbol{A}.} \tag{1.6}$$

Substituting (1.6) into (1.3b) we find that $-\boldsymbol{E} - j\omega\boldsymbol{A}$ is curl-free, and so can be written as the gradient of the so-called electric scalar potential Φ [V]:

$$\boxed{\boldsymbol{E} = -j\omega\boldsymbol{A} - \nabla\Phi.} \tag{1.7}$$

To derive the differential equations for $\boldsymbol{A}$ and Φ we begin with the identity

$$\nabla \times \nabla \times \boldsymbol{A} = \nabla \times \mu\boldsymbol{H} = \mu\nabla \times \boldsymbol{H} + \nabla\mu \times \boldsymbol{H} \tag{1.8}$$

and use Equations (1.3a) and (1.6) to eliminate $\boldsymbol{H}$:

$$\nabla\nabla \cdot \boldsymbol{A} - \nabla^2\boldsymbol{A} = j\omega\epsilon\mu\boldsymbol{E} + \mu\boldsymbol{J} + \nabla\mu \times \left(\frac{1}{\mu}\nabla \times \boldsymbol{A}\right). \tag{1.9}$$

Note that we also employed the identity $\nabla \times \nabla \times \boldsymbol{A} = \nabla\nabla \cdot \boldsymbol{A} - \nabla^2\boldsymbol{A}$. Now eliminating $\boldsymbol{E}$ using (1.7) we obtain

$$\nabla^2\boldsymbol{A} + k^2\boldsymbol{A} + \nabla\mu \times \left(\frac{1}{\mu}\nabla \times \boldsymbol{A}\right) - \nabla\left[\nabla \cdot \boldsymbol{A} + j\omega\mu\epsilon\Phi\right] = -\mu\boldsymbol{J}. \tag{1.10}$$

Since the divergence of the magnetic vector potential is as yet unspecified, we may apply the Lorentz gauge, $\nabla \cdot \boldsymbol{A} = -j\omega\epsilon\mu\Phi$, and set the quantity in square brackets above to zero:

$$\boxed{\nabla^2\boldsymbol{A} + k^2\boldsymbol{A} + \frac{\nabla\mu}{\mu} \times \nabla \times \boldsymbol{A} = -\mu\boldsymbol{J}.} \tag{1.11}$$

Equation (1.11) is the fundamental wave equation for the magnetic vector potential under the Lorentz gauge in an inhomogeneous medium.

An equation for Φ is now obtained by employing the identity $\boldsymbol{\nabla} \cdot \epsilon \boldsymbol{E} = \boldsymbol{E} \cdot \boldsymbol{\nabla}\epsilon + \epsilon \boldsymbol{\nabla} \cdot \boldsymbol{E}$ in (1.5a) and then eliminating $\boldsymbol{E}$ using (1.7):

$$
\begin{aligned}
q_{\mathrm{e}} &= \boldsymbol{E} \cdot \boldsymbol{\nabla}\epsilon + \epsilon \boldsymbol{\nabla} \cdot \boldsymbol{E} \\
&= -(j\omega\boldsymbol{A} + \boldsymbol{\nabla}\Phi) \cdot \boldsymbol{\nabla}\epsilon - \epsilon \boldsymbol{\nabla} \cdot (j\omega\boldsymbol{A} + \boldsymbol{\nabla}\Phi).
\end{aligned}
\tag{1.12}
$$

After invoking the Lorentz gauge this can be written as

$$
\boxed{\nabla^2\Phi + k^2\Phi + \frac{\boldsymbol{\nabla}\Phi \cdot \boldsymbol{\nabla}\epsilon}{\epsilon} = -\frac{q_{\mathrm{e}}}{\epsilon} - \frac{j\omega\boldsymbol{A} \cdot \boldsymbol{\nabla}\epsilon}{\epsilon}.}
\tag{1.13}
$$

Equation (1.13) is the wave equation for the electric scalar potential under the Lorentz gauge in an inhomogeneous medium.

1.1.1   Piecewise Homogeneous Medium

Suppose that the spatial domain U of the boundary value problem for which Maxwell's Equations are to be solved consists of a disjoint union of a finite number N of homogeneous regions U_i, as in the case of a stratified medium:

$$
U = \bigcup_{i=1}^{N} U_i,
\tag{1.14}
$$

and suppose that the permittivity and permeability of the ith region are the constants ϵ_i and μ_i, respectively, with corresponding wavenumber k_i. Then, for points within the ith medium, the terms involving the gradient of the permittivity and permeability are zero, and the potentials within the ith region are solutions to

$$
\nabla^2\boldsymbol{A}^{(i)} + k_i^2\boldsymbol{A}^{(i)} = -\mu_i\boldsymbol{J},
\tag{1.15a}
$$

$$
\nabla^2\Phi^{(i)} + k_i^2\Phi^{(i)} = -q_{\mathrm{e}}/\epsilon_i.
\tag{1.15b}
$$

If the ith region contains no sources, then the potentials in that region are solutions to the Helmholtz equation:

$$
\nabla^2\boldsymbol{A}^{(i)} + k_i^2\boldsymbol{A}^{(i)} = \boldsymbol{0},
\tag{1.16a}
$$

$$
\nabla^2\Phi^{(i)} + k_i^2\Phi^{(i)} = 0.
\tag{1.16b}
$$

1.2   Maxwell's Equations for Magnetic Sources

Under the assumptions listed in the introduction, and postulating the existence of only magnetic sources, Maxwell's curl equations (Ampere's Law and Faraday's Law) take the form

$$
\boldsymbol{\nabla} \times \boldsymbol{H} = j\omega\epsilon\boldsymbol{E}
\tag{1.17a}
$$

$$
\boldsymbol{\nabla} \times \boldsymbol{E} = -j\omega\mu\boldsymbol{H} - \boldsymbol{M}
\tag{1.17b}
$$

where E is the electric field vector [V/m], H is the magnetic field vector [A/m], and M is the magnetic current density [V/m^2]. When combined with the equation of continuity

$$\nabla \cdot M + j\omega q_{\mathrm{m}} = 0 \tag{1.18}$$

we obtain the divergence relations

$$\nabla \cdot \epsilon E = 0 \tag{1.19a}$$

$$\nabla \cdot \mu H = q_{\mathrm{m}}, \tag{1.19b}$$

where q_{m} is the magnetic charge density, with units of [Wb/m^3]. The fact that ϵE is divergenceless leads to the introduction of the electric vector potential F having units of [As/m]:

$$\boxed{\epsilon E = \nabla \times F.} \tag{1.20}$$

Substituting (1.20) into (1.17a) we find that $j\omega F - H$ is curl-free, and so can be written as the gradient of the so-called magnetic scalar potential Ψ [A]:

$$\boxed{H = j\omega F - \nabla\Psi.} \tag{1.21}$$

To derive the differential equations for F and Ψ we begin with the identity

$$\nabla \times \nabla \times F = \nabla \times \epsilon E = \epsilon \nabla \times E + \nabla\epsilon \times E \tag{1.22}$$

and use Equations (1.17b) and (1.20) to eliminate E:

$$\nabla\nabla \cdot F - \nabla^2 F = -j\omega\epsilon\mu H - \epsilon M + \nabla\epsilon \times \left(\frac{1}{\epsilon}\nabla \times F \right). \tag{1.23}$$

Note that we also employed the identity $\nabla \times \nabla \times F = \nabla\nabla \cdot F - \nabla^2 F$. Now eliminating H using (1.21) we obtain

$$\nabla^2 F + k^2 F + \nabla\epsilon \times \left(\frac{1}{\epsilon}\nabla \times F \right) - \nabla\left[\nabla \cdot F - j\omega\mu\epsilon\Psi \right] = \epsilon M. \tag{1.24}$$

Since the divergence of the electric vector potential is as yet unspecified, we may apply the Lorentz gauge, $\nabla \cdot F = j\omega\epsilon\mu\Psi$, and set the quantity in square brackets above to zero:

$$\boxed{\nabla^2 F + k^2 F + \frac{\nabla\epsilon}{\epsilon} \times \nabla \times F = \epsilon M.} \tag{1.25}$$

Equation (1.25) is the fundamental wave equation for the electric vector potential under the Lorentz gauge in an inhomogeneous medium.

An equation for Ψ is now obtained by employing the identity $\boldsymbol{\nabla} \cdot \mu \boldsymbol{H} = \boldsymbol{H} \cdot \boldsymbol{\nabla}\mu + \mu \boldsymbol{\nabla} \cdot \boldsymbol{H}$ in (1.19b) and then eliminating $\boldsymbol{H}$ using (1.21):

$$
\begin{aligned}
q_{\mathrm{m}} &= \boldsymbol{H} \cdot \boldsymbol{\nabla}\mu + \mu \boldsymbol{\nabla} \cdot \boldsymbol{H} \\
&= (j\omega \boldsymbol{F} - \boldsymbol{\nabla}\Psi) \cdot \boldsymbol{\nabla}\mu + \mu \boldsymbol{\nabla} \cdot (j\omega \boldsymbol{F} - \boldsymbol{\nabla}\Psi).
\end{aligned}
\tag{1.26}
$$

After invoking the Lorentz gauge this can be written as

$$
\boxed{\nabla^2 \Psi + k^2 \Psi + \frac{\boldsymbol{\nabla}\Psi \cdot \boldsymbol{\nabla}\mu}{\mu} = -\frac{q_{\mathrm{m}}}{\mu} + \frac{j\omega \boldsymbol{F} \cdot \boldsymbol{\nabla}\mu}{\mu}.}
\tag{1.27}
$$

Equation (1.27) is the wave equation for the electric scalar potential under the Lorentz gauge in an inhomogeneous medium.

1.2.1 Piecewise Homogeneous Medium

Suppose that the spatial domain U of the boundary value problem for which Maxwell's Equations are to be solved consists of a disjoint union of a finite number N of homogeneous regions U_i, as in the case of a stratified medium:

$$
U = \bigcup_{i=1}^{N} U_i,
\tag{1.28}
$$

and suppose that the permittivity and permeability of the ith region are the constants ϵ_i and μ_i, respectively, with corresponding wavenumber k_i. Then, for points within the ith medium, the terms involving the gradient of the permittivity and permeability are zero, and the potentials within the ith region are solutions to

$$
\nabla^2 \boldsymbol{F}^{(i)} + k_i^2 \boldsymbol{F}^{(i)} = \epsilon_i \boldsymbol{M},
\tag{1.29a}
$$

$$
\nabla^2 \Psi^{(i)} + k_i^2 \Psi^{(i)} = -q_{\mathrm{m}}/\mu_i.
\tag{1.29b}
$$

If the ith region contains no sources, then the potentials in that region are solutions to the Helmholtz equation:

$$
\nabla^2 \boldsymbol{F}^{(i)} + k_i^2 \boldsymbol{F}^{(i)} = \mathbf{0},
\tag{1.30a}
$$

$$
\nabla^2 \Psi^{(i)} + k_i^2 \Psi^{(i)} = 0.
\tag{1.30b}
$$

1.3 Duality

We note that the cases of electric-only and magnetic-only sources are duals. Any valid equation involving electromagnetic quantities has a dual equation which can be obtained by applying the following rules:

1. Interchange μ and ϵ.

2. Electric quantities are replaced by their corresponding magnetic quantity.

3. Magnetic quantities are replaced by the negative of their corresponding electric quantity.

The mappings between original and dual quantities are given in Table 1.1.

Original → Dual
$\mu \rightarrow \epsilon$
$\epsilon \rightarrow \mu$
$k \rightarrow k$
$\eta \rightarrow 1/\eta$
$\boldsymbol{E} \rightarrow \boldsymbol{H}$
$\boldsymbol{J} \rightarrow \boldsymbol{M}$
$\boldsymbol{F} \rightarrow \boldsymbol{A}$
$\Phi \rightarrow \Psi$
$q_{\mathrm{e}} \rightarrow q_{\mathrm{m}}$
$\boldsymbol{H} \rightarrow -\boldsymbol{E}$
$\boldsymbol{M} \rightarrow -\boldsymbol{J}$
$\boldsymbol{A} \rightarrow -\boldsymbol{F}$
$\Psi \rightarrow -\Phi$
$q_{\mathrm{m}} \rightarrow -q_{\mathrm{e}}$

Table 1.1: Electromagnetic dual quantities.

1.4   Fourier Transform Definitions

1.4.1   One-dimensional Transform

The Fourier transform of a function $f : \mathbb{R} \rightarrow \mathbb{C}$ is $\tilde{f} = \mathscr{F}\{f\}$, where

$$\tilde{f}(k) = \int_{-\infty}^{\infty} f(x)e^{jkx}\mathrm{d}x, \tag{1.31}$$

so that

$$f(x) = \frac{1}{2\pi} \int_{-\infty}^{\infty} \tilde{f}(k)e^{-jkx}\mathrm{d}k. \tag{1.32}$$

The completeness statement is

$$\delta(x) = \frac{1}{2\pi} \int_{-\infty}^{\infty} e^{\pm jkx}\mathrm{d}k \tag{1.33}$$

and Parseval's relation is

$$\int_{-\infty}^{\infty} f(x)g^*(x)\, \mathrm{d}x = \frac{1}{2\pi} \int_{-\infty}^{\infty} \tilde{f}(k)\tilde{g}^*(k)\, \mathrm{d}k. \tag{1.34}$$

Finally, if

$$h(x) = \int_{-\infty}^{\infty} f(x')g(x-x')\, \mathrm{d}x' \tag{1.35}$$

then the convolution theorem states that

$$\tilde{h}(k) = \tilde{f}(k)\tilde{g}(k). \tag{1.36}$$

1.4.2 Two-dimensional Transform

The Fourier transform of a function $f : \mathbb{R} \times \mathbb{R} \to \mathbb{C}$ is $\tilde{f} = \mathcal{F}\{f\}$, where

$$\tilde{f}(k_x, k_y) = \int_{-\infty}^{\infty} \int_{-\infty}^{\infty} f(x,y)e^{j(k_x x + k_y y)}\, \mathrm{d}x\mathrm{d}y, \tag{1.37}$$

so that

$$f(x,y) = \frac{1}{4\pi^2} \int_{-\infty}^{\infty} \int_{-\infty}^{\infty} \tilde{f}(k_x, k_y)e^{-j(k_x x + k_y y)}\, \mathrm{d}k_x\mathrm{d}k_y. \tag{1.38}$$

The completeness statement is

$$\delta(x)\delta(y) = \frac{1}{4\pi^2} \int_{-\infty}^{\infty} \int_{-\infty}^{\infty} e^{\pm j(k_x x + k_y y)}\, \mathrm{d}k_x\mathrm{d}k_y \tag{1.39}$$

and Parseval's relation is

$$\int_{-\infty}^{\infty} \int_{-\infty}^{\infty} f(x,y)g^*(x,y)\, \mathrm{d}x\mathrm{d}y = \frac{1}{4\pi^2} \int_{-\infty}^{\infty} \int_{-\infty}^{\infty} \tilde{f}(k_x, k_y)\tilde{g}^*(k_x, k_y)\, \mathrm{d}k_x\mathrm{d}k_y. \tag{1.40}$$

Finally, if

$$h(x,y) = \int_{-\infty}^{\infty} \int_{-\infty}^{\infty} f(x',y')g(x-x', y-y')\, \mathrm{d}x'\mathrm{d}y' \tag{1.41}$$

then the convolution theorem states that

$$\tilde{h}(k_x, k_y) = \tilde{f}(k_x, k_y)\tilde{g}(k_x, k_y). \tag{1.42}$$

<center>Chapter 2</center>

Periodicity, Reciprocal Lattice, Floquet Modes

This chapter discusses the direct and reciprocal lattice vectors, and defines the Floquet modes that can exist in the dielectric regions.

2.1   The Direct Lattice

We consider a structure with discrete translational invariance in two space dimensions. The periodicity is characterized by the *direct lattice vectors* s_1 and s_2, a pair of real vectors satisfying

$$s_1 \cdot \hat{z} = s_2 \cdot \hat{z} = 0, \quad A \equiv \hat{z} \cdot s_1 \times s_2 > 0. \tag{2.1}$$

The structure is invariant to a translation consisting of any integer number of shifts in the s_1 or s_2 directions. Such periodicity is exhibited by idealized models of frequency selective surfaces (FSSs) and phased arrays, for example. This periodicity gives rise to the concept of the direct lattice, the set of points $\boldsymbol{\rho}_{mn} = \hat{x}x_{mn} + \hat{y}y_{mn}$ satisfying

$$\boldsymbol{\rho}_{mn} = ms_1 + ns_2, \quad \text{for } m \text{ and } n \text{ any integers.} \tag{2.2}$$

A periodic structure and its direct lattice is shown in Figure 2.1.

2.2   Periodic Boundary Conditions and the Unit Cell

We now assume that an electromagnetic excitation of some type is applied to the structure. In the case of a FSS, the excitation takes the form of an incident plane wave. In the case of a phased array, the excitation may be an incident plane wave, or perhaps a set of incoming waveguide modes in each of the excitation ports of the radiating elements. Denote the spatial variation of the excitation by the function $V(\boldsymbol{r})$. We insist that the function V satisfy the following quasi-periodicity condition:

$$V(\boldsymbol{r} + ms_1 + ns_2) = V(\boldsymbol{r})e^{-j(m\psi_1 + n\psi_2)}, \quad \text{for any integers } m \text{ and } n \tag{2.3}$$
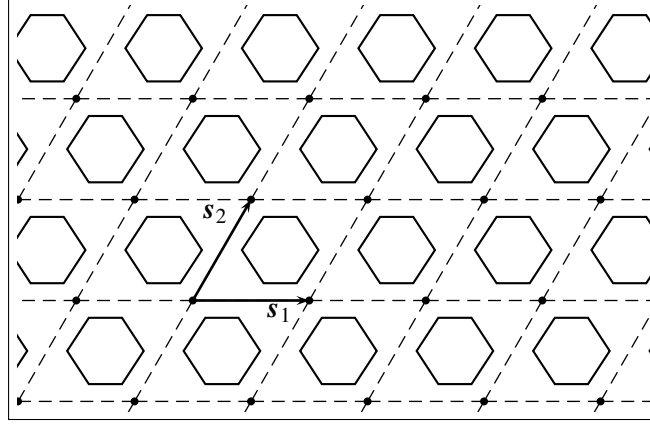
<center>8</center>

Figure 2.1: A frequency selective surface consisting of a thin metal plate with hexagonal perforations, and the associated direct lattice. The location selected for the lattice origin is arbitrary.

where ψ_1 and ψ_2 are given real numbers, which we will refer to as the "unit cell incremental phase shifts". By the translational invariance of Maxwell's equations and given the discrete translational invariance of the structure, it is clear that all electromagnetic fields, charges, etc., resulting from the given excitation must also satisfy (2.3), which we refer to as the "Floquet boundary condition."

Since the fields throughout the structure satisfy Equation (2.3), it suffices to restrict consideration to a single unit cell U, defined[1] as the set of points $\boldsymbol{r}$ satisfying

$$U = \{\boldsymbol{r} : \ \boldsymbol{r} = \xi_1 \boldsymbol{s}_1 + \xi_2 \boldsymbol{s}_2 + \hat{\boldsymbol{z}} z, \quad 0 \le \xi_1, \xi_2 \le 1\}, \tag{2.4}$$

where ξ_1 and ξ_2 are the so-called "normalized area coordinates," each constrained to the interval $[0, 1]$. We seek a set of modes that can propagate in the unit cell, subject to an appropriate set of boundary conditions to be stated below. Let $E(\boldsymbol{r})$ be some rectangular component of electric or magnetic field evaluated at a point $\boldsymbol{r} = \hat{\boldsymbol{x}} x + \hat{\boldsymbol{y}} y + \hat{\boldsymbol{z}} z = \xi_1 \boldsymbol{s}_1 + \xi_2 \boldsymbol{s}_2 + \hat{\boldsymbol{z}} z$ within the unit cell. Then the quasi-periodic boundary condition can be expressed as

$$E(\boldsymbol{s}_1 + \xi_2 \boldsymbol{s}_2 + \hat{\boldsymbol{z}} z) = E(\xi_2 \boldsymbol{s}_2 + \hat{\boldsymbol{z}} z) e^{-j\psi_1} \tag{2.5a}$$

$$E(\xi_1 \boldsymbol{s}_1 + \boldsymbol{s}_2 + \hat{\boldsymbol{z}} z) = E(\xi_1 \boldsymbol{s}_1 + \hat{\boldsymbol{z}} z) e^{-j\psi_2} \tag{2.5b}$$

which must hold for all z and for all ξ_1 and ξ_2 in the interval $[0, 1]$.

2.2.1   Mode Potentials

Following the formalism of Section 5.1 of [3], for both TE and TM modes we seek mode potentials $\Psi(\boldsymbol{\rho}) = \Psi(x, y)$ that satisfy the two-dimensional Helmholtz equation

$$\nabla_t^2 \Psi + k_c^2 \Psi = 0 \tag{2.6}$$

------

[1]The definition of a unit cell is not unique. The present definition is most useful for our purposes.

within the unit cell in addition to the boundary conditions (2.5). To simplify the following derivation, let $f(\xi_1, \xi_2) = \Psi(\xi_1 s_1 + \xi_2 s_2) = \Psi(x, y)$. Then the boundary condition (2.5) satisfied by Ψ can be expressed more simply in terms of f as

$$f(1, \xi_2) = f(0, \xi_2)e^{-j\psi_1} \tag{2.7a}$$

$$f(\xi_1, 1) = f(\xi_1, 0)e^{-j\psi_2} \tag{2.7b}$$

Note that f is periodic in ξ_1 and ξ_2 with unit period except for the progressive phase shifts ψ_1 and ψ_2. This motivates us to consider the function $f(\xi_1, \xi_2)e^{j(\xi_1\psi_1 + \xi_2\psi_2)}$ which is indeed periodic and can therefore be expanded in a double Fourier series:

$$f(\xi_1, \xi_2)e^{j(\xi_1\psi_1 + \xi_2\psi_2)} = \sum_{m=-\infty}^{\infty} \sum_{n=-\infty}^{\infty} f_{mn} e^{-j(m2\pi\xi_1 + n2\pi\xi_2)}$$

or equivalently

$$f(\xi_1, \xi_2) = \sum_{m=-\infty}^{\infty} \sum_{n=-\infty}^{\infty} f_{mn} e^{-j[\xi_1(\psi_1 + m2\pi) + \xi_2(\psi_2 + n2\pi)]}. \tag{2.8}$$

We wish to write Equation (2.8) explicitly in terms of $\rho = \hat{x}x + \hat{y}y$. Recalling that $\rho = \xi_1 s_1 + \xi_2 s_2$ and writing the relation in matrix form yields

$$\begin{bmatrix} x \\ y \end{bmatrix} = \begin{bmatrix} s_{1x} & s_{2x} \\ s_{1y} & s_{2y} \end{bmatrix} \begin{bmatrix} \xi_1 \\ \xi_2 \end{bmatrix}. \tag{2.9}$$

Inverting, we obtain

$$\begin{aligned} \begin{bmatrix} \xi_1 \\ \xi_2 \end{bmatrix} &= \frac{1}{A} \begin{bmatrix} s_{2y} & -s_{2x} \\ -s_{1y} & s_{1x} \end{bmatrix} \begin{bmatrix} x \\ y \end{bmatrix} \\ &= \frac{1}{A} \begin{bmatrix} s_{2y}x - s_{2x}y \\ -s_{1y}x + s_{1x}y \end{bmatrix} \\ &= \frac{1}{A} \begin{bmatrix} s_2 \times \hat{z} \cdot \rho \\ \hat{z} \times s_1 \cdot \rho \end{bmatrix} \\ &= \frac{1}{2\pi} \begin{bmatrix} \beta_1 \cdot \rho \\ \beta_2 \cdot \rho \end{bmatrix} \end{aligned} \tag{2.10}$$

where

$$\beta_1 = \frac{2\pi}{A} s_2 \times \hat{z}, \quad \beta_2 = \frac{2\pi}{A} \hat{z} \times s_1, \tag{2.11}$$

are the *reciprocal lattice vectors* [4, 5] and $A = \hat{z} \cdot s_1 \times s_2$ is the area of the unit cell. Substituting (2.11) into (2.8), we obtain the desired representation of the mode potential:

$$f(\xi_1, \xi_2) = \Psi(x, y) = \sum_{m=-\infty}^{\infty} \sum_{n=-\infty}^{\infty} f_{mn} e^{-j\beta_{mn} \cdot \rho} \tag{2.12}$$
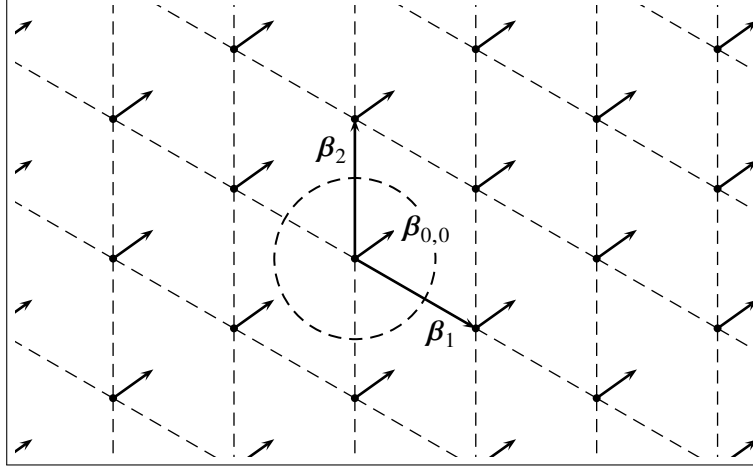
Figure 2.2: The reciprocal lattice for the structure of Figure 2.1. Note that this lattice is a scaled and rotated (by 90°) version of the direct lattice. Modes are located at the tips of the small, offset vectors. Propagating modes lie within the dashed circle of radius k centered on the origin. The offset vector $\boldsymbol{\beta}_{00}$ accounts for the effects of the impressed phase shift.

where

$$\boldsymbol{\beta}_{mn} = \boldsymbol{\beta}_{00} + m\boldsymbol{\beta}_1 + n\boldsymbol{\beta}_2, \tag{2.13a}$$

$$\boldsymbol{\beta}_{00} = \frac{\psi_1}{2\pi}\boldsymbol{\beta}_1 + \frac{\psi_2}{2\pi}\boldsymbol{\beta}_2. \tag{2.13b}$$

We see that the mode potentials assume the form of a discrete set of plane waves for both TE and TM modes. The cutoff wavenumber k_c of a plane wave with transverse propagation vector $\boldsymbol{\beta}_{mn}$ is given by

$$k_c = \beta_{mn} \equiv \sqrt{\boldsymbol{\beta}_{mn} \cdot \boldsymbol{\beta}_{mn}}. \tag{2.14}$$

For a lossless medium a finite number of modes may satisfy $k > \beta_{mn}$; these are the propagating modes. The remaining modes, comprising a denumerably infinite set, are cut-off (or evanescent). The situation is depicted in Figure 2.2 for the structure of Figure 2.1.

Following the prescription given in [3], we may now write down the explicit forms of the modal fields:

2.2.2   TE modes

Oblique Incidence

We first assume that $\beta_{mn} \neq 0$, in which case the modal fields are

$$\Psi_{mn}^{\text{TE}}(\boldsymbol{\rho}) = \frac{c_{mn}^{\text{TE}}}{k\eta\beta_{mn}} e^{-j\boldsymbol{\beta}_{mn}\cdot\boldsymbol{\rho}} \tag{2.15a}$$

$$\gamma_{mn} = \sqrt{\beta_{mn}^2 - k^2} \qquad \text{(1st quadrant)} \tag{2.15b}$$

$$Z_{mn}^{\text{TE}} = \frac{1}{Y_{mn}^{\text{TE}}} = \frac{jk\eta}{\gamma_{mn}} \tag{2.15c}$$

$$(\hat{\boldsymbol{x}}\hat{\boldsymbol{x}} + \hat{\boldsymbol{y}}\hat{\boldsymbol{y}}) \cdot \boldsymbol{H}_{mn}^{\text{TE}}(\boldsymbol{r}) = \pm\gamma_{mn}e^{\pm\gamma_{mn}z}\,\boldsymbol{\nabla}_t\Psi_{mn}^{\text{TE}}$$

$$= \mp j\gamma_{mn}\Psi_{mn}^{\text{TE}}e^{\pm\gamma_{mn}z}\boldsymbol{\beta}_{mn}$$

$$= \pm c_{mn}^{\text{TE}}Y_{mn}^{\text{TE}}e^{-j\boldsymbol{\beta}_{mn}\cdot\boldsymbol{\rho}\pm\gamma_{mn}z}\hat{\boldsymbol{\beta}}_{mn} \tag{2.15d}$$

$$\hat{\boldsymbol{z}} \cdot \boldsymbol{H}_{mn}^{\text{TE}}(\boldsymbol{r}) = \beta_{mn}^2\Psi_{mn}^{\text{TE}}e^{\pm\gamma_{mn}z}$$

$$= c_{mn}^{\text{TE}}\frac{\beta_{mn}}{k\eta}e^{-j\boldsymbol{\beta}_{mn}\cdot\boldsymbol{\rho}\pm\gamma_{mn}z} \tag{2.15e}$$

$$\boldsymbol{E}_{mn}^{\text{TE}}(\boldsymbol{r}) = \pm Z_{mn}^{\text{TE}}\hat{\boldsymbol{z}} \times \boldsymbol{H}_{mn}(\boldsymbol{r})$$

$$= c_{mn}^{\text{TE}}e^{-j\boldsymbol{\beta}_{mn}\cdot\boldsymbol{\rho}\pm\gamma_{mn}z}\hat{\boldsymbol{z}} \times \hat{\boldsymbol{\beta}}_{mn} \tag{2.15f}$$

where we have used $\hat{\boldsymbol{\beta}}_{mn} = \boldsymbol{\beta}_{mn}/\beta_{mn}$.

Normal Incidence

In the case where $\beta_{mn} = 0$, we use the following convention:

$$\hat{\boldsymbol{\beta}}_{mn} = \hat{\boldsymbol{x}}, \tag{2.16}$$

so that the final formulas in (2.15) remain valid.

2.2.3   TM modes

Oblique Incidence

We first assume that $\beta_{mn} \neq 0$, in which case

$$\Psi_{mn}^{\mathrm{TM}}(\boldsymbol{\rho}) = \frac{\pm j c_{mn}^{\mathrm{TM}}}{\gamma_{mn}\beta_{mn}} e^{-j\boldsymbol{\beta}_{mn}\cdot\boldsymbol{\rho}} \tag{2.17a}$$

$$\gamma_{mn} = \sqrt{\beta_{mn}^2 - k^2} \qquad \text{(1st quadrant)} \tag{2.17b}$$

$$Y_{mn}^{\mathrm{TM}} = \frac{1}{Z_{mn}^{\mathrm{TM}}} = \frac{jk}{\eta\gamma_{mn}} \tag{2.17c}$$

$$\begin{aligned}
(\hat{\boldsymbol{x}}\hat{\boldsymbol{x}} + \hat{\boldsymbol{y}}\hat{\boldsymbol{y}}) \cdot \boldsymbol{E}_{mn}^{\mathrm{TM}}(\boldsymbol{r}) &= \pm\gamma_{mn} e^{\pm\gamma_{mn}z} \, \boldsymbol{\nabla}_t \Psi_{mn}^{\mathrm{TM}} \\
&= \mp j\gamma_{mn}\Psi_{mn}^{\mathrm{TM}} e^{\pm\gamma_{mn}z}\boldsymbol{\beta}_{mn} \\
&= c_{mn}^{\mathrm{TM}} e^{-j\boldsymbol{\beta}_{mn}\cdot\boldsymbol{\rho}\pm\gamma_{mn}z}\hat{\boldsymbol{\beta}}_{mn}
\end{aligned} \tag{2.17d}$$

$$\begin{aligned}
\hat{\boldsymbol{z}} \cdot \boldsymbol{E}_{mn}^{\mathrm{TM}}(\boldsymbol{r}) &= \beta_{mn}^2 \, \Psi_{mn}^{\mathrm{TM}} e^{\pm\gamma_{mn}z} \\
&= \pm j c_{mn}^{\mathrm{TM}}\frac{\beta_{mn}}{\gamma_{mn}} e^{-j\boldsymbol{\beta}_{mn}\cdot\boldsymbol{\rho}\pm\gamma_{mn}z}
\end{aligned} \tag{2.17e}$$

$$\begin{aligned}
\boldsymbol{H}_{mn}^{\mathrm{TM}}(\boldsymbol{r}) &= \mp Y_{mn}^{\mathrm{TM}}\hat{\boldsymbol{z}} \times \boldsymbol{E}_{mn}^{\mathrm{TM}}(\boldsymbol{r}) \\
&= \mp c_{mn}^{\mathrm{TM}} Y_{mn}^{\mathrm{TM}} e^{-j\boldsymbol{\beta}_{mn}\cdot\boldsymbol{\rho}\pm\gamma_{mn}z}\hat{\boldsymbol{z}} \times \hat{\boldsymbol{\beta}}_{mn}
\end{aligned} \tag{2.17f}$$

Normal Incidence

In the case where $\beta_{mn} = 0$, we again employ the convention (2.16), so that the final formulas in (2.17) remain valid.

2.2.4   Mode Normalization

So far we have not specified values for the set of mode normalization constants $\{c_{mn}^{\mathrm{TE}}\}$ and $\{c_{mn}^{\mathrm{TM}}\}$. These can be specified in any convenient manner. We will choose a normalization that allows us to easily interpret the incident and reflected traveling wave variables in terms of power transported by the modes. Consider a source-free slab of the unit cell bounded by $z = $ constant planes, filled with homogeneous dielectric material. Taking account of the results of Sections 2.2.2 and 2.2.3, we see that the transverse components of the most general electromagnetic field that can exist in this region can be written as

$$(\hat{\boldsymbol{x}}\hat{\boldsymbol{x}} + \hat{\boldsymbol{y}}\hat{\boldsymbol{y}}) \cdot \boldsymbol{E}(\boldsymbol{r}) = \sum_{(p,m,n)\in S} \boldsymbol{e}_{pmn}(x, y) \left(a_{pmn}e^{-\gamma_{mn}z} + b_{pmn}e^{\gamma_{mn}z}\right), \tag{2.18a}$$

$$(\hat{\boldsymbol{x}}\hat{\boldsymbol{x}} + \hat{\boldsymbol{y}}\hat{\boldsymbol{y}}) \cdot \boldsymbol{H}(\boldsymbol{r}) = \sum_{(p,m,n)\in S} \boldsymbol{h}_{pmn}(x, y) \left(a_{pmn}e^{-\gamma_{mn}z} - b_{pmn}e^{\gamma_{mn}z}\right), \tag{2.18b}$$

where the summations are taken over the set of integer triples $S = \{(p, m, n) \in \{1, 2\} \times \mathbb{Z} \times \mathbb{Z}\}$, $\mathbb{Z}$ is the set of all integers, $p = 1$ corresponds to TE modes, and $p = 2$ corresponds to TM modes. The modal fields $\boldsymbol{e}_{pmn}$ and $\boldsymbol{h}_{pmn}$ are given explicitly by

$$\boldsymbol{e}_{1mn} = c_{1mn}\hat{z} \times \hat{\boldsymbol{\beta}}_{mn} e^{-j\boldsymbol{\beta}_{mn} \cdot \boldsymbol{\rho}} \tag{2.19a}$$

$$\boldsymbol{e}_{2mn} = c_{2mn}\hat{\boldsymbol{\beta}}_{mn} e^{-j\boldsymbol{\beta}_{mn} \cdot \boldsymbol{\rho}} \tag{2.19b}$$

$$\boldsymbol{h}_{pmn} = Y_{pmn}\hat{z} \times \boldsymbol{e}_{pmn} \tag{2.19c}$$

where

$$Y_{1mn} = Y_{mn}^{\text{TE}}, \quad c_{1mn} = c_{mn}^{\text{TE}} \tag{2.20a}$$

$$Y_{2mn} = Y_{mn}^{\text{TM}}, \quad c_{2mn} = c_{mn}^{\text{TM}}. \tag{2.20b}$$

By virtue of the orthogonality of the Floquet modes (see Appendix A), the complex power P traveling down the unit cell in the z direction can be expressed as a sum of the individual complex powers transported by each mode:

$$
\begin{aligned}
P &= \iint_{U'} \boldsymbol{E} \times \boldsymbol{H}^* \cdot \hat{z}\, \mathrm{d}A \\
&= \sum_{(p,m,n)\in S} (a_{pmn} + b_{pmn})(a_{pmn}^* - b_{pmn}^*) \iint_{U'} \boldsymbol{e}_{pmn} \times \boldsymbol{h}_{pmn}^* \cdot \hat{z}\, \mathrm{d}A \\
&= \sum_{(p,m,n)\in S} \left[|a_{pmn}|^2 - |b_{pmn}|^2 - 2j\, \mathrm{Im}\left\{a_{pmn}b_{pmn}^*\right\} \right] P_{pmn}
\end{aligned}
\tag{2.21}
$$

where U' is the restriction of the unit cell to the plane $z = 0$, and

$$P_{pmn} = \iint_{U'} \boldsymbol{e}_{pmn} \times \boldsymbol{h}_{pmn}^* \cdot \hat{z}\, \mathrm{d}A = |c_{pmn}|^2 Y_{pmn}^* A \tag{2.22}$$

is the complex power associated with each unit-strength positive-going mode. Its value depends on the choice of mode normalization constant c_{pmn}, which has not yet been specified. Note that if P_{pmn} is equal to 1, then the time-average (real) power carried down the guide in the $+z$ direction is just $|a_{pmn}|^2 - |b_{pmn}|^2$, consistent with the usual definition of traveling wave variables [6]. Such a normalization is not possible, since in many cases of practical interest, P_{pmn} has zero real part. Consider the case of a lossless medium with $\beta_{mn} > k$. Then γ_{mn} is pure real, so that Y_{pmn} is pure imaginary. It follows from Equation (2.22) that P_{pmn} is pure imaginary, since A and $|c_{pmn}|$ are both pure real. Therefore, we content ourselves with setting the magnitude of P_{pmn} equal to $P_0 \equiv$ one watt:

$$P_{pmn} = \frac{Y_{pmn}^*}{|Y_{pmn}|} P_0. \tag{2.23}$$

Substituting (2.23) into (2.22) determines the value of the mode normalization constant (up to an arbitrary phase):

$$|c_{pmn}| = \sqrt{\frac{P_0}{A|Y_{pmn}|}}. \tag{2.24}$$

This choice results in a unitary scattering matrix for propagating modes in lossless media. It will be convenient for later work to choose the phase of c_{pmn} as follows:

$$c_{pmn} = \sqrt{\frac{P_0}{AY_{pmn}}}. \tag{2.25}$$

where we agree to take that square root of Y_{pmn} having positive real part.

Chapter 3

Generalized Scattering Matrix

3.1 Introduction

This chapter documents the form of the GSM (generalized scattering matrix) used in the PSSFSS program and provides formulas for the scattering parameters of several canonical structures needed in the analysis of an FSS (Frequency Selective Surface). These include a dielectric interface, a dielectric slab, and the cascade interconnection of two FSS structures.

3.2 Definition of the GSM

We consider a structure with two-dimensional periodicity as described in Chapter 2. The structure occupies the region $z_1 \leq z \leq z_2$, as shown in Figure 3.1. It is bounded by the two half-spaces denoted as Region 1 and Region 2. Each is characterized by its electrical parameters μ_i, ϵ_i, k_i, and η_i, $i = 1, 2$, which are the permittivity, permeability, intrinsic wavenumber, and intrinsic impedance, respectively. Given the lattice vectors s_1 and s_2 and impressed phasings ψ_1 and ψ_2, as defined in Chapter 2, we may expand the transverse fields in each of Regions 1 and 2 in terms of incident and
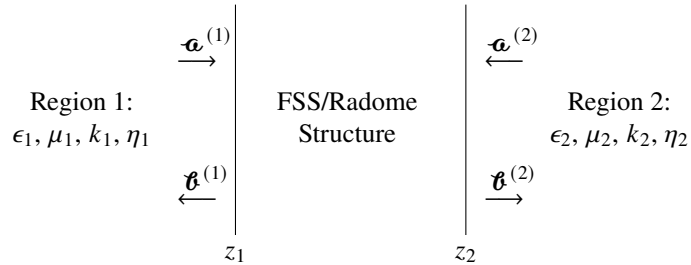

Figure 3.1: A structure to be characterized by its GSM occupies the region $z_1 \leq z \leq z_2$. It is bounded on each side by (possibly dissimilar) homogeneous, dielectric half-spaces.

reflected Floquet modes:

$$(\hat{x}\hat{x} + \hat{y}\hat{y}) \cdot \boldsymbol{E}^{(1)}(\boldsymbol{r}) = \sum_{q=1}^{N_1} \boldsymbol{e}_q^{(1)}(x, y) \left(a_q^{(1)} e^{-\gamma_q^{(1)}(z-z_1)} + b_q^{(1)} e^{\gamma_q^{(1)}(z-z_1)}\right), \tag{3.1a}$$

$$(\hat{x}\hat{x} + \hat{y}\hat{y}) \cdot \boldsymbol{H}^{(1)}(\boldsymbol{r}) = \sum_{q=1}^{N_1} \boldsymbol{h}_q^{(1)}(x, y) \left(a_q^{(1)} e^{-\gamma_q^{(1)}(z-z_1)} - b_q^{(1)} e^{\gamma_q^{(1)}(z-z_1)}\right), \tag{3.1b}$$

$$(\hat{x}\hat{x} + \hat{y}\hat{y}) \cdot \boldsymbol{E}^{(2)}(\boldsymbol{r}) = \sum_{q=1}^{N_2} \boldsymbol{e}_q^{(2)}(x, y) \left(a_q^{(2)} e^{\gamma_q^{(2)}(z-z_2)} + b_q^{(2)} e^{-\gamma_q^{(2)}(z-z_2)}\right), \tag{3.1c}$$

$$(\hat{x}\hat{x} + \hat{y}\hat{y}) \cdot \boldsymbol{H}^{(2)}(\boldsymbol{r}) = \sum_{q=1}^{N_2} \boldsymbol{h}_q^{(2)}(x, y) \left(-a_q^{(2)} e^{\gamma_q^{(2)}(z-z_2)} + b_q^{(2)} e^{-\gamma_q^{(2)}(z-z_2)}\right). \tag{3.1d}$$

Superscripted numbers in parentheses are used in Equations (3.1) as region designators. The sums are taken over the set of modes in each region, which for convenience are enumerated with a single index q, rather than the triple index (p, m, n) as was used in Section 2.2. We will make use of both subscripting schemes, employing whichever is most convenient in a particular formula. Although the limits on the sums should be infinite in principle, the numbers of modes in each region are truncated to a finite value (N_1 modes in Region 1 and N_2 in Region 2) so that a numerical evaluation can be accomplished. In general the modes are sorted prior to enumeration so that those with the smallest values of β_{mn} are retained in the finite sums.

The generalized scattering matrix $\boldsymbol{\mathcal{S}}$ expresses the linear relationship between the incident and scattered Floquet modal coefficients evaluated at each terminal plane of the FSS structure. This relationship is written in partitioned form as

$$\begin{bmatrix} \boldsymbol{b}^{(1)} \\ \boldsymbol{b}^{(2)} \end{bmatrix} = \begin{bmatrix} \boldsymbol{\mathcal{S}}^{11} & \boldsymbol{\mathcal{S}}^{12} \\ \boldsymbol{\mathcal{S}}^{21} & \boldsymbol{\mathcal{S}}^{22} \end{bmatrix} \begin{bmatrix} \boldsymbol{a}^{(1)} \\ \boldsymbol{a}^{(2)} \end{bmatrix} \tag{3.2}$$

where

$$\boldsymbol{a}^{(1)} = \begin{bmatrix} a_1^{(1)} \\ a_2^{(1)} \\ a_3^{(1)} \\ \vdots \\ a_{N_1}^{(1)} \end{bmatrix}, \quad \boldsymbol{b}^{(1)} = \begin{bmatrix} b_1^{(1)} \\ b_2^{(1)} \\ b_3^{(1)} \\ \vdots \\ b_{N_1}^{(1)} \end{bmatrix}, \quad \boldsymbol{a}^{(2)} = \begin{bmatrix} a_1^{(2)} \\ a_2^{(2)} \\ a_3^{(2)} \\ \vdots \\ a_{N_2}^{(2)} \end{bmatrix}, \quad \boldsymbol{b}^{(2)} = \begin{bmatrix} b_1^{(2)} \\ b_2^{(2)} \\ b_3^{(2)} \\ \vdots \\ b_{N_2}^{(2)} \end{bmatrix}, \tag{3.3}$$

and $\boldsymbol{\mathcal{S}}^{11} \in \mathbb{C}^{N_1 \times N_1}$, $\boldsymbol{\mathcal{S}}^{12} \in \mathbb{C}^{N_1 \times N_2}$, $\boldsymbol{\mathcal{S}}^{21} \in \mathbb{C}^{N_2 \times N_1}$, $\boldsymbol{\mathcal{S}}^{22} \in \mathbb{C}^{N_2 \times N_2}$. We see that the entries of the $\boldsymbol{\mathcal{S}}^{11}$ and $\boldsymbol{\mathcal{S}}^{22}$ matrices are reflection coefficients while those of $\boldsymbol{\mathcal{S}}^{12}$ and $\boldsymbol{\mathcal{S}}^{21}$ are transmission coefficients.

3.3   GSM of a Dielectric Interface

Consider the case where $z_1 = z_2 = 0$ and there is no FSS present at the junction plane. The resulting structure is then just the interface between two homogeneous half-spaces.

3.3.1   Wave Incident from Region 1

TE Mode Incident

The transverse components of the incident field are

$$(\hat{x}\hat{x} + \hat{y}\hat{y}) \cdot E^{\text{inc}} = c_{1mn}^{(1)} e^{-j\beta_{mn} \cdot \rho - \gamma_{mn}^{(1)} z} \hat{z} \times \hat{\beta}_{mn} \tag{3.4a}$$

$$(\hat{x}\hat{x} + \hat{y}\hat{y}) \cdot H^{\text{inc}} = -c_{1mn}^{(1)} Y_{1mn}^{(1)} e^{-j\beta_{mn} \cdot \rho - \gamma_{mn}^{(1)} z} \hat{\beta}_{mn} \tag{3.4b}$$

The transverse components of the reflected field are

$$(\hat{x}\hat{x} + \hat{y}\hat{y}) \cdot E^{\text{r}} = R_{1mn}^{(1)} c_{1mn}^{(1)} e^{-j\beta_{mn} \cdot \rho + \gamma_{mn}^{(1)} z} \hat{z} \times \hat{\beta}_{mn} \tag{3.5a}$$

$$(\hat{x}\hat{x} + \hat{y}\hat{y}) \cdot H^{\text{r}} = R_{1mn}^{(1)} c_{1mn}^{(1)} Y_{1mn}^{(1)} e^{-j\beta_{mn} \cdot \rho + \gamma_{mn}^{(1)} z} \hat{\beta}_{mn} \tag{3.5b}$$

The transverse components of the transmitted field are

$$(\hat{x}\hat{x} + \hat{y}\hat{y}) \cdot E^{\text{t}} = T_{1mn}^{(2)} c_{1mn}^{(2)} e^{-j\beta_{mn} \cdot \rho - \gamma_{mn}^{(2)} z} \hat{z} \times \hat{\beta}_{mn} \tag{3.6a}$$

$$(\hat{x}\hat{x} + \hat{y}\hat{y}) \cdot H^{\text{t}} = -T_{1mn}^{(2)} c_{1mn}^{(2)} Y_{1mn}^{(2)} e^{-j\beta_{mn} \cdot \rho - \gamma_{mn}^{(2)} z} \hat{\beta}_{mn} \tag{3.6b}$$

The unknown reflection and transmission coefficients $R_{1mn}^{(1)}$ and $T_{1mn}^{(2)}$ are determined by equating the total transverse electric and magnetic fields at each side of the interface:

$$(\hat{x}\hat{x} + \hat{y}\hat{y}) \cdot \left[E^{\text{inc}}(0,0,0) + E^{\text{r}}(0,0,0) \right] = (\hat{x}\hat{x} + \hat{y}\hat{y}) \cdot E^{\text{t}}(0,0,0), \tag{3.7a}$$

$$(\hat{x}\hat{x} + \hat{y}\hat{y}) \cdot \left[H^{\text{inc}}(0,0,0) + H^{\text{r}}(0,0,0) \right] = (\hat{x}\hat{x} + \hat{y}\hat{y}) \cdot H^{\text{t}}(0,0,0). \tag{3.7b}$$

This procedure results in the following system of equations for the transmission and reflection coefficient:

$$1 + R_{1mn}^{(1)} = \frac{c_{1mn}^{(2)}}{c_{1mn}^{(1)}} T_{1mn}^{(2)} = \frac{\sqrt{Y_{1mn}^{(1)}}}{\sqrt{Y_{1mn}^{(2)}}} T_{1mn}^{(2)} \tag{3.8a}$$

$$1 - R_{1mn}^{(1)} = \frac{c_{1mn}^{(2)} Y_{1mn}^{(2)}}{c_{1mn}^{(1)} Y_{1mn}^{(1)}} T_{1mn}^{(2)} = \frac{\sqrt{Y_{1mn}^{(2)}}}{\sqrt{Y_{1mn}^{(1)}}} T_{1mn}^{(2)} \tag{3.8b}$$

where we have made use of Equation (2.25). One can easily solve for $R_{1mn}^{(1)}$ by dividing the equations and recalling that

$$y = \frac{1-x}{1+x} \iff x = \frac{1-y}{1+y}. \tag{3.9}$$

The result is

$$R_{1mn}^{(1)} = \frac{Y_{1mn}^{(1)} - Y_{1mn}^{(2)}}{Y_{1mn}^{(1)} + Y_{1mn}^{(2)}} = \frac{Z_{1mn}^{(2)} - Z_{1mn}^{(1)}}{Z_{1mn}^{(2)} + Z_{1mn}^{(1)}}, \tag{3.10}$$

$$T_{1mn}^{(2)} = \frac{2\sqrt{Y_{1mn}^{(1)}}\sqrt{Y_{1mn}^{(2)}}}{Y_{1mn}^{(1)} + Y_{1mn}^{(2)}} = \frac{2\sqrt{Z_{1mn}^{(1)}}\sqrt{Z_{1mn}^{(2)}}}{Z_{1mn}^{(1)} + Z_{1mn}^{(2)}}. \tag{3.11}$$

TM Mode Incident

The transverse components of the incident field are

$$(\hat{x}\hat{x} + \hat{y}\hat{y}) \cdot \boldsymbol{E}^{\mathrm{inc}} = c_{2mn}^{(1)} e^{-j\beta_{mn}\cdot\rho - \gamma_{mn}^{(1)} z} \hat{\boldsymbol{\beta}}_{mn} \tag{3.12a}$$

$$(\hat{x}\hat{x} + \hat{y}\hat{y}) \cdot \boldsymbol{H}^{\mathrm{inc}} = c_{2mn}^{(1)} Y_{2mn}^{(1)} e^{-j\beta_{mn}\cdot\rho - \gamma_{mn}^{(1)} z} \hat{z} \times \hat{\boldsymbol{\beta}}_{mn} \tag{3.12b}$$

The transverse components of the reflected field are

$$(\hat{x}\hat{x} + \hat{y}\hat{y}) \cdot \boldsymbol{E}^{\mathrm{r}} = R_{2mn}^{(1)} c_{2mn}^{(1)} e^{-j\beta_{mn}\cdot\rho + \gamma_{mn}^{(1)} z} \hat{\boldsymbol{\beta}}_{mn} \tag{3.13a}$$

$$(\hat{x}\hat{x} + \hat{y}\hat{y}) \cdot \boldsymbol{H}^{\mathrm{r}} = -R_{2mn}^{(1)} c_{2mn}^{(1)} Y_{2mn}^{(1)} e^{-j\beta_{mn}\cdot\rho + \gamma_{mn}^{(1)} z} \hat{z} \times \hat{\boldsymbol{\beta}}_{mn} \tag{3.13b}$$

The transverse components of the transmitted field are

$$(\hat{x}\hat{x} + \hat{y}\hat{y}) \cdot \boldsymbol{E}^{\mathrm{t}} = T_{2mn}^{(2)} c_{2mn}^{(2)} e^{-j\beta_{mn}\cdot\rho - \gamma_{mn}^{(2)} z} \hat{\boldsymbol{\beta}}_{mn} \tag{3.14a}$$

$$(\hat{x}\hat{x} + \hat{y}\hat{y}) \cdot \boldsymbol{H}^{\mathrm{t}} = -T_{2mn}^{(2)} c_{2mn}^{(2)} Y_{2mn}^{(2)} e^{-j\beta_{mn}\cdot\rho - \gamma_{mn}^{(2)} z} \hat{z} \times \hat{\boldsymbol{\beta}}_{mn} \tag{3.14b}$$

When the total transverse fields are equated at the plane $z = 0$, we again arrive at the set of equations (3.8) for the unknowns $R_{2mn}^{(1)}$ and $T_{2mn}^{(2)}$. Therefore, the TM reflection and transmission coefficients for a wave incident from Region 1 are identical to the TE coefficients:

$$R_{2mn}^{(1)} = \frac{Y_{2mn}^{(1)} - Y_{2mn}^{(2)}}{Y_{2mn}^{(1)} + Y_{2mn}^{(2)}} = \frac{Z_{2mn}^{(2)} - Z_{2mn}^{(1)}}{Z_{2mn}^{(2)} + Z_{2mn}^{(1)}}, \tag{3.15}$$

$$T_{2mn}^{(2)} = \frac{2\sqrt{Y_{2mn}^{(1)}}\sqrt{Y_{2mn}^{(2)}}}{Y_{2mn}^{(1)} + Y_{2mn}^{(2)}} = \frac{2\sqrt{Z_{2mn}^{(1)}}\sqrt{Z_{2mn}^{(2)}}}{Z_{2mn}^{(1)} + Z_{2mn}^{(2)}}. \tag{3.16}$$

3.3.2   Wave Incident from Region 2

TE Mode Incident

The transverse components of the incident field are

$$(\hat{x}\hat{x} + \hat{y}\hat{y}) \cdot \boldsymbol{E}^{\mathrm{inc}} = c_{1mn}^{(2)} e^{-j\boldsymbol{\beta}_{mn}\cdot\boldsymbol{\rho}+\gamma_{mn}^{(2)}z}\hat{z} \times \hat{\boldsymbol{\beta}}_{mn} \tag{3.17a}$$

$$(\hat{x}\hat{x} + \hat{y}\hat{y}) \cdot \boldsymbol{H}^{\mathrm{inc}} = c_{1mn}^{(2)} Y_{1mn}^{(2)} e^{-j\boldsymbol{\beta}_{mn}\cdot\boldsymbol{\rho}+\gamma_{mn}^{(2)}z}\hat{\boldsymbol{\beta}}_{mn} \tag{3.17b}$$

The transverse components of the reflected field are

$$(\hat{x}\hat{x} + \hat{y}\hat{y}) \cdot \boldsymbol{E}^{\mathrm{r}} = R_{1mn}^{(2)} c_{1mn}^{(2)} e^{-j\boldsymbol{\beta}_{mn}\cdot\boldsymbol{\rho}-\gamma_{mn}^{(2)}z}\hat{z} \times \hat{\boldsymbol{\beta}}_{mn} \tag{3.18a}$$

$$(\hat{x}\hat{x} + \hat{y}\hat{y}) \cdot \boldsymbol{H}^{\mathrm{r}} = -R_{1mn}^{(2)} c_{1mn}^{(2)} Y_{1mn}^{(2)} e^{-j\boldsymbol{\beta}_{mn}\cdot\boldsymbol{\rho}-\gamma_{mn}^{(2)}z}\hat{\boldsymbol{\beta}}_{mn} \tag{3.18b}$$

The transverse components of the transmitted field are

$$(\hat{x}\hat{x} + \hat{y}\hat{y}) \cdot \boldsymbol{E}^{\mathrm{t}} = T_{1mn}^{(1)} c_{1mn}^{(1)} e^{-j\boldsymbol{\beta}_{mn}\cdot\boldsymbol{\rho}+\gamma_{mn}^{(1)}z}\hat{z} \times \hat{\boldsymbol{\beta}}_{mn} \tag{3.19a}$$

$$(\hat{x}\hat{x} + \hat{y}\hat{y}) \cdot \boldsymbol{H}^{\mathrm{t}} = T_{1mn}^{(1)} c_{1mn}^{(1)} Y_{1mn}^{(1)} e^{-j\boldsymbol{\beta}_{mn}\cdot\boldsymbol{\rho}+\gamma_{mn}^{(1)}z}\hat{\boldsymbol{\beta}}_{mn} \tag{3.19b}$$

Equating the total transverse electric and magnetic field across the $z = 0$ plane results in the following system of equations for the transmission and reflection coefficient:

$$1 + R_{1mn}^{(2)} = \frac{c_{1mn}^{(1)}}{c_{1mn}^{(2)}} T_{1mn}^{(1)} = \frac{\sqrt{Y_{1mn}^{(2)}}}{\sqrt{Y_{1mn}^{(1)}}} T_{1mn}^{(1)} \tag{3.20a}$$

$$1 - R_{1mn}^{(2)} = \frac{c_{1mn}^{(1)} Y_{1mn}^{(1)}}{c_{1mn}^{(2)} Y_{1mn}^{(2)}} T_{1mn}^{(1)} = \frac{\sqrt{Y_{1mn}^{(1)}}}{\sqrt{Y_{1mn}^{(2)}}} T_{1mn}^{(1)}. \tag{3.20b}$$

We note that these are identical to Equations (3.8) with the roles of Regions 1 and 2 reversed. Therefore, the solution is

$$R_{1mn}^{(2)} = -R_{1mn}^{(1)} = \frac{Y_{1mn}^{(2)} - Y_{1mn}^{(1)}}{Y_{1mn}^{(2)} + Y_{1mn}^{(1)}} = \frac{Z_{1mn}^{(1)} - Z_{1mn}^{(2)}}{Z_{1mn}^{(1)} + Z_{1mn}^{(2)}}, \tag{3.21}$$

$$T_{1mn}^{(1)} = T_{1mn}^{(2)} = \frac{2\sqrt{Y_{1mn}^{(2)}}\sqrt{Y_{1mn}^{(1)}}}{Y_{1mn}^{(2)} + Y_{1mn}^{(1)}} = \frac{2\sqrt{Z_{1mn}^{(2)}}\sqrt{Z_{1mn}^{(1)}}}{Z_{1mn}^{(2)} + Z_{1mn}^{(1)}}. \tag{3.22}$$

TM Mode Incident

The results for TM incidence are identical to the TE case, as they were for a wave incident from Region 1.

3.3.3   Summary

Considering the results of Sections 3.3.1 and 3.3.2, we can write the GSM of the dielectric interface in the following form:

$$\mathcal{S} = \begin{bmatrix} \mathcal{R}^{(1)} & \mathcal{T}^\mathsf{T} \\ \mathcal{T} & \mathcal{R}^{(2)} \end{bmatrix} \tag{3.23}$$

where

$$R_{qq'}^{(1)} = -R_{q'q}^{(2)} = \frac{Y_{p_q m_q n_q}^{(1)} - Y_{p_q m_q n_q}^{(2)}}{Y_{p_q m_q n_q}^{(1)} + Y_{p_q m_q n_q}^{(2)}} \, \delta_{p_q p_{q'}} \delta_{m_q m_{q'}} \delta_{n_q n_{q'}}, \tag{3.24a}$$

$$T_{qq'} = \frac{2\sqrt{Y_{p_q m_q n_q}^{(1)}} \sqrt{Y_{p_q m_q n_q}^{(2)}}}{Y_{p_q m_q n_q}^{(1)} + Y_{p_q m_q n_q}^{(2)}} \, \delta_{p_q p_{q'}} \delta_{m_q m_{q'}} \delta_{n_q n_{q'}}. \tag{3.24b}$$

Note that even though the matrices $\mathcal{T}$, $\mathcal{R}^{(1)}$, and $\mathcal{R}^{(2)}$ are diagonal, $\mathcal{T}$ is not square, unless $N_1 = N_2$; i.e., the number of modes used in Regions 1 and 2 is the same. Only in this case is it true that $\mathcal{R}^{(2)} = -\mathcal{R}^{(1)}$.

It is also important to realize that the two radicands in Eq. (3.24b) must not be combined under a single radical, since, for general complex numbers a and b, $\sqrt{ab} \neq \sqrt{a}\sqrt{b}$.

3.4   GSM of a Dielectric Slab

We consider the case where Regions 1 and 2 are identical, there is no FSS present, and $z_2 - z_1 = L$. In this case we will always insist that $N_2 = N_1 = N$ (same number of modes in each region). It is simple to see that all reflection coefficients are identically zero, and the transmission coefficients are just the propagation factors of each mode:

$$\mathcal{S} = \begin{bmatrix} \mathbf{0} & \mathcal{P} \\ \mathcal{P} & \mathbf{0} \end{bmatrix} \tag{3.25}$$

where $\mathcal{P}$ is the propagator matrix [7]

$$\mathcal{P} = \mathrm{diag}\left\{ e^{-\gamma_{m_1 n_1} L}, e^{-\gamma_{m_2 n_2} L}, \ldots, e^{-\gamma_{m_N n_N} L} \right\} \tag{3.26}$$

3.5   GSM of a Cascade

In this section we consider the cascade connection of a pair of FSS structures as shown in Figure 3.2. We have two FSS structures A and B, with the Region 2 terminal plane of A coinciding with the Region 1 terminal plane of B. The scattering matrix for A is $\mathcal{A}$ and the scattering matrix for B is $\mathcal{B}$. Note that the number of modes used in Region 2 of device A must equal the number of modes used in Region 1 of device B. In fact, these two regions are really the same region, and the Floquet modes defined for each device for this common region are in fact identical.
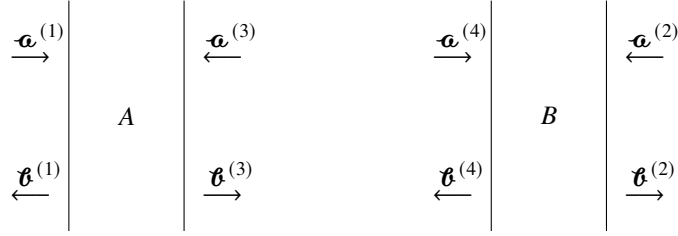
Figure 3.2: A structure consisting of a pair of FSS structures connected in cascade.

The goal of this section is to find the scattering matrix $\mathcal{S}$ that relates $\boldsymbol{a}^{(1)}$ and $\boldsymbol{a}^{(2)}$ to $\boldsymbol{b}^{(1)}$ and $\boldsymbol{b}^{(2)}$ under the interconnection condition:

$$\begin{bmatrix} \boldsymbol{b}^{(3)} \\ \boldsymbol{b}^{(4)} \end{bmatrix} = \begin{bmatrix} \mathbf{0} & \mathcal{I} \\ \mathcal{I} & \mathbf{0} \end{bmatrix} \begin{bmatrix} \boldsymbol{a}^{(3)} \\ \boldsymbol{a}^{(4)} \end{bmatrix}, \tag{3.27}$$

where $\mathcal{I}$ is the identity matrix. Each device satisfies its own scattering relation:

$$\begin{bmatrix} \boldsymbol{b}^{(1)} \\ \boldsymbol{b}^{(3)} \end{bmatrix} = \begin{bmatrix} \mathcal{A}^{11} & \mathcal{A}^{12} \\ \mathcal{A}^{21} & \mathcal{A}^{22} \end{bmatrix} \begin{bmatrix} \boldsymbol{a}^{(1)} \\ \boldsymbol{a}^{(3)} \end{bmatrix} \tag{3.28a}$$

$$\begin{bmatrix} \boldsymbol{b}^{(4)} \\ \boldsymbol{b}^{(2)} \end{bmatrix} = \begin{bmatrix} \mathcal{B}^{11} & \mathcal{B}^{12} \\ \mathcal{B}^{21} & \mathcal{B}^{22} \end{bmatrix} \begin{bmatrix} \boldsymbol{a}^{(4)} \\ \boldsymbol{a}^{(2)} \end{bmatrix}. \tag{3.28b}$$

In light of (3.27), it is useful to partition the scattering relations (3.28) in the following manner:

$$\begin{bmatrix} \boldsymbol{b}^{(1)} \\ \boldsymbol{b}^{(2)} \end{bmatrix} = \begin{bmatrix} \mathcal{A}^{11} & \mathbf{0} \\ \mathbf{0} & \mathcal{B}^{22} \end{bmatrix} \begin{bmatrix} \boldsymbol{a}^{(1)} \\ \boldsymbol{a}^{(2)} \end{bmatrix} + \begin{bmatrix} \mathcal{A}^{12} & \mathbf{0} \\ \mathbf{0} & \mathcal{B}^{21} \end{bmatrix} \begin{bmatrix} \boldsymbol{a}^{(3)} \\ \boldsymbol{a}^{(4)} \end{bmatrix} \tag{3.29a}$$

$$\begin{bmatrix} \boldsymbol{b}^{(3)} \\ \boldsymbol{b}^{(4)} \end{bmatrix} = \begin{bmatrix} \mathcal{A}^{21} & \mathbf{0} \\ \mathbf{0} & \mathcal{B}^{12} \end{bmatrix} \begin{bmatrix} \boldsymbol{a}^{(1)} \\ \boldsymbol{a}^{(2)} \end{bmatrix} + \begin{bmatrix} \mathcal{A}^{22} & \mathbf{0} \\ \mathbf{0} & \mathcal{B}^{11} \end{bmatrix} \begin{bmatrix} \boldsymbol{a}^{(3)} \\ \boldsymbol{a}^{(4)} \end{bmatrix}. \tag{3.29b}$$

Equating (3.27) and (3.29b), one can solve for $\boldsymbol{a}^{(3)}$ and $\boldsymbol{a}^{(4)}$ in terms of $\boldsymbol{a}^{(1)}$ and $\boldsymbol{a}^{(2)}$:

$$\begin{aligned}
\begin{bmatrix} \boldsymbol{a}^{(3)} \\ \boldsymbol{a}^{(4)} \end{bmatrix} &= \begin{bmatrix} -\mathcal{A}^{22} & \mathcal{I} \\ \mathcal{I} & -\mathcal{B}^{11} \end{bmatrix}^{-1} \begin{bmatrix} \mathcal{A}^{21} & \mathbf{0} \\ \mathbf{0} & \mathcal{B}^{12} \end{bmatrix} \begin{bmatrix} \boldsymbol{a}^{(1)} \\ \boldsymbol{a}^{(2)} \end{bmatrix} \\
&= \begin{bmatrix} \mathcal{C}^{11} & \mathcal{C}^{12} \\ \mathcal{C}^{21} & \mathcal{C}^{22} \end{bmatrix} \begin{bmatrix} \mathcal{A}^{21} & \mathbf{0} \\ \mathbf{0} & \mathcal{B}^{12} \end{bmatrix} \begin{bmatrix} \boldsymbol{a}^{(1)} \\ \boldsymbol{a}^{(2)} \end{bmatrix} \\
&= \begin{bmatrix} \mathcal{C}^{11}\mathcal{A}^{21} & \mathcal{C}^{12}\mathcal{B}^{12} \\ \mathcal{C}^{21}\mathcal{A}^{21} & \mathcal{C}^{22}\mathcal{B}^{12} \end{bmatrix} \begin{bmatrix} \boldsymbol{a}^{(1)} \\ \boldsymbol{a}^{(2)} \end{bmatrix}
\end{aligned} \tag{3.30}$$

where

$$
\begin{bmatrix} \mathcal{C}^{11} & \mathcal{C}^{12} \\ \mathcal{C}^{21} & \mathcal{C}^{22} \end{bmatrix} \equiv \begin{bmatrix} -\mathcal{A}^{22} & \mathcal{I} \\ \mathcal{I} & -\mathcal{B}^{11} \end{bmatrix}^{-1}
$$

$$
= \begin{bmatrix} \mathcal{B}^{11}(\mathcal{I} - \mathcal{A}^{22}\mathcal{B}^{11})^{-1} & (\mathcal{I} - \mathcal{B}^{11}\mathcal{A}^{22})^{-1} \\ (\mathcal{I} - \mathcal{A}^{22}\mathcal{B}^{11})^{-1} & \mathcal{A}^{22}(\mathcal{I} - \mathcal{B}^{11}\mathcal{A}^{22})^{-1} \end{bmatrix}, \tag{3.31}
$$

a result obtainable using [8, Exercise 1.3.12]. For conciseness, we make the following definitions.

$$
\mathcal{G}^{AB} \equiv (\mathcal{I} - \mathcal{A}^{22}\mathcal{B}^{11})^{-1}, \qquad \mathcal{G}^{BA} \equiv (\mathcal{I} - \mathcal{B}^{11}\mathcal{A}^{22})^{-1} \tag{3.32}
$$

so that

$$
\begin{bmatrix} \mathcal{C}^{11} & \mathcal{C}^{12} \\ \mathcal{C}^{21} & \mathcal{C}^{22} \end{bmatrix} = \begin{bmatrix} \mathcal{B}^{11}\mathcal{G}^{AB} & \mathcal{G}^{BA} \\ \mathcal{G}^{AB} & \mathcal{A}^{22}\mathcal{G}^{BA} \end{bmatrix} \tag{3.33}
$$

and (3.30) can be written as

$$
\begin{bmatrix} a^{(3)} \\ a^{(4)} \end{bmatrix} = \begin{bmatrix} \mathcal{B}^{11}\mathcal{G}^{AB}\mathcal{A}^{21} & \mathcal{G}^{BA}\mathcal{B}^{12} \\ \mathcal{G}^{AB}\mathcal{A}^{21} & \mathcal{A}^{22}\mathcal{G}^{BA}\mathcal{B}^{12} \end{bmatrix} \begin{bmatrix} a^{(1)} \\ a^{(2)} \end{bmatrix}. \tag{3.34}
$$

We can now substitute (3.34) into (3.29a) to obtain

$$
\begin{bmatrix} b^{(1)} \\ b^{(2)} \end{bmatrix} = \left\{ \begin{bmatrix} \mathcal{A}^{11} & 0 \\ 0 & \mathcal{B}^{22} \end{bmatrix} + \begin{bmatrix} \mathcal{A}^{12} & 0 \\ 0 & \mathcal{B}^{21} \end{bmatrix} \begin{bmatrix} \mathcal{B}^{11}\mathcal{G}^{AB}\mathcal{A}^{21} & \mathcal{G}^{BA}\mathcal{B}^{12} \\ \mathcal{G}^{AB}\mathcal{A}^{21} & \mathcal{A}^{22}\mathcal{G}^{BA}\mathcal{B}^{12} \end{bmatrix} \right\} \begin{bmatrix} a^{(1)} \\ a^{(2)} \end{bmatrix}
$$

$$
= \begin{bmatrix} \mathcal{A}^{11} + \mathcal{A}^{12}\mathcal{B}^{11}\mathcal{G}^{AB}\mathcal{A}^{21} & \mathcal{A}^{12}\mathcal{G}^{BA}\mathcal{B}^{12} \\ \mathcal{B}^{21}\mathcal{G}^{AB}\mathcal{A}^{21} & \mathcal{B}^{22} + \mathcal{B}^{21}\mathcal{A}^{22}\mathcal{G}^{BA}\mathcal{B}^{12} \end{bmatrix} \begin{bmatrix} a^{(1)} \\ a^{(2)} \end{bmatrix}
$$

so that the composite scattering matrix is

$$
\mathcal{S} = \begin{bmatrix} \mathcal{S}^{11} & \mathcal{S}^{12} \\ \mathcal{S}^{21} & \mathcal{S}^{22} \end{bmatrix} = \begin{bmatrix} \mathcal{A}^{11} + \mathcal{A}^{12}\mathcal{B}^{11}\mathcal{G}^{AB}\mathcal{A}^{21} & \mathcal{A}^{12}\mathcal{G}^{BA}\mathcal{B}^{12} \\ \mathcal{B}^{21}\mathcal{G}^{AB}\mathcal{A}^{21} & \mathcal{B}^{22} + \mathcal{B}^{21}\mathcal{A}^{22}\mathcal{G}^{BA}\mathcal{B}^{12} \end{bmatrix}. \tag{3.35}
$$

3.5.1   Device A is a Dielectric Slab

In the case where device *A* is just a dielectric slab, we have

$$
\mathcal{A} = \begin{bmatrix} 0 & \mathcal{P} \\ \mathcal{P} & 0 \end{bmatrix} \tag{3.36}
$$

where $\mathcal{P}$ is defined in Equation (3.26). $\mathcal{G}^{AB}$ and $\mathcal{G}^{BA}$ both reduce to the unit matrix, and the formula given in (3.35) for the composite scattering matrix simplifies to

$$
\begin{bmatrix} \mathcal{S}^{11} & \mathcal{S}^{12} \\ \mathcal{S}^{21} & \mathcal{S}^{22} \end{bmatrix} = \begin{bmatrix} \mathcal{P}\mathcal{B}^{11}\mathcal{P} & \mathcal{P}\mathcal{B}^{12} \\ \mathcal{B}^{21}\mathcal{P} & \mathcal{B}^{22} \end{bmatrix}. \tag{3.37}
$$

3.5.2   Device B is a Dielectric Slab

In the case where device B is just a dielectric slab, we have

$$\mathcal{B} = \begin{bmatrix} \mathbf{0} & \mathcal{P} \\ \mathcal{P} & \mathbf{0} \end{bmatrix} \tag{3.38}$$

where $\mathcal{P}$ is defined in Equation (3.26). $\mathcal{G}^{AB}$ and $\mathcal{G}^{BA}$ both reduce to the unit matrix, and the formula given in (3.35) for the composite scattering matrix simplifies to

$$\begin{bmatrix} \mathcal{S}^{11} & \mathcal{S}^{12} \\ \mathcal{S}^{21} & \mathcal{S}^{22} \end{bmatrix} = \begin{bmatrix} \mathcal{A}^{11} & \mathcal{A}^{12}\mathcal{P} \\ \mathcal{P}\mathcal{A}^{21} & \mathcal{P}\mathcal{A}^{22}\mathcal{P} \end{bmatrix}. \tag{3.39}$$

Chapter 4

Mixed Potential Green's Functions for Abutted Half-Spaces

In this chapter, we derive an efficient method of evaluating the potential Green's functions needed for the PSSFSS program. The structure for which the potential Green's functions are desired consists of two layers, as shown in Figure 4.1. The coordinate system origin is located in the interface between layers 1 and 2 and the z axis points into layer 2. Both layers are semi-infinite in the z direction and translationally invariant in the x and y directions. Each layer $i = 1, 2$ is characterized by a complex permittivity ϵ_i and permeability μ_i, each of which lies either in the fourth quadrant of the complex plane, or on the real axis. The medium intrinsic wavenumbers are $k_i = \omega\sqrt{\mu_i \epsilon_i}$.

We will use the shorthand notation $\sum\limits_{m,n}$ to denote the double sum $\sum\limits_{m=-\infty}^{\infty} \sum\limits_{n=-\infty}^{\infty}$.

Region 1: $z < 0$ Region 2: $z > 0$
$\epsilon_1, \mu_1, k_1, \eta_1$ $\epsilon_2, \mu_2, k_2, \eta_2$
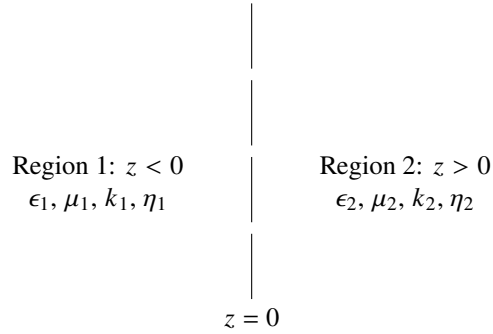
$z = 0$

Figure 4.1: The two-layer structure for which the Green's functions are desired.

4.1   Derivation of Modal Series

4.1.1   Magnetic Vector Potential

The assumed source is the electric current density

$$J(r) = \hat{x} \sum_{m,n} \delta(r - \rho' - m s_1 - n s_2) e^{-j(m\psi_1 + n\psi_2)} \tag{4.1}$$

where, as usual

$$r = \hat{x}x + \hat{y}y + \hat{z}z \tag{4.2a}$$

$$\rho = \hat{x}x + \hat{y}y \tag{4.2b}$$

$$r' = \hat{x}x' + \hat{y}y' + \hat{z}z' \tag{4.2c}$$

$$\rho' = \hat{x}x' + \hat{y}y'. \tag{4.2d}$$

The electric current density J can also be expanded into a series of Floquet modes as follows:

$$J(r) = \hat{x} \frac{\delta(z)}{A} \sum_{m,n} e^{-j\beta_{mn} \cdot (\rho - \rho')} \tag{4.3}$$

The surface current density is

$$J_s(\rho) = \int_{-\infty}^{\infty} J(r) \, dz = \hat{x} \frac{1}{A} \sum_{m,n} e^{-j\beta_{mn} \cdot (\rho - \rho')} \tag{4.4}$$

The region i magnetic vector potential $A^{(i)}$ satisfies the Helmholtz equation

$$(\nabla^2 + k_i^2) A^{(i)} = 0, \tag{4.5}$$

the radiation condition as $|z| \rightarrow \infty$, and the following interface conditions at $z = 0$ obtained from the fundamental boundary conditions on E and H:

$$A_x^{(1)} = A_x^{(2)}, \tag{4.6a}$$

$$\frac{1}{\mu_1} A_z^{(1)} = \frac{1}{\mu_2} A_z^{(2)}, \tag{4.6b}$$

$$\frac{1}{\mu_1} \frac{\partial A_x^{(1)}}{\partial z} - \frac{1}{\mu_2} \frac{\partial A_x^{(2)}}{\partial z} = \hat{x} \cdot J_s, \tag{4.6c}$$

$$\frac{1}{k_1^2} \left(\frac{\partial A_x^{(1)}}{\partial x} + \frac{\partial A_z^{(1)}}{\partial z} \right) = \frac{1}{k_2^2} \left(\frac{\partial A_x^{(2)}}{\partial x} + \frac{\partial A_z^{(2)}}{\partial z} \right). \tag{4.6d}$$

It is well known that the interface conditions require two components of $\boldsymbol{A}$. We follow the standard procedure and choose $\boldsymbol{A}^{(i)} = \hat{\boldsymbol{x}}A_x^{(i)} + \hat{\boldsymbol{z}}A_z^{(i)}$. Writing $\boldsymbol{A}$ as a series of Floquet modes we have

$$\boldsymbol{A}^{(i)} = \sum_{m,n} \left(\hat{\boldsymbol{x}}A_{mn}^{(i)} + \hat{\boldsymbol{z}}B_{mn}^{(i)} \right) e^{-j\boldsymbol{\beta}_{mn}\cdot(\boldsymbol{\rho}-\boldsymbol{\rho}')-\gamma_{mn}^{(i)}|z|}, \tag{4.7}$$

where

$$\gamma_{mn}^{(i)} = \sqrt{\boldsymbol{\beta}_{mn}\cdot\boldsymbol{\beta}_{mn} - k_i^2}. \tag{4.8}$$

Because the modal expansions consist of a series of orthogonal functions, each term (mode) must independently obey the stated boundary conditions. To satisfy (4.6a), let $A_{mn}^{(1)} = A_{mn}^{(2)} \equiv a_{mn}$. To satisfy (4.6b), let $B_{mn}^{(i)} = \mu_i b_{mn}$. The series for $\boldsymbol{A}$ can then be written as

$$\boldsymbol{A}^{(i)} = \sum_{m,n} \left(\hat{\boldsymbol{x}}a_{mn} + \hat{\boldsymbol{z}}\mu_i b_{mn} \right) e^{-j\boldsymbol{\beta}_{mn}\cdot(\boldsymbol{\rho}-\boldsymbol{\rho}')-\gamma_{mn}^{(i)}|z|}. \tag{4.9}$$

From (4.6c) we obtain

$$\frac{1}{\mu_1}\gamma_{mn}^{(1)}a_{mn} + \frac{1}{\mu_2}\gamma_{mn}^{(2)}a_{mn} = \frac{1}{A}$$

so that

$$a_{mn} = \frac{\tilde{\mu}}{2A}\frac{\mu_1 + \mu_2}{\mu_1\gamma_{mn}^{(2)} + \mu_2\gamma_{mn}^{(1)}} \tag{4.10}$$

where

$$\tilde{\mu} = \frac{2\mu_1\mu_2}{\mu_1 + \mu_2}. \tag{4.11}$$

From (4.6d) we obtain

$$\frac{1}{\mu_1\epsilon_1}\left(-j\beta_{mnx}a_{mn} + \gamma_{mn}^{(1)}\mu_1 b_{mn} \right) = \frac{1}{\mu_2\epsilon_2}\left(-j\beta_{mnx}a_{mn} - \gamma_{mn}^{(2)}\mu_2 b_{mn} \right)$$

where $\beta_{mnx} = \hat{\boldsymbol{x}}\cdot\boldsymbol{\beta}_{mn}$. After some algebraic manipulations the expression for b_{mn} is obtained.

$$b_{mn} = \frac{\mu_1\epsilon_1 - \mu_2\epsilon_2}{A}\frac{-j\beta_{mnx}}{(\epsilon_1\gamma_{mn}^{(2)} + \epsilon_2\gamma_{mn}^{(1)})(\mu_1\gamma_{mn}^{(2)} + \mu_2\gamma_{mn}^{(1)})} \tag{4.12}$$

4.1.2 Scalar Electric Potential

Using the Lorentz gauge the electric scalar potential Φ is

$$\Phi^{(i)}(\boldsymbol{r}) = \frac{j}{\omega\mu_i\epsilon_i}\boldsymbol{\nabla}\cdot\boldsymbol{A}^{(i)}$$

$$= \frac{j}{\omega\mu_i\epsilon_i}\sum_{m,n}\left(-j\beta_{mnx}a_{mn} - \gamma_{mn}^{(i)}\,\mathrm{sgn}(z)\mu_i b_{mn} \right) e^{-j\boldsymbol{\beta}_{mn}\cdot(\boldsymbol{\rho}-\boldsymbol{\rho}')-\gamma_{mn}^{(i)}|z|} \tag{4.13}$$

To aid in simplifying this summand, let us define $F^{(i)} = -j\beta_x a - \gamma^{(i)} \operatorname{sgn}(z)\mu_i b$, where for simplicity we have temporarily omitted the subscript mn. Proceeding with the algebra:

$$
\begin{aligned}
F^{(i)} &= \frac{-j\beta_x}{A\mu_i \epsilon_i} \left[\frac{\mu_1 \mu_2}{\mu_1 \gamma^{(2)} + \mu_2 \gamma^{(1)}} - \frac{\gamma^{(i)} \operatorname{sgn}(z)\mu_i (\mu_1 \epsilon_1 - \mu_2 \epsilon_2)}{\left(\epsilon_1 \gamma^{(2)} + \epsilon_2 \gamma^{(1)}\right)\left(\mu_1 \gamma^{(2)} + \mu_2 \gamma^{(1)}\right)} \right] \\
&= -j\beta_x \frac{\mu_1 \mu_2 \epsilon_1 \gamma^{(2)} + \mu_1 \mu_2 \epsilon_2 \gamma^{(1)} - \gamma^{(i)} \operatorname{sgn}(z)\mu_i (\mu_1 \epsilon_1 - \mu_2 \epsilon_2)}{A\mu_i \epsilon_i \left(\epsilon_1 \gamma^{(2)} + \epsilon_2 \gamma^{(1)}\right)\left(\mu_1 \gamma^{(2)} + \mu_2 \gamma^{(1)}\right)}
\end{aligned} \tag{4.14}
$$

Evaluated in Region 2 $(z > 0)$ this expression becomes

$$
\begin{aligned}
F^{(2)} &= -j\beta_x \frac{\mu_1 \mu_2 \epsilon_1 \gamma^{(2)} + \mu_1 \mu_2 \epsilon_2 \gamma^{(1)} - \gamma^{(2)} \mu_2 (\mu_1 \epsilon_1 - \mu_2 \epsilon_2)}{A\mu_2 \epsilon_2 \left(\epsilon_1 \gamma^{(2)} + \epsilon_2 \gamma^{(1)}\right)\left(\mu_1 \gamma^{(2)} + \mu_2 \gamma^{(1)}\right)} \\
&= -j\beta_x \frac{\mu_1 \epsilon_1 \gamma^{(2)} + \mu_1 \epsilon_2 \gamma^{(1)} - \gamma^{(2)} (\mu_1 \epsilon_1 - \mu_2 \epsilon_2)}{A\epsilon_2 \left(\epsilon_1 \gamma^{(2)} + \epsilon_2 \gamma^{(1)}\right)\left(\mu_1 \gamma^{(2)} + \mu_2 \gamma^{(1)}\right)} \\
&= -j\beta_x \frac{\mu_1 \gamma^{(1)} + \mu_2 \gamma^{(2)}}{A\left(\epsilon_1 \gamma^{(2)} + \epsilon_2 \gamma^{(1)}\right)\left(\mu_1 \gamma^{(2)} + \mu_2 \gamma^{(1)}\right)}
\end{aligned} \tag{4.15}
$$

A similar derivation for Region 1 yields

$$
\begin{aligned}
F^{(1)} &= -j\beta_x \frac{\mu_2 \epsilon_1 \gamma^{(2)} + \mu_2 \epsilon_2 \gamma^{(1)} + \gamma^{(1)} (\mu_1 \epsilon_1 - \mu_2 \epsilon_2)}{A\epsilon_1 \left(\epsilon_1 \gamma^{(2)} + \epsilon_2 \gamma^{(1)}\right)\left(\mu_1 \gamma^{(2)} + \mu_2 \gamma^{(1)}\right)} \\
&= -j\beta_x \frac{\mu_1 \gamma^{(1)} + \mu_2 \gamma^{(2)}}{A\left(\epsilon_1 \gamma^{(2)} + \epsilon_2 \gamma^{(1)}\right)\left(\mu_1 \gamma^{(2)} + \mu_2 \gamma^{(1)}\right)} \\
&= F^{(2)}.
\end{aligned} \tag{4.16}
$$

The expression for Φ is therefore

$$
\Phi^{(i)}(\boldsymbol{r}) = \frac{j}{\omega A} \sum_{m,n} -j\beta_{mnx} \frac{(\mu_1 \gamma_{mn}^{(1)} + \mu_2 \gamma_{mn}^{(2)}) e^{-j\boldsymbol{\beta}_{mn} \cdot (\boldsymbol{\rho} - \boldsymbol{\rho}') - \gamma_{mn}^{(i)} |z|}}{(\epsilon_1 \gamma_{mn}^{(2)} + \epsilon_2 \gamma_{mn}^{(1)})(\mu_1 \gamma_{mn}^{(2)} + \mu_2 \gamma_{mn}^{(1)})} \tag{4.17}
$$

From the equation of continuity we find that the electric charge density q_e that gives rise to Φ is

$$
q_e = \frac{j}{\omega} \boldsymbol{\nabla} \cdot \boldsymbol{J} = \frac{j}{\omega} \boldsymbol{\nabla} \cdot [\hat{\boldsymbol{x}}\delta(x - x')\delta(y - y')\delta(z)] = \frac{j}{\omega} \delta'(x - x')\delta(y - y')\delta(z) \tag{4.18}
$$

To determine an expression for the Green's function G^Φ for the electric scalar potential, note that

$$
\Phi(\boldsymbol{r}) = \iiint G^\Phi(\boldsymbol{r} - \boldsymbol{r}_0) q_e(\boldsymbol{r}_0) \, \mathrm{d}V_0 = \frac{-j}{\omega} \frac{\partial G^\Phi(\boldsymbol{r} - \boldsymbol{\rho}')}{\partial x'} = \frac{j}{\omega} \frac{\partial G^\Phi(\boldsymbol{r} - \boldsymbol{\rho}')}{\partial x} \tag{4.19}
$$

so that

$$
\frac{\partial G^\Phi}{\partial x} = \frac{\omega}{j} \Phi. \tag{4.20}
$$

Comparing (4.17) and (4.20) we conclude that the expression for the Green's function is

$$G^{\Phi}(\boldsymbol{r} - \boldsymbol{\rho}') = \frac{1}{2\bar{\epsilon}A} \sum_{m,n} \frac{(\epsilon_1 + \epsilon_2)(\mu_1\gamma_{mn}^{(1)} + \mu_2\gamma_{mn}^{(2)})}{(\epsilon_1\gamma_{mn}^{(2)} + \epsilon_2\gamma_{mn}^{(1)})(\mu_1\gamma_{mn}^{(2)} + \mu_2\gamma_{mn}^{(1)})} e^{-j\boldsymbol{\beta}_{mn}\cdot(\boldsymbol{\rho}-\boldsymbol{\rho}')-\gamma_{mn}^{(i)}|z|} \tag{4.21}$$

where $\bar{\epsilon} = \dfrac{\epsilon_1 + \epsilon_2}{2}$.

4.1.3 Summary of Source Plane Potentials

For convenience we list here the four potential Green's functions that will be required for the moment method analysis. Those for the electric vector potential $\boldsymbol{F}$ and magnetic scalar potential Ψ are obtained from those of $\boldsymbol{A}$ and Φ, respectively, via duality.

$$G_{xx}^{A}(\boldsymbol{\rho} - \boldsymbol{\rho}') = \frac{\tilde{\mu}}{2A} \sum_{m,n} \frac{\mu_1 + \mu_2}{\mu_1\gamma_{mn}^{(2)} + \mu_2\gamma_{mn}^{(1)}} e^{-j\boldsymbol{\beta}_{mn}\cdot(\boldsymbol{\rho}-\boldsymbol{\rho}')} \tag{4.22a}$$

$$G^{\Phi}(\boldsymbol{\rho} - \boldsymbol{\rho}') = \frac{1}{2\bar{\epsilon}A} \sum_{m,n} \frac{(\epsilon_1 + \epsilon_2)(\mu_1\gamma_{mn}^{(1)} + \mu_2\gamma_{mn}^{(2)})}{(\epsilon_1\gamma_{mn}^{(2)} + \epsilon_2\gamma_{mn}^{(1)})(\mu_1\gamma_{mn}^{(2)} + \mu_2\gamma_{mn}^{(1)})} e^{-j\boldsymbol{\beta}_{mn}\cdot(\boldsymbol{\rho}-\boldsymbol{\rho}')} \tag{4.22b}$$

$$G_{xx}^{F}(\boldsymbol{\rho} - \boldsymbol{\rho}') = -\frac{\tilde{\epsilon}}{2A} \sum_{m,n} \frac{\epsilon_1 + \epsilon_2}{\epsilon_1\gamma_{mn}^{(2)} + \epsilon_2\gamma_{mn}^{(1)}} e^{-j\boldsymbol{\beta}_{mn}\cdot(\boldsymbol{\rho}-\boldsymbol{\rho}')} \tag{4.22c}$$

$$G^{\Psi}(\boldsymbol{\rho} - \boldsymbol{\rho}') = \frac{1}{2\bar{\mu}A} \sum_{m,n} \frac{(\mu_1 + \mu_2)(\epsilon_1\gamma_{mn}^{(1)} + \epsilon_2\gamma_{mn}^{(2)})}{(\mu_1\gamma_{mn}^{(2)} + \mu_2\gamma_{mn}^{(1)})(\epsilon_1\gamma_{mn}^{(2)} + \epsilon_2\gamma_{mn}^{(1)})} e^{-j\boldsymbol{\beta}_{mn}\cdot(\boldsymbol{\rho}-\boldsymbol{\rho}')} \tag{4.22d}$$

where

$$\tilde{\mu} = \frac{2\mu_1\mu_2}{\mu_1 + \mu_2}, \quad \bar{\epsilon} = \frac{\epsilon_1 + \epsilon_2}{2}, \quad \tilde{\epsilon} = \frac{2\epsilon_1\epsilon_2}{\epsilon_1 + \epsilon_2}, \quad \bar{\mu} = \frac{\mu_1 + \mu_2}{2}. \tag{4.23}$$

It should be noted that these series represent only a formal solution of Maxwell's equations. They are at best only conditionally convergent and are completely unsuitable for direct numerical evaluation. In fact, it is easy to see that these series can not be absolutely convergent, for as $\boldsymbol{\rho} \to \boldsymbol{\rho}'$ the Green's functions increase in magnitude without bound, a singularity that is proportional to $1/\|\boldsymbol{\rho} - \boldsymbol{\rho}'\|$. It is desirable to extract this singularity as an explicit term, so that it can be integrated in closed form, as in [9]. The next section describes the technique used to perform this extraction and accelerate the series for efficient evaluation.

4.2 Series Acceleration

We now manipulate the series in Equations (4.22) to arrive at an efficient, wide-band formulation. In the process, the Green's functions will be expressed as the sum of several absolutely, uniformly convergent series. Our strategy is to find the first few terms of an asymptotic expansion of the summands in a suitably chosen variable. Applying a Kummer's transformation, these terms are

subtracted from the original summand, leaving a spectral sum with greatly accelerated convergence. The sum of the asymptotic terms is then accelerated by means of the Poisson transformation (which converts it to a spatial sum) after which it is recombined with the spectral sum. A careful choice of the expansion variable ensures that all sums are rapidly convergent and provides the wide-band capability described below.

4.2.1   Kummer's Transformation

Let u be an appropriately chosen positive *smoothing factor*; define

$$\kappa_{mn} = \sqrt{\boldsymbol{\beta}_{mn} \cdot \boldsymbol{\beta}_{mn} + u^2} \tag{4.24}$$

and

$$w_i \equiv w(\mu_i, \epsilon_i) = \sqrt{\omega^2 \mu_i \epsilon_i + u^2} = \sqrt{k_i^2 + u^2}, \quad i = 1, 2 \tag{4.25}$$

so that

$$\gamma_{mn}^{(i)} \equiv \gamma_{mn}(\mu_i, \epsilon_i) = \sqrt{\kappa_{mn}^2 - u^2 - \omega^2 \mu_i \epsilon_i} = \kappa_{mn}\sqrt{1 - \left(\frac{w_i}{\kappa_{mn}}\right)^2} \tag{4.26}$$

The original summands in (4.22) will be expanded in series of reciprocal powers of κ_{mn}. The smoothing factor u should be chosen large enough to ensure that the spatial series of asymptotic terms converges rapidly, yet small enough so that after only a few terms, the differences between the original summands of (4.22) and their asymptotic expansions are negligible.

Consider first the summand for magnetic vector potential given in (4.22a):

$$A_{mn}(\mu_1, \epsilon_1, \mu_2, \epsilon_2) \equiv \frac{\mu_1 + \mu_2}{\mu_1 \gamma_{mn}(\mu_2, \epsilon_2) + \mu_2 \gamma_{mn}(\mu_1, \epsilon_1)} = \frac{\mu_1 + \mu_2}{\mu_1 \gamma_{mn}^{(2)} + \mu_2 \gamma_{mn}^{(1)}}$$

$$= \frac{1}{\kappa_{mn}} \frac{\mu_1 + \mu_2}{\mu_1 \sqrt{1 - w_2^2/\kappa_{mn}^2} + \mu_2 \sqrt{1 - w_1^2/\kappa_{mn}^2}} \tag{4.27}$$

An asymptotic expansion of the summand A_{mn} for large κ_{mn} can be found by determining the first few coefficients in the MacLaurin series of the function

$$f(x) = x \frac{\mu_1 + \mu_2}{\mu_1 \sqrt{1 - w_2^2 x^2} + \mu_2 \sqrt{1 - w_1^2 x^2}}. \tag{4.28}$$

This task was accomplished with the aid of a computer algebra system with the result

$$A_{mn} = \frac{c_1}{\kappa_{mn}} + \frac{c_3}{\kappa_{mn}^3} + O(\kappa_{mn}^{-5}), \tag{4.29}$$

where

$$c_1 = 1, \quad c_3(\mu_1, \epsilon_1, \mu_2, \epsilon_2) = \frac{\mu_1 w^2(\mu_2, \epsilon_2) + \mu_2 w^2(\mu_1, \epsilon_1)}{2(\mu_1 + \mu_2)} = \frac{\mu_1 w_2^2 + \mu_2 w_1^2}{2(\mu_1 + \mu_2)}. \tag{4.30}$$

Now consider the summand for the electric scalar potential Green's function, Equation (4.22b).

$$
\begin{aligned}
\Phi_{mn} &\equiv \frac{(\epsilon_1 + \epsilon_2)(\mu_1 \gamma_{mn}^{(1)} + \mu_2 \gamma_{mn}^{(2)})}{(\epsilon_1 \gamma_{mn}^{(2)} + \epsilon_2 \gamma_{mn}^{(1)})(\mu_1 \gamma_{mn}^{(2)} + \mu_2 \gamma_{mn}^{(1)})} \\[2mm]
&= \frac{1}{\kappa_{mn}} \frac{(\epsilon_1 + \epsilon_2)\left(\mu_1 \sqrt{1 - \frac{w_1^2}{\kappa_{mn}^2}} + \mu_2 \sqrt{1 - \frac{w_2^2}{\kappa_{mn}^2}}\right)}{\left(\epsilon_1 \sqrt{1 - \frac{w_2^2}{\kappa_{mn}^2}} + \epsilon_2 \sqrt{1 - \frac{w_1^2}{\kappa_{mn}^2}}\right)\left(\mu_1 \sqrt{1 - \frac{w_2^2}{\kappa_{mn}^2}} + \mu_2 \sqrt{1 - \frac{w_1^2}{\kappa_{mn}^2}}\right)}
\end{aligned} \tag{4.31}
$$

A MacLaurin expansion of this summand in the variable $1/\kappa_{mn}$ yields the result

$$\Phi_{mn} = \frac{d_1}{\kappa_{mn}} + \frac{d_3}{\kappa_{mn}^3} + O(\kappa_{mn}^{-5}), \tag{4.32}$$

where

$$d_1 = 1, \tag{4.33a}$$

$$d_3(\mu_1, \epsilon_1, \mu_2, \epsilon_2) = \frac{\mu_1[w_2^2(2\epsilon_1 + \epsilon_2) - w_1^2 \epsilon_1] + \mu_2[w_1^2(\epsilon_1 + 2\epsilon_2) - w_2^2 \epsilon_2]}{2(\mu_1 + \mu_2)(\epsilon_1 + \epsilon_2)}. \tag{4.33b}$$

The potential Green's functions can now be written as (note that we are showing the explicit dependence of the Green's functions on the material parameters of Regions 1 and 2):

$$G_{xx}^A(\boldsymbol{\rho} - \boldsymbol{\rho}'; \mu_1, \epsilon_1, \mu_2, \epsilon_2) = \tilde{\mu}\left\{\Sigma_{M1}(\mu_1, \epsilon_1, \mu_2, \epsilon_2) + \frac{u}{4\pi}\left[\Sigma_{S1} + \frac{c_3(\mu_1, \epsilon_1, \mu_2, \epsilon_2)}{u^2}\Sigma_{S2}\right]\right\} \tag{4.34a}$$

$$G^\Phi(\boldsymbol{\rho} - \boldsymbol{\rho}'; \mu_1, \epsilon_1, \mu_2, \epsilon_2) = \frac{1}{\tilde{\epsilon}}\left\{\Sigma_{M2}(\mu_1, \epsilon_1, \mu_2, \epsilon_2) + \frac{u}{4\pi}\left[\Sigma_{S1} + \frac{d_3(\mu_1, \epsilon_1, \mu_2, \epsilon_2)}{u^2}\Sigma_{S2}\right]\right\} \tag{4.34b}$$

$$G_{xx}^F(\boldsymbol{\rho} - \boldsymbol{\rho}'; \mu_1, \epsilon_1, \mu_2, \epsilon_2) = -\tilde{\epsilon}\left\{\Sigma_{M1}(\epsilon_1, \mu_1, \epsilon_2, \mu_2) + \frac{u}{4\pi}\left[\Sigma_{S1} + \frac{c_3(\epsilon_1, \mu_1, \epsilon_2, \mu_2)}{u^2}\Sigma_{S2}\right]\right\} \tag{4.34c}$$

$$G^\Psi(\boldsymbol{\rho} - \boldsymbol{\rho}'; \mu_1, \epsilon_1, \mu_2, \epsilon_2) = \frac{1}{\tilde{\mu}}\left\{\Sigma_{M2}(\epsilon_1, \mu_1, \epsilon_2, \mu_2) + \frac{u}{4\pi}\left[\Sigma_{S1} + \frac{d_3(\epsilon_1, \mu_1, \epsilon_2, \mu_2)}{u^2}\Sigma_{S2}\right]\right\} \tag{4.34d}$$

where

$$\Sigma_{M1}(x_1, y_1, x_2, y_2) = \frac{1}{2A}\sum_{m,n}$$

$$\left[\frac{x_1 + x_2}{x_1 \gamma_{mn}(x_2, y_2) + x_2 \gamma_{mn}(x_1, y_1)} - \frac{1}{\kappa_{mn}} - \frac{c_3(x_1, y_1, x_2, y_2)}{\kappa_{mn}^3}\right] e^{-j\boldsymbol{\beta}_{mn}\cdot(\boldsymbol{\rho}-\boldsymbol{\rho}')} \tag{4.35}$$

$$\Sigma_{M2}(x_1, y_1, x_2, y_2) = \frac{1}{2A} \sum_{m,n}$$

$$\left[\frac{(y_1 + y_2)(x_1 \gamma_{mn}(x_1, y_1) + x_2 \gamma_{mn}(x_2, y_2))}{(y_1 \gamma_{mn}(x_2, y_2) + y_2 \gamma_{mn}(x_1, y_1))(x_1 \gamma_{mn}(x_2, y_2) + x_2 \gamma_{mn}(x_1, y_1))} \right.$$

$$\left. - \frac{1}{\kappa_{mn}} - \frac{d_3(x_1, x_2, y_1, y_2)}{\kappa_{mn}^3} \right] e^{-j\boldsymbol{\beta}_{mn} \cdot (\boldsymbol{\rho} - \boldsymbol{\rho}')} \quad (4.36)$$

$$\Sigma_{S1}(x_1, y_1, x_2, y_2) = \frac{2\pi}{uA} \sum_{m,n} \frac{1}{\kappa_{mn}} e^{-j\boldsymbol{\beta}_{mn} \cdot (\boldsymbol{\rho} - \boldsymbol{\rho}')} \quad (4.37)$$

$$\Sigma_{S2}(x_1, y_1, x_2, y_2) = \frac{2\pi u}{A} \sum_{m,n} \frac{1}{\kappa_{mn}^3} e^{-j\boldsymbol{\beta}_{mn} \cdot (\boldsymbol{\rho} - \boldsymbol{\rho}')}. \quad (4.38)$$

The modal series Σ_{M1} and Σ_{M2} are in a form suitable for direct numerical evaluation. They are absolutely convergent since their summands decay as $(\gamma_{mn}^{(i)})^{-5}$. Considered as a function of $\boldsymbol{\rho} - \boldsymbol{\rho}'$, they are uniformly convergent and extremely smooth, since all of their singularities have been subtracted off. This suggests that an efficient method of evaluation is to tabulate the series on a grid of points in the unit cell using the fast Fourier transform (FFT). Then, a low-order bivariate interpolation scheme can be used to evaluate the functions at arbitrary points in the unit cell. More will said on this topic later, in Section 5.4.

The (soon to be) spatial sums Σ_{S1} and Σ_{S2} are still slowly convergent, especially Σ_{S1} which is at best only conditionally convergent. However, they are in a form suitable for application of the Poisson summation formula, as discussed in the next section.

4.2.2 Application of the Poisson Transformation

We now wish to accelerate the convergence of the double sums

$$S_l = \frac{1}{2A} \sum_{m,n} \frac{e^{-j\left[\left(\frac{\psi_1}{2\pi}+m\right)\boldsymbol{\beta}_1 + \left(\frac{\psi_2}{2\pi}+n\right)\boldsymbol{\beta}_2\right] \cdot (\boldsymbol{\rho} - \boldsymbol{\rho}')}}{\kappa_{mn}^l} \quad (4.39)$$

for $l = 1$ and 3. For m and n defined as *real* variables, let

$$f_l(m, n) = \frac{e^{-j\left[\left(\frac{\psi_1}{2\pi}+m\right)\boldsymbol{\beta}_1 + \left(\frac{\psi_2}{2\pi}+n\right)\boldsymbol{\beta}_2\right] \cdot (\boldsymbol{\rho} - \boldsymbol{\rho}')}}{2A\left[\left\|\left(\frac{\psi_1}{2\pi} + m\right)\boldsymbol{\beta}_1 + \left(\frac{\psi_2}{2\pi} + n\right)\boldsymbol{\beta}_2\right\|^2 + u^2\right]^{l/2}}. \quad (4.40)$$

Then by the Poisson summation formula [10, p. 139], [11]

$$S_l = \sum_{m,n} f_l(m, n) = \sum_{m,n} F_l(2\pi m, 2\pi n) \quad (4.41)$$

where

$$F_l(\zeta,\eta) = \int_{-\infty}^{\infty} \int_{-\infty}^{\infty} f_l(m,n) e^{j(\zeta m + \eta n)} \, \mathrm{d}m \, \mathrm{d}n. \tag{4.42}$$

Let

$$\mu = \frac{\psi_1}{2\pi} + m \quad \text{and} \quad \nu = \frac{\psi_2}{2\pi} + n, \tag{4.43}$$

so

$$F_l(\zeta,\eta) = \frac{e^{-j\left(\frac{\psi_1}{2\pi}\zeta + \frac{\psi_2}{2\pi}\eta\right)}}{2A} \int_{-\infty}^{\infty} \int_{-\infty}^{\infty} \frac{e^{-j(\mu\boldsymbol{\beta}_1 + \nu\boldsymbol{\beta}_2)\cdot(\boldsymbol{\rho}-\boldsymbol{\rho}')} e^{j(\mu\zeta + \nu\eta)}}{(\|\mu\boldsymbol{\beta}_1 + \nu\boldsymbol{\beta}_2\|^2 + u^2)^{l/2}} \, \mathrm{d}\mu \, \mathrm{d}\nu \tag{4.44}$$

In order to proceed we now introduce the change of variables

$$\mu\boldsymbol{\beta}_1 + \nu\boldsymbol{\beta}_2 = \hat{\boldsymbol{x}} k_x + \hat{\boldsymbol{y}} k_y = \boldsymbol{k}. \tag{4.45}$$

The differential elements of area in the k_x-k_y and μ-ν planes are related as follows:

$$\mathrm{d}k_x \, \mathrm{d}k_y = \mathrm{d}\mu \, \mathrm{d}\nu \, \|\boldsymbol{\beta}_1 \times \boldsymbol{\beta}_2\| = \mathrm{d}\mu \, \mathrm{d}\nu \frac{4\pi^2}{\|\boldsymbol{s}_1 \times \boldsymbol{s}_2\|} = \mathrm{d}\mu \, \mathrm{d}\nu \frac{4\pi^2}{A}. \tag{4.46}$$

Recalling the properties of the direct and reciprocal lattice vectors

$$\boldsymbol{\beta}_1 \cdot \boldsymbol{s}_1 = 2\pi, \quad \boldsymbol{\beta}_1 \cdot \boldsymbol{s}_2 = 0 \tag{4.47a}$$

$$\boldsymbol{\beta}_2 \cdot \boldsymbol{s}_2 = 2\pi, \quad \boldsymbol{\beta}_2 \cdot \boldsymbol{s}_1 = 0 \tag{4.47b}$$

we see that

$$\mu = \boldsymbol{k} \cdot \boldsymbol{s}_1/(2\pi), \quad \nu = \boldsymbol{k} \cdot \boldsymbol{s}_2/(2\pi),$$

so that Equation (4.44) can be written as

$$F_l(\zeta,\eta) = \frac{e^{-j\left(\frac{\psi_1}{2\pi}\zeta + \frac{\psi_2}{2\pi}\eta\right)}}{4\pi} B_l\left(\boldsymbol{\rho} - \boldsymbol{\rho}' - \frac{\zeta \boldsymbol{s}_1 + \eta \boldsymbol{s}_2}{2\pi}\right) \tag{4.48}$$

where

$$B_l(\boldsymbol{\rho}) \equiv \frac{1}{2\pi} \int_{-\infty}^{\infty} \int_{-\infty}^{\infty} \frac{e^{-j\boldsymbol{k}\cdot\boldsymbol{\rho}}}{(\|\boldsymbol{k}\|^2 + u^2)^{l/2}} \, \mathrm{d}k_x \, \mathrm{d}k_y \tag{4.49}$$

The form of the integrand in (4.49) immediately suggests a transformation to polar coordinates:

$$k_x = k_\rho \cos\theta, \quad k_y = k_\rho \sin\theta$$
$$x = \rho \cos\phi, \quad y = \rho \sin\phi$$

yielding

$$
\begin{aligned}
B_l(\boldsymbol{\rho}) &= \frac{1}{2\pi} \int_0^{\infty} \int_0^{2\pi} \frac{e^{-jk_\rho\rho\cos(\theta-\phi)}}{(k_\rho^2 + u^2)^{l/2}} k_\rho \, \mathrm{d}\theta \, \mathrm{d}k_\rho \\
&= \int_0^{\infty} \frac{J_0(k_\rho\rho)}{(k_\rho^2 + u^2)^{l/2}} k_\rho \, \mathrm{d}k_\rho,
\end{aligned}
\tag{4.50}
$$

which is recognized as a Hankel (Fourier-Bessel) transform that depends only on $\rho = \|\boldsymbol{\rho}\|$. The case $l = 1$ is given in [12, Eqn. (5.15.5)]:

$$B_1(\boldsymbol{\rho}) = \int_0^{\infty} \frac{J_0(k_\rho \rho)}{(k_\rho^2 + u^2)^{1/2}} \, k_\rho \, \mathrm{d}k_\rho = \frac{e^{-u\rho}}{\rho}. \tag{4.51}$$

B_3 is easily evaluated by noting that

$$\frac{\partial B_1(\boldsymbol{\rho})}{\partial u} = -e^{-u\rho}$$

$$= \frac{\partial}{\partial u} \int_0^{\infty} \frac{J_0(k_\rho \rho)}{(k_\rho^2 + u^2)^{1/2}} \, k_\rho \, \mathrm{d}k_\rho$$

$$= -u \int_0^{\infty} \frac{J_0(k_\rho \rho)}{(k_\rho^2 + u^2)^{3/2}} \, k_\rho \, \mathrm{d}k_\rho$$

$$= -u B_3(\boldsymbol{\rho}) \tag{4.52}$$

so that

$$B_3(\boldsymbol{\rho}) = \frac{1}{u} e^{-u\rho}. \tag{4.53}$$

We then have

$$F_l(2\pi m, 2\pi n) = \frac{1}{4\pi} e^{-j(m\psi_1 + n\psi_2)} B_l(\boldsymbol{\rho}_{mn}) \tag{4.54}$$

where

$$\boldsymbol{\rho}_{mn} = \boldsymbol{\rho} - \boldsymbol{\rho}' - m\boldsymbol{s}_1 - n\boldsymbol{s}_2 \tag{4.55}$$

is the vector from the (m, n)th translational image of the source point to the observation point. The spatial series are thus given explicitly by the formulas:

$$\Sigma_{S1} = \sum_{m,n} \frac{e^{-u\rho_{mn}}}{u\rho_{mn}} e^{-j(m\psi_1 + n\psi_2)} \tag{4.56a}$$

$$\Sigma_{S2} = \sum_{m,n} e^{-u\rho_{mn}} e^{-j(m\psi_1 + n\psi_2)}. \tag{4.56b}$$

Let us take note of the following facts regarding these series:

- The free-space singularity is explicitly recovered in the $m = n = 0$ term of the first series in Σ_{S1} and Σ_{S2}.

- The summands exhibit exponential decay with ρ_{mn}. An astute choice of u will assure convergence using only a few rings in the summation lattice.

- These series consist of frequency-independent terms, which are then multiplied by the frequency-dependent constants c_3 and d_3 before being combined. Therefore, it is possible to compute the contribution of the frequency-independent sums to the interaction matrix

that occurs in the moment method procedure once, prior to sweeping the analysis frequency. These contributions can be weighted appropriately and combined at each desired analysis frequency, avoiding redundant calculations and saving large amounts of execution time. In this sense the formulation of the periodic Green's functions can be said to be "wide-band." If this approach is pursued, it makes sense to choose u relatively small, so that the convergence of the modal series is enhanced, since these will have to be evaluated at each frequency while the spatial series will be evaluated only once.

Chapter 5

Green's Functions for Multiply Stratified Medium

In the previous chapter, a method was derived to efficiently evaluate the potential Green's functions for a geometry consisting of the abutment of two half-spaces under quasi-periodic boundary conditions. This chapter extends the results to handle an arbitrary number of dielectric slabs.

The structure for which the potential Green's functions are desired consists of N layers, as shown in Figure 5.1. The structure is laterally invariant, with each dielectric layer being homogeneous and
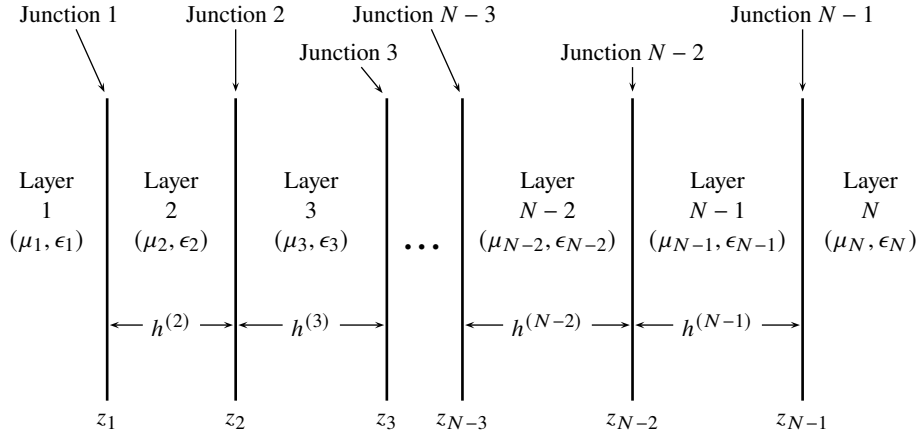
Figure 5.1: The structure under consideration is a stack of $N \geq 2$ dielectric layers. Layers 1 and N are semi-infinite in extent. For $2 \leq i \leq N - 1$, layer i lies in the region $z_{i-1} < z < z_i$, is of thickness $h^{(i)} = z_i - z_{i-1}$, and is characterized by permeability μ_i and permittivity ϵ_i.

isotropic. Each layer $i = 1, 2, \ldots, N$ is characterized by a complex permittivity ϵ_i and permeability μ_i, each of which lies either in the fourth quadrant of the complex plane, or on the real axis. The medium intrinsic wavenumbers are $k_i = \omega\sqrt{\mu_i\epsilon_i}$.

We will conntinue the use of the shorthand notation $\sum\limits_{m,n}$ to denote the double sum $\sum\limits_{m=-\infty}^{\infty}\sum\limits_{n=-\infty}^{\infty}$.

As in the Chapter 4 we are interested in determining the potential Green's functions $G_{xx}^{A}(\boldsymbol{\rho}-\boldsymbol{\rho}',z,z')$, $G_{xx}^{F}(\boldsymbol{\rho}-\boldsymbol{\rho}',z,z')$, $G^{\Phi}(\boldsymbol{\rho}-\boldsymbol{\rho}',z,z')$, and $G^{\Psi}(\boldsymbol{\rho}-\boldsymbol{\rho}',z,z')$ evaluated for both observation point z and source point z' located at one of the interface planes: $z=z'=z_s$, $s=1,2,\ldots,N-1$. To accomplish this task we will make use of the transmission line Green's function (TLGF) formalism of [13]. Therefore, we must first determine the relationship between the quasi-periodic Green's functions and those discussed in [13]. We investigate this relationship in the next section.

5.1   The Discrete Spectrum of Quasi-Periodic Functions

Let us suppose that we are given the complex-valued function $f:\mathbb{R}^2\to\mathbb{C}$ and its two-dimensional Fourier transform $\tilde{f}:\mathbb{R}^2\to\mathbb{C}$. They are obtained from each other by the transform relations

$$\tilde{f}(\boldsymbol{k})=\iint_{\mathbb{R}^2}f(\boldsymbol{\rho})e^{j\boldsymbol{k}\cdot\boldsymbol{\rho}}\,\mathrm{d}x\,\mathrm{d}y,\quad f(\boldsymbol{\rho})=\frac{1}{4\pi^2}\iint_{\mathbb{R}^2}\tilde{f}(\boldsymbol{k})e^{-j\boldsymbol{k}\cdot\boldsymbol{\rho}}\,\mathrm{d}k_x\,\mathrm{d}k_y,\tag{5.1}$$

where $\boldsymbol{\rho}=\hat{\boldsymbol{x}}x+\hat{\boldsymbol{y}}y$ and $\boldsymbol{k}=\hat{\boldsymbol{x}}k_x+\hat{\boldsymbol{y}}k_y$. We now define a quasi-periodic[1] function f_p as

$$f_p(\boldsymbol{\rho})=\sum_{m,n}f(\boldsymbol{\rho}-m\boldsymbol{s}_1-n\boldsymbol{s}_2)e^{-j(m\psi_1+n\psi_2)}\tag{5.2}$$

with Fourier transform $\tilde{f}_p$. We are interested in determining the relationship between $\tilde{f}_p$ and $\tilde{f}$.

Applying the transform integral to f_p and interchanging the order of summation and integration we obtain

$$\tilde{f}_p(\boldsymbol{k})=\sum_{m,n}\iint_{\mathbb{R}^2}f(\boldsymbol{\rho}-m\boldsymbol{s}_1-n\boldsymbol{s}_2)e^{-j(m\psi_1+n\psi_2)}e^{j\boldsymbol{k}\cdot\boldsymbol{\rho}}\,\mathrm{d}x\,\mathrm{d}y$$

$$=\sum_{m,n}e^{-j(m\psi_1+n\psi_2)}\iint_{\mathbb{R}^2}f(\boldsymbol{\rho})e^{j\boldsymbol{k}\cdot(\boldsymbol{\rho}+m\boldsymbol{s}_1+n\boldsymbol{s}_2)}\,\mathrm{d}x\,\mathrm{d}y$$

$$=\sum_{m,n}e^{-j(m\psi_1+n\psi_2)}e^{j\boldsymbol{k}\cdot(m\boldsymbol{s}_1+n\boldsymbol{s}_2)}\iint_{\mathbb{R}^2}f(\boldsymbol{\rho})e^{j\boldsymbol{k}\cdot\boldsymbol{\rho}}\,\mathrm{d}x\,\mathrm{d}y$$

$$=\tilde{f}(\boldsymbol{k})\sum_{m,n}e^{-j(m\psi_1+n\psi_2)}e^{j\boldsymbol{k}\cdot(m\boldsymbol{s}_1+n\boldsymbol{s}_2)}.\tag{5.3}$$

We now recall the reciprocal lattice vectors

$$\boldsymbol{\beta}_1=\frac{2\pi}{A}\boldsymbol{s}_2\times\hat{\boldsymbol{z}},\quad\boldsymbol{\beta}_2=\frac{2\pi}{A}\hat{\boldsymbol{z}}\times\boldsymbol{s}_1,\tag{5.4}$$

---

[1]"Quasi-periodic" because of the incremental phase shifts ψ_1 and ψ_2 applied to the otherwise periodic function.

where $A = \|\mathbf{s}_1 \times \mathbf{s}_2\|$ is the unit cell area, and make use of the property $\boldsymbol{\beta}_p \cdot \mathbf{s}_q = 2\pi\delta_{pq}$, $p, q \in \{1, 2\}$. We also introduce the change of variables $\mathbf{k} = \xi\boldsymbol{\beta}_1 + \eta\boldsymbol{\beta}_2 + \boldsymbol{\beta}_{00}$, where

$$\boldsymbol{\beta}_{00} = \boldsymbol{\beta}_1\frac{\psi_1}{2\pi} + \boldsymbol{\beta}_2\frac{\psi_2}{2\pi} \tag{5.5}$$

so that (5.3) becomes

$$
\begin{aligned}
\tilde{f}_p(\xi\boldsymbol{\beta}_1 + \eta\boldsymbol{\beta}_2 + \boldsymbol{\beta}_{00}) &= \tilde{f}(\xi\boldsymbol{\beta}_1 + \eta\boldsymbol{\beta}_2 + \boldsymbol{\beta}_{00}) \sum_{m,n} e^{-j(m\psi_1+n\psi_2)} e^{j(\xi\boldsymbol{\beta}_1+\eta\boldsymbol{\beta}_2+\boldsymbol{\beta}_{00})\cdot(m\mathbf{s}_1+n\mathbf{s}_2)} \\
&= \tilde{f}(\xi\boldsymbol{\beta}_1 + \eta\boldsymbol{\beta}_2 + \boldsymbol{\beta}_{00}) \sum_{m,n} e^{-j(m\psi_1+n\psi_2)} e^{j[m(2\pi\xi+\psi_1)+n(2\pi\eta+\psi_2)]} \\
&= \tilde{f}(\xi\boldsymbol{\beta}_1 + \eta\boldsymbol{\beta}_2 + \boldsymbol{\beta}_{00}) \sum_{m,n} e^{j2\pi(m\xi+n\eta)} \\
&= \tilde{f}(\xi\boldsymbol{\beta}_1 + \eta\boldsymbol{\beta}_2 + \boldsymbol{\beta}_{00}) \sum_{m,n} \delta(\xi - m)\,\delta(\eta - n) \\
&= \sum_{m,n} \tilde{f}(m\boldsymbol{\beta}_1 + n\boldsymbol{\beta}_2 + \boldsymbol{\beta}_{00})\delta(\xi - m)\,\delta(\eta - n) \\
&= \sum_{m,n} \tilde{f}(\boldsymbol{\beta}_{mn})\delta(\xi - m)\,\delta(\eta - n) \tag{5.6}
\end{aligned}
$$

where we have used the well-known Fourier series representation of a train of delta functions and defined $\boldsymbol{\beta}_{mn} = m\boldsymbol{\beta}_1 + n\boldsymbol{\beta}_2 + \boldsymbol{\beta}_{00}$.

The area element in the spectral domain is

$$\mathrm{d}k_x\,\mathrm{d}k_y = \mathrm{d}\xi\,\mathrm{d}\eta\,\|\boldsymbol{\beta}_1 \times \boldsymbol{\beta}_2\| = \frac{4\pi^2}{A}\,\mathrm{d}\xi\,\mathrm{d}\eta \tag{5.7}$$

and the inversion integral applied to (5.6) becomes

$$
\begin{aligned}
f_p(\boldsymbol{\rho}) &= \frac{1}{4\pi^2} \iint_{\mathbb{R}^2} \tilde{f}_p(\mathbf{k})e^{-j\mathbf{k}\cdot\boldsymbol{\rho}}\,\mathrm{d}k_x\,\mathrm{d}k_y \\
&= \frac{1}{A} \iint_{\mathbb{R}^2} \sum_{m,n} \tilde{f}(\boldsymbol{\beta}_{mn})\delta(\xi - m)\,\delta(\eta - n)e^{-j(\xi\boldsymbol{\beta}_1+\eta\boldsymbol{\beta}_2+\boldsymbol{\beta}_{00})\cdot\boldsymbol{\rho}}\,\mathrm{d}\xi\,\mathrm{d}\eta \\
&= \frac{1}{A} \sum_{m,n} \tilde{f}(\boldsymbol{\beta}_{mn})e^{-j\boldsymbol{\beta}_{mn}\cdot\boldsymbol{\rho}}. \tag{5.8}
\end{aligned}
$$

Equation (5.8) is the important, well-known result that the quasi-periodic function f_p can be recovered by sampling the spectrum of the corresponding "isolated" function f at locations determined by the reciprocal lattice and impressed phasing. It allows us to find the potential Green's functions for the quasi-periodic array of point sources in the multilayered structure from the spectral representations of the isolated-source Green's functions presented in [13].

5.2   Potential Green's Functions (Electric Sources)

5.2.1   Magnetic Vector Potential

According to [13] the Fourier transform of the magnetic vector potential Green's function (for an isolated source at $\boldsymbol{\rho}' = \mathbf{0}$) is

$$\tilde{G}_{xx}^{A}(\boldsymbol{k}, z, z') = \frac{1}{j\omega} V_{\mathrm{i}}^{\mathrm{TE}}(\boldsymbol{k}, z, z') \tag{5.9}$$

where we have multiplied their result by μ_0 to be consistent with our definition of the potential Green's function, and $V_{\mathrm{i}}^{\mathrm{TE}}(\boldsymbol{k}, z, z')$ is the TE transmission line Green's function (TLGF) for the voltage observed at z due to a unit current source at z', using an equivalent circuit appropriate for a plane wave whose dependence on the transverse spatial variables x and y is of the form $e^{-j\boldsymbol{k}\cdot\boldsymbol{\rho}}$. From Equation (5.8) we then find that

$$G_{xx}^{A}(\boldsymbol{\rho} - \boldsymbol{\rho}', z_s, z_s) = \frac{1}{j\omega A} \sum_{m,n} V_{\mathrm{i}}^{\mathrm{TE}}(\boldsymbol{\beta}_{mn}, z_s, z_s) e^{-j\boldsymbol{\beta}_{mn}\cdot(\boldsymbol{\rho}-\boldsymbol{\rho}')}. \tag{5.10}$$

5.2.2   Scalar Electric Potential

According to [13] the Fourier transform of the so-called "scalar potential kernel" (for an isolated point charge associated with a horizontal current source at $\boldsymbol{\rho}' = \mathbf{0}$) is

$$\tilde{K}^{\Phi}(\boldsymbol{k}, z, z') = \frac{-j\omega\epsilon_0}{\boldsymbol{k}\cdot\boldsymbol{k}} \left[V_{\mathrm{i}}^{\mathrm{TE}}(\boldsymbol{k}, z, z') - V_{\mathrm{i}}^{\mathrm{TM}}(\boldsymbol{k}, z, z') \right] \tag{5.11}$$

where $V_{\mathrm{i}}^{\mathrm{TM}}(\boldsymbol{k}, z, z')$ is the TM transmission line Green's function (TLGF) for the voltage observed at z due to a unit current source at z'. Dividing by ϵ_0 to be consistent with our definition of the potential Green's function and using Equation (5.8) we obtain

$$G^{\Phi}(\boldsymbol{\rho} - \boldsymbol{\rho}', z_s, z_s) = \frac{-j\omega}{A} \sum_{m,n} \frac{V_{\mathrm{i}}^{\mathrm{TE}}(\boldsymbol{\beta}_{mn}, z_s, z_s) - V_{\mathrm{i}}^{\mathrm{TM}}(\boldsymbol{\beta}_{mn}, z_s, z_s)}{\beta_{mn}^2} e^{-j\boldsymbol{\beta}_{mn}\cdot(\boldsymbol{\rho}-\boldsymbol{\rho}')}. \tag{5.12}$$

5.2.3   Evaluation of Transmission Line Green's Functions

Referring to Equations (5.10) and (5.12) we see that the problem is reduced to evaluating the TLGFs $V_{\mathrm{i}}^{\mathrm{TE}}$ and $V_{\mathrm{i}}^{\mathrm{TM}}$. The equivalent transmission line circuit needed to accomplish this task is shown in Figure 5.2. The equivalent circuit consists of a series of cascaded transmission lines, each characterized by its modal characteristic impedance $Z_{pmn}^{(i)}$ and complex attenuation constant $\gamma_{mn}^{(i)}$. The termination impedances at the ends of the structure are equal to the characteristic impedances of the respective semi-infinite lines, and the entire structure is excited by a unit current generator located at $z = z_s$. To calculate $V_{\mathrm{i}}^{\mathrm{TE}}$, the modal impedances of the TE Floquet modes are used in the equivalent circuit; for $V_{\mathrm{i}}^{\mathrm{TM}}$ we employ the TM modal impedances. The desired quantity is the
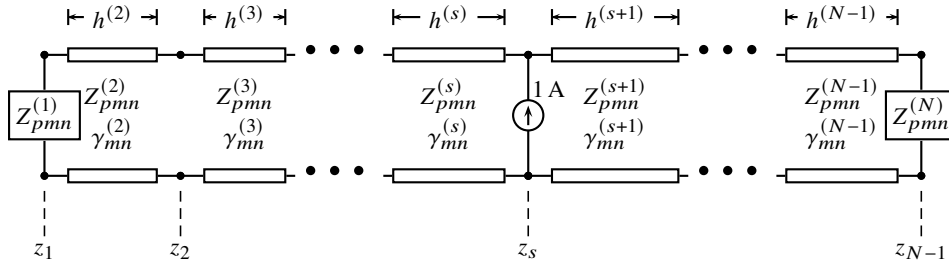
Figure 5.2: Equivalent transmission line circuit used to find transmission line Green's functions. We set $p = 1$ when evaluating V_i^{TE} and $p = 2$ for V_i^{TM}. Superscripted quantities in parentheses are region designators. m and n are modal indices associated with the transverse variation of the modal fields.

voltage across the structure at $z = z_s$. Since we have a unit current generator at $z = z_s$ the voltage there is equal to the total impedance at that point:

$$V_i^p(\beta_{mn}, z_s, z_s) = Z_{pmn}^{\text{tot}}(z_s) = \cfrac{1}{\cfrac{1}{\overleftarrow{Z}_{pmn}(z_s)} + \cfrac{1}{\overrightarrow{Z}_{pmn}(z_s)}} = \frac{\overleftarrow{Z}_{pmn}(z_s)\,\overrightarrow{Z}_{pmn}(z_s)}{\overleftarrow{Z}_{pmn}(z_s) + \overrightarrow{Z}_{pmn}(z_s)}, \qquad (5.13)$$

where p takes on the value 1 (TE) or 2 (TM), and $\overleftarrow{Z}_{pmn}(z_s)$ and $\overrightarrow{Z}_{pmn}(z_s)$ are the impedances seen looking to the left and right, respectively, at $z = z_s$. These latter quantities are easily determined using the following recursive formulas derived from elementary transmission line theory:

$$\overleftarrow{Z}_{pmn}(z_1) = Z_{pmn}^{(1)} \qquad (5.14\text{a})$$

$$\overleftarrow{Z}_{pmn}(z_i) = Z_{pmn}^{(i)}\frac{\overleftarrow{Z}_{pmn}(z_{i-1}) + Z_{pmn}^{(i)}\tanh(\gamma_{mn}^{(i)}h^{(i)})}{Z_{pmn}^{(i)} + \overleftarrow{Z}_{pmn}(z_{i-1})\tanh(\gamma_{mn}^{(i)}h^{(i)})}, \qquad i = 2, 3, \ldots, s \qquad (5.14\text{b})$$

$$\overrightarrow{Z}_{pmn}(z_{N-1}) = Z_{pmn}^{(N)} \qquad (5.14\text{c})$$

$$\overrightarrow{Z}_{pmn}(z_i) = Z_{pmn}^{(i+1)}\frac{\overrightarrow{Z}_{pmn}(z_{i+1}) + Z_{pmn}^{(i+1)}\tanh(\gamma_{mn}^{(i+1)}h^{(i+1)})}{Z_{pmn}^{(i+1)} + \overrightarrow{Z}_{pmn}(z_{i+1})\tanh(\gamma_{mn}^{(i+1)}h^{(i+1)})},$$
$$i = N - 2, N - 3, \ldots, s. \qquad (5.14\text{d})$$

5.2.4   Series Acceleration

At this point, we have expressed the Green's functions for the magnetic vector potential and electric scalar potential as a pair of modal series, as given in Equations (5.10) and (5.12). In order to accelerate the convergence of these series we need to examine their asymptotic behavior. Note that the summands for both V_i^{TE} and V_i^{TM} involve $\overleftarrow{Z}_{pmn}(z_s)$ and $\overrightarrow{Z}_{pmn}(z_s)$, both of which are of a

similar form:

$$\overleftarrow{Z}_{pmn}(z_s) = Z_{pmn}^{(s)} \frac{\overleftarrow{Z}_{pmn}(z_{s-1}) + Z_{pmn}^{(i)} \tanh(\gamma_{mn}^{(i)} h^{(s)})}{Z_{pmn}^{(s)} + \overleftarrow{Z}_{pmn}(z_{s-1}) \tanh(\gamma_{mn}^{(s)} h^{(s)})} \tag{5.15}$$

The behavior of this quantity for large values of the spectral variables m and n is determined by examining the following asymptotic representation of the hyperbolic tangent function:

$$\tanh x = \frac{1 - e^{-2x}}{1 + e^{-2x}} \sim (1 - e^{-2x}) \times (1 - e^{-2x} + e^{-4x} - e^{-6x} + \cdots)$$

$$= 1 - 2e^{-2x} + 2e^{-4x} - 2e^{-6x} + \cdots \tag{5.16}$$

from which we see that the hyperbolic tangent function rapidly approaches unity for large arguments. In fact, one can approximate $\tanh x \approx 1$ for $x > 7$ with an error less than 2×10^{-6}. Therefore, the large argument approximation to the transmission line Green's function (assuming that the layers on each side of the source plane are of nonvanishing thickness) is

$$V_i^p(\boldsymbol{\beta}_{mn}, z_s, z_s) \sim \frac{Z_{pmn}^{(s)} Z_{pmn}^{(s+1)}}{Z_{pmn}^{(s)} + Z_{pmn}^{(s+1)}} \tag{5.17}$$

which, when substituted into Equations (5.10) and (5.12) results in exactly the same formulas as presented for the two-layer Green's functions of Chapter 4. We conclude that the asymptotic behavior for the Green's functions is exactly the same as for a two-layer structure consisting of the regions on either side of the source plane, infinitely extended. The acceleration technique is thus the same as that presented in Chapter 4.

The source-plane potential Green's functions can now be written in their final, accelerated form as

$$G_{xx}^A(\boldsymbol{\rho} - \boldsymbol{\rho}', z_s, z_s) = \tilde{\mu}\left\{\Sigma_{m1} + \frac{u}{4\pi}\left[\Sigma_{S1} + \frac{c_3(\mu_s, \epsilon_s, \mu_{s+1}, \epsilon_{s+1})}{u^2}\Sigma_{S2}\right]\right\} \tag{5.18a}$$

$$G^\Phi(\boldsymbol{\rho} - \boldsymbol{\rho}', z_s, z_s) = \frac{1}{\tilde{\epsilon}}\left\{\Sigma_{m2} + \frac{u}{4\pi}\left[\Sigma_{S1} + \frac{d_3(\mu_s, \epsilon_s, \mu_{s+1}, \epsilon_{s+1})}{u^2}\Sigma_{S2}\right]\right\} \tag{5.18b}$$

where

$$\Sigma_{m1} = \frac{1}{2A}\sum_{m,n}\left[\frac{2V_i^{\mathrm{TE}}(\boldsymbol{\beta}_{mn}, z_s, z_s)}{j\omega\tilde{\mu}} - \frac{1}{\kappa_{mn}} - \frac{c_3(\mu_s, \epsilon_s, \mu_{s+1}, \epsilon_{s+1})}{\kappa_{mn}^3}\right]e^{-j\boldsymbol{\beta}_{mn}\cdot(\boldsymbol{\rho}-\boldsymbol{\rho}')} \tag{5.19a}$$

$$\Sigma_{m2} = \frac{1}{2A}\sum_{m,n}\left(2j\omega\tilde{\epsilon}\frac{V_i^{\mathrm{TM}}(\boldsymbol{\beta}_{mn}, z_s, z_s) - V_i^{\mathrm{TE}}(\boldsymbol{\beta}_{mn}, z_s, z_s)}{\beta_{mn}^2}\right.$$

$$\left. - \frac{1}{\kappa_{mn}} - \frac{d_3(\mu_s, \epsilon_s, \mu_{s+1}, \epsilon_{s+1})}{\kappa_{mn}^3}\right)e^{-j\boldsymbol{\beta}_{mn}\cdot(\boldsymbol{\rho}-\boldsymbol{\rho}')} \tag{5.19b}$$

and

$$\tilde{\mu} = \frac{2\mu_s\mu_{s+1}}{\mu_s + \mu_{s+1}}, \qquad \bar{\epsilon} = \frac{\epsilon_s + \epsilon_{s+1}}{2}. \tag{5.20}$$

The symbols c_3 and d_3 used above are defined in Chapter 4.

5.3   Potential Green's Functions (Magnetic Sources)

5.3.1   Electric Vector Potential

Using the definitions from Chapter 1, we can obtain the expression for the electric vector potential via duality from that of the magnetic vector potential:

$$G_{xx}^F(\rho - \rho', z, z') = \frac{-1}{j\omega A} \sum_{m,n} I_v^{TM}(\beta_{mn}, z, z') e^{-j\beta_{mn}\cdot(\rho - \rho')}. \tag{5.21}$$

where $I_v^{TM}(\beta_{mn}, z, z')$ is the transmission line current at z' due to a unit series voltage source located at z' for the TM equivalent circuit.

5.3.2   Scalar Magnetic Potential

Using duality to transform the scalar electric potential we obtain

$$G^\Psi(\rho - \rho', z, z') = \frac{-j\omega}{A} \sum_{m,n} \frac{I_v^{TM}(\beta_{mn}, z, z') - I_v^{TE}(\beta_{mn}, z, z')}{\beta_{mn}^2} e^{-j\beta_{mn}\cdot(\rho - \rho')}. \tag{5.22}$$

5.3.3   Evaluation of Transmission Line Green's Functions

The equivalent circuit for the magnetic source Green's function differs from that of the electric sources. In the integral equation formulation, it is assumed that a perfectly conducting wall is inserted at $z = z_s$, with the sources impressed at both z_s^- and z_s^+. Therefore, we will require two pairs of potential Green's functions, denoted as $\overleftarrow{G}_{xx}^F$, $\overleftarrow{G}^\Psi$, $\overrightarrow{G}_{xx}^F$, and $\overrightarrow{G}^\Psi$. The former two are due to sources impressed at z_s^- (to the left of the ground plane) and the latter two are for sources at z_s^+ (to the right of the ground plane.) The equivalent circuits for the left- and right-looking sources are shown in Figure 5.3. Since we have unit voltage sources driving each equivalent circuit, it is apparent that the source currents are just admittances, so that

$$\overleftarrow{I}_v^p(\beta_{mn}, z_s, z_s) = \overleftarrow{Y}_{pmn}(z_s), \qquad \overrightarrow{I}_v^p(\beta_{mn}, z_s, z_s) = \overrightarrow{Y}_{pmn}(z_s). \tag{5.23}$$
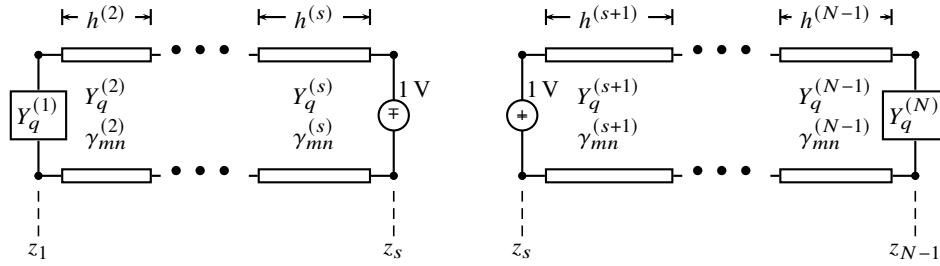
Figure 5.3: Equivalent transmission line circuits used to find magnetic source transmission line Green's functions. We set $p = 1$ when evaluating I_v^{TE} and $p = 2$ for I_v^{TM}.

These admittances are easily found using the following recursive formulas derived from elementary transmission line theory:

$$\overrightarrow{Y}_{pmn}(z_{N-1}) = Y_{pmn}^{(N)} \tag{5.24a}$$

$$\overrightarrow{Y}_{pmn}(z_i) = Y_{pmn}^{(i+1)} \frac{\overrightarrow{Y}_{pmn}(z_{i+1}) + Y_{pmn}^{(i+1)} \tanh(\gamma_{mn}^{(i+1)} h^{(i+1)})}{Y_{pmn}^{(i+1)} + \overrightarrow{Y}_{pmn}(z_{i+1}) \tanh(\gamma_{mn}^{(i+1)} h^{(i+1)})},$$
$$i = N - 2, N - 3, \ldots, s. \tag{5.24b}$$

$$\overleftarrow{Y}_{pmn}(z_1) = Y_{pmn}^{(1)}, \tag{5.24c}$$

$$\overleftarrow{Y}_{pmn}(z_i) = Y_{pmn}^{(i)} \frac{\overleftarrow{Y}_{pmn}(z_{i-1}) + Y_{pmn}^{(i)} \tanh(\gamma_{mn}^{(i)} h^{(i)})}{Y_{pmn}^{(i)} + \overleftarrow{Y}_{pmn}(z_{i-1}) \tanh(\gamma_{mn}^{(i)} h^{(i)})},$$
$$i = 2, 3, \ldots, s. \tag{5.24d}$$

5.3.4   Series Acceleration

The asymptotic form of the magnetic source Green's functions summands are equal to twice the summand for a similar source radiating in a homogeneous medium, with permittivity and permeability equal to either Region s (for left-looking sources) or Region $s + 1$ (for right-looking sources.) Applying the acceleration techniques of Chapter 4 then results in the final formulas

$$G_{xx}^F(\boldsymbol{\rho} - \boldsymbol{\rho}', z_s, z_s) \equiv \overleftarrow{G}_{xx}^F(\boldsymbol{\rho} - \boldsymbol{\rho}', z_s, z_s) + \overrightarrow{G}_{xx}^F(\boldsymbol{\rho} - \boldsymbol{\rho}', z_s, z_s)$$

$$= -\epsilon_0 \left[\Sigma_{m1}' + \frac{u\bar{\epsilon}}{\pi\epsilon_0} \Sigma_{s1} + \frac{c_3^{(s)} \epsilon_s + c_3^{(s+1)} \epsilon_{s+1}}{2\pi u \epsilon_0} \Sigma_{s2} \right] \tag{5.25a}$$

$$G^{\Psi}(\boldsymbol{\rho} - \boldsymbol{\rho}', z_s, z_s) = \overleftarrow{G}^{\Psi}(\boldsymbol{\rho} - \boldsymbol{\rho}', z_s, z_s) + \overrightarrow{G}^{\Psi}(\boldsymbol{\rho} - \boldsymbol{\rho}', z_s, z_s)$$

$$= \frac{1}{\mu_0} \left[\Sigma_{m2}' + \frac{u\mu_0}{\pi\tilde{\mu}} \Sigma_{s1} + \frac{\mu_0}{2\pi u} \left(\frac{d_3^{(s)}}{\mu_s} + \frac{d_3^{(s+1)}}{\mu_{s+1}} \right) \Sigma_{s2} \right] \tag{5.25b}$$

where

$$\Sigma'_{m1} =$$

$$\frac{1}{A} \sum_{m,n} \left[\frac{\overleftarrow{Y}_{2mn}(z_s) + \overrightarrow{Y}_{2mn}(z_s)}{j\omega\epsilon_0} - \frac{2\bar{\epsilon}}{\epsilon_0} \kappa_{mn}^{-1} - \frac{\epsilon_s c_3^{(s)} + \epsilon_{s+1} c_3^{(s+1)}}{\epsilon_0} \kappa_{mn}^{-3} \right] e^{-j\beta_{mn}\cdot(\rho-\rho')} \quad (5.26a)$$

$$\Sigma'_{m2} =$$

$$\frac{1}{A} \sum_{m,n} \left\{ \left(\frac{\overleftarrow{Y}_{2mn}(z_s) + \overrightarrow{Y}_{2mn}(z_s)}{j\omega\epsilon_0} k_0^2 + j\omega\mu_0 \left[\overleftarrow{Y}_{1mn}(z_s) + \overrightarrow{Y}_{1mn}(z_s) \right] \right) \middle/ \beta_{mn}^2 \right.$$

$$\left. - \frac{2\mu_0}{\tilde{\mu}} \kappa_{mn}^{-1} - \mu_0 \left(\frac{d_3^{(s)}}{\mu_s} + \frac{d_3^{(s+1)}}{\mu_{s+1}} \right) \kappa_{mn}^{-3} \right\} e^{-j\beta_{mn}\cdot(\rho-\rho')} \quad (5.26b)$$

and

$$c_3^{(i)} = c_3(\mu_i, \epsilon_i, \mu_i, \epsilon_i), \quad d_3^{(i)} = d_3(\mu_i, \epsilon_i, \mu_i, \epsilon_i). \quad (5.27)$$

5.4 FFT Evaluation of the Modal Difference Series

The modal series in (4.35), (4.36), (5.18), (5.19), and (5.26) represent extremely smooth functions of $\rho - \rho'$, since their singularities have been subtracted out. Therefore, an efficient and accurate method of evaluating them is to tabulate and then interpolate using a low-order bivariate polynomial interpolation scheme, such as [14, Eq. 25.2.7]. Here we consider a method of rapidly tabulating the functions over the unit cell using the Fast Fourier Transform (FFT).

The modal series are all of the form

$$f(\rho - \rho') = \sum_{m=-\infty}^{\infty} \sum_{n=-\infty}^{\infty} f_{(m,n)} e^{-j(\beta_{00}+m\beta_1+n\beta_2)\cdot(\rho-\rho')}. \quad (5.28)$$

We introduce the change of variables

$$\rho - \rho' = \xi_1 s_1 + \xi_2 s_2. \quad (5.29)$$

It is clear that for any points ρ and ρ' in the unit cell, the difference vector $\rho - \rho'$ can be represented by Equation (5.29) with $-1 \le \xi_1, \xi_2 < 1$. We can further restrict evaluation of the series to the range $0 \le \xi_1, \xi_2 < 1$ by making use of the translational formula

$$f((\xi_1 + m)s_1 + (\xi_2 + n)s_2) = e^{-j(m\psi_1+n\psi_2)} f(\xi_1 s_1 + \xi_2 s_2) \quad (5.30)$$

which holds for any integers m and n. Given $\rho - \rho'$ one can easily determine ξ_1 and ξ_2 using

$$\xi_i = \frac{1}{2\pi} \beta_i \cdot (\rho - \rho'), \quad i = 1, 2. \quad (5.31)$$

With (5.29), the series in (5.28) becomes

$$f(\xi_1 s_1 + \xi_2 s_2) = e^{-j(\xi_1 \psi_1 + \xi_2 \psi_2)} \sum_{m=-\infty}^{\infty} \sum_{n=-\infty}^{\infty} f_{(m,n)} e^{-j2\pi(m\xi_1 + n\xi_2)}. \tag{5.32}$$

We now assume that the summand is nonzero only for $-\frac{M}{2} \le m \le \frac{M}{2} - 1$ and $-\frac{N}{2} \le n \le \frac{N}{2} - 1$, where M and N are some convenient integer powers of 2. Then

$$f(\xi_1 s_1 + \xi_2 s_2) = e^{-j(\xi_1 \psi_1 + \xi_2 \psi_2)} \sum_{m=-\frac{M}{2}}^{\frac{M}{2}-1} \sum_{n=-\frac{N}{2}}^{\frac{N}{2}-1} f_{(m,n)} e^{-j2\pi(m\xi_1 + n\xi_2)}$$

$$= e^{-j(\xi_1 \psi_1 + \xi_2 \psi_2)} \sum_{m=0}^{M-1} \sum_{n=0}^{N-1} f_{(m-\frac{M}{2}, n-\frac{N}{2})} e^{-j2\pi[(m-\frac{M}{2})\xi_1 + (n-\frac{N}{2})\xi_2]}$$

$$= e^{-j[\xi_1(\psi_1 - M\pi) + \xi_2(\psi_2 - N\pi)]} \sum_{m=0}^{M-1} \sum_{n=0}^{N-1} f_{(m-\frac{M}{2}, n-\frac{N}{2})} e^{-j2\pi(m\xi_1 + n\xi_2)}. \tag{5.33}$$

Finally, we restrict evaluation to the set of points

$$\xi_1 = p/M, \ p = 0, 1, 2, \ldots, M - 1, \qquad \xi_2 = q/N, \ q = 0, 1, 2, \ldots, N - 1$$

so that the expression for the sum becomes

$$f\left(\frac{p}{M} s_1 + \frac{q}{N} s_2\right) =$$

$$e^{j[p(\pi - \psi_1/M) + q(\pi - \psi_2/N)]} \sum_{m=0}^{M-1} \sum_{n=0}^{N-1} f_{(m-\frac{M}{2}, n-\frac{N}{2})} e^{-j2\pi(mp/M + nq/N)},$$

$$p = 0, 1, 2, \ldots, M - 1, \quad q = 0, 1, 2, \ldots, N - 1. \tag{5.34}$$

The double sum in (5.34) constitutes a two-dimensional discrete Fourier transform (DFT). It can be evaluated efficiently for all desired p and q values via a single application of the two-dimensional fast Fourier transform (FFT) using the facilities built into Julia.

Chapter 6

Calculation of Incident Fields and GSM Entries

6.1 Introduction

In Chapter refchap:gfstratified a method was presented to efficiently evaluate the potential Green's functions for a multiply stratified medium under quasi-periodic boundary conditions. In order to make use of this Green's function in a periodic moment method procedure, it is also necessary to compute the incident fields and pick off the scattering matrix entries for the multiply stratified medium. This chapter provides solutions for these tasks.

We will assume that the single FSS sheet is located at interface number s, located between layers s and $s + 1$, where $1 \leq s < N$.

6.2 Electric Current Unknowns

6.2.1 Calculation of Incident Fields

In this case the incident field is the field that would exist in the structure in the absence of the unknown electric currents (and the metalization which they represent). That is, the incident field is the field present in the pure radome case, with primary excitation from an incoming normalized Floquet mode with unit excitation coefficient.

There are two cases to consider. In the first case, the primary excitation is a Region 1 Floquet mode propagating in the $+z$ direction. In the second case, the exciting wave is a Region N Floquet mode propagating in the $-z$ direction.

Region 1 Incidence

The primary excitation is a plane wave incident from Region 1 with transverse electric field given by

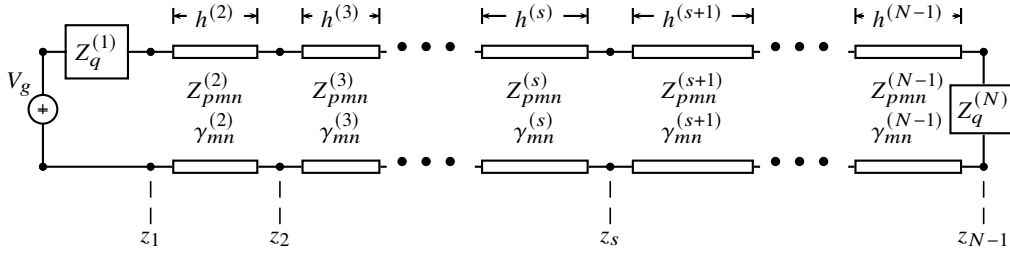$$\boldsymbol{e}_q^{(1)}(x, y)e^{-\gamma^{(1)}(z-z_1)} \tag{6.1}$$

Figure 6.1: Equivalent transmission line circuit used to find incident electric field for a plane wave incident from Region 1.

where q is the modal triple index $q = (p_q, m_q, n_q)$. The transmission line equivalent circuit for determining the incident field present at any desired junction plane is shown in Figure 6.1. We choose the generator voltage $V_g = 2$ to supply a unit incoming voltage wave. The total incident (both incoming and reflected) electric field at $z = z_1$ is then

$$\bar{\boldsymbol{I}}_z \cdot \boldsymbol{E}^{\text{inc}}(x, y, z_1) = V(z_1) e_q^{(1)}(x, y) = \frac{V_g}{2}(1 + S_{qq}^{11}) e_q^{(1)}(x, y) \tag{6.2}$$

where S_{qq}^{11} is the partial GSM entry due to the incident fields. We can find $V(z_1)$ using the transmission line equivalent circuit. The voltage and current at the junction plane $z = z_1$ are

$$V(z_1) = \frac{V_g \vec{Z}(z_1)}{\vec{Z}(z_1) + Z_q^{(1)}}, \quad I(z_1) = \frac{V_g}{\vec{Z}(z_1) + Z_q^{(1)}} \tag{6.3}$$

where $\vec{Z}(z_i)$ is the impedance seen looking to the right at $z = z_i$. The right-looking impedances seen at the junction planes are easily determined using the following recursive formulas derived from elementary transmission line theory:

$$\vec{Z}(z_{N-1}) = Z_q^{(N)} \tag{6.4a}$$

$$\vec{Z}(z_i) = Z_q^{(i+1)} \frac{\vec{Z}(z_{i+1}) + Z_q^{(i+1)} \tanh(\gamma_q^{(i+1)} h^{(i+1)})}{Z_q^{(i+1)} + \vec{Z}(z_{i+1}) \tanh(\gamma_q^{(i+1)} h^{(i+1)})},$$
$$i = N - 2, N - 3, \dots, 1. \tag{6.4b}$$

A similar recursive procedure can be used to calculate the equivalent circuit voltages and currents at each of the remaining junction planes:

$$V(z_i) = V(z_{i-1}) \cosh(\gamma_q^{(i)} h^{(i)}) - Z_q^{(i)} I(z_{i-1}) \sinh(\gamma_q^{(i)} h^{(i)}), \quad I(z_i) = \frac{V(z_i)}{\vec{Z}(z_i)}$$
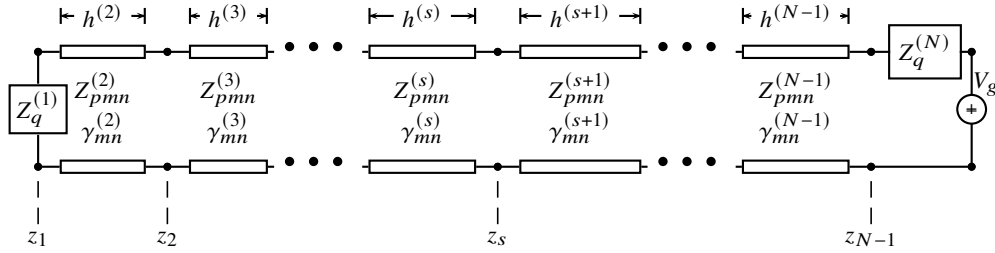$$i = 2, 3, \dots, N - 1. \tag{6.5}$$

Figure 6.2: Equivalent transmission line circuit used to find incident electric field for a plane wave incident from Region N.

The total incident (both incoming and reflected) electric field at $z = z_s$ is then

$$\bar{I}_z \cdot E^{\text{inc}}(x, y, z_s) = V(z_s) e_q^{(1)}(x, y) = V(z_s) \frac{c_q^{(1)}}{c_q^{(s)}} e_q^{(s)}(x, y), \qquad (6.6)$$

where we used the fact that $e_q^{(1)}/c_q^{(1)} = e_q^{(s)}/c_q^{(s)}$.

The partial transmission scattering parameter (due to the incident field) S_{qq}^{21} is obtained from the equivalent circuit voltage at $z = z_{N-1}$:

$$\bar{I} \cdot E^{\text{inc}}(x, y, z_{N-1}) = V(z_{N-1}) e_q^{(1)}(x, y) = S_{qq}^{21} e_q^{(N)}(x, y). \qquad (6.7)$$

Since $e_q^{(1)}/c_q^{(1)} = e_q^{(N)}/c_q^{(N)}$ we find that

$$S_{qq}^{21} = V(z_{N-1}) \frac{c_q^{(1)}}{c_q^{(N)}}. \qquad (6.8)$$

Region N Incidence

The primary excitation is a plane wave incident from Region N with transverse electric field given by

$$e_q^{(N)}(x, y) e^{\gamma^{(1)}(z - z_{N-1})} \qquad (6.9)$$

where q is the modal triple index $q = (p_q, m_q, n_q)$. The transmission line equivalent circuit for determining the incident field present at any desired junction plane is shown in Figure 6.2. We choose the generator voltage $V_g = 2$ to supply a unit incoming voltage wave. The total incident (both incoming and reflected) electric field at $z = z_{N-1}$ is

$$\bar{I}_z \cdot E^{\text{inc}}(x, y, z_{N-1}) = V(z_{N-1}) e_q^{(N)}(x, y) = (1 + S_{qq}^{22}) e_q^{(N)}(x, y) \qquad (6.10)$$

where S_{qq}^{22} is the partial GSM entry due to the incident fields. We can find $V(z_{N-1})$ using the transmission line equivalent circuit. The voltage and current at the junction plane $z = z_{N-1}$ are

$$V(z_{N-1}) = \frac{V_g \overleftarrow{Z}(z_{N-1})}{\overleftarrow{Z}(z_{N-1}) + Z_q^{(N)}}, \quad I(z_{N-1}) = \frac{-V_g}{\overleftarrow{Z}(z_{N-1}) + Z_q^{(N)}} \tag{6.11}$$

where $\overleftarrow{Z}(z_i)$ is the impedance seen looking to the left at $z = z_i$. The left-looking impedances seen at the junction planes are easily determined using the following recursive formulas derived from elementary transmission line theory:

$$\overleftarrow{Z}(z_1) = Z_q^{(1)} \tag{6.12a}$$

$$\overleftarrow{Z}(z_i) = Z_q^{(i)} \frac{\overleftarrow{Z}(z_{i-1}) + Z_q^{(i)} \tanh(\gamma_q^{(i)} h^{(i)})}{Z_q^{(i)} + \overleftarrow{Z}(z_{i-1}) \tanh(\gamma_q^{(i)} h^{(i)})},$$

$$i = 2, 3, \dots, N-1. \tag{6.12b}$$

A similar recursive procedure can be used to calculate the equivalent circuit voltages and currents at each of the remaining junction planes:

$$\begin{cases} V(z_i) = V(z_{i+1}) \cosh(\gamma_q^{(i+1)} h^{(i+1)}) + Z_q^{(i+1)} I(z_{i+1}) \sinh(\gamma_q^{(i+1)} h^{(i+1)}), \\ I(z_i) = -V(z_i)/\overleftarrow{Z}(z_i) \end{cases}$$

$$i = N-2, N-3 \dots, 1. \tag{6.13}$$

The total incident (both incoming and reflected) electric field at $z = z_s$ is then

$$\bar{I}_z \cdot E^{\text{inc}}(x, y, z_s) = V(z_s) e_q^{(N)}(x, y) = V(z_s) \frac{c_q^{(N)}}{c_q^{(s+1)}} e_q^{(s+1)}(x, y), \tag{6.14}$$

where we used the fact that $e_q^{(N)}/c_q^{(N)} = e_q^{(s+1)}/c_q^{(s+1)}$.

The partial transmission scattering parameter (due to the incident field) S_{qq}^{12} is obtained from the equivalent circuit voltage at $z = z_1$:

$$\bar{I} \cdot E^{\text{inc}}(x, y, z_1) = V(z_1) e_q^{(N)}(x, y) = S_{qq}^{12} e_q^{(1)}(x, y). \tag{6.15}$$

Since $e_q^{(N)}/c_q^{(N)} = e_q^{(1)}/c_q^{(1)}$ we find that

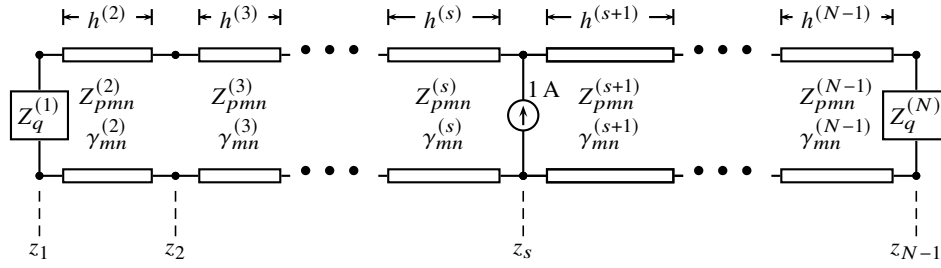$$S_{qq}^{12} = V(z_1) \frac{c_q^{(N)}}{c_q^{(1)}}. \tag{6.16}$$

Figure 6.3: Equivalent transmission line circuit used to find scattered fields. We set $p = 1$ when evaluating V_i^{TE} and $p = 2$ for V_i^{TM}. Superscripted quantities in parentheses are region designators.

6.2.2 Calculation of (scattered) GSM entries

We now assume that the electric surface currents $\boldsymbol{J}_s$ on the FSS sheet located at $z = z_s$ have been obtained using the method of moments. We seek expressions for the outgoing wave coefficients $\{b_q^{(1)}\}$ and $\{b_q^{(N)}\}$ in the scattered field expansions

$$\boldsymbol{E}^{\text{sc}}(x, y, z) = \begin{cases} \sum_q b_q^{(1)} \boldsymbol{e}_q^{(1)}(x, y) e^{j\gamma_q^{(1)}(z-z_1)} & (z < z_1) \\ \sum_q b_q^{(N)} \boldsymbol{e}_q^{(N)}(x, y) e^{-j\gamma_q^{(N)}(z-z_{N-1})} & (z > z_{N-1}). \end{cases} \quad (6.17)$$

These coefficients are the partial GSM entries due to the scattered (radiated by the induced surface currents) fields. Using the results of [13] we find that they are given by

$$b_q^{(1)} = -\hat{\boldsymbol{t}}_q \cdot \tilde{\boldsymbol{J}}_s(\boldsymbol{\beta}_{m_q,n_q}) \frac{V_i^{pq}(\boldsymbol{\beta}_{m_q,n_q}, z_1, z_s)}{A c_q^{(1)}} \quad (6.18a)$$

$$b_q^{(N)} = -\hat{\boldsymbol{t}}_q \cdot \tilde{\boldsymbol{J}}_s(\boldsymbol{\beta}_{m_q,n_q}) \frac{V_i^{pq}(\boldsymbol{\beta}_{m_q,n_q}, z_{N-1}, z_s)}{A c_q^{(N)}} \quad (6.18b)$$

where V_i^p is the transmission line Green's function for the voltage due to a unit current source for either the TE ($p = 1$) or TM ($p = 2$) equivalent circuit, shown in Figure 6.3. Since we have a unit

current source at $z = z_s$ the voltage there is equal to the total impedance at that point:

$$V_i^p(\boldsymbol{\beta}_{m_q,n_q}, z_s, z_s) = Z^{\text{tot}}(z_s) = \frac{1}{\frac{1}{\overleftarrow{Z}(z_s)} + \frac{1}{\overrightarrow{Z}(z_s)}} = \frac{\overleftarrow{Z}(z_s)\,\overrightarrow{Z}(z_s)}{\overleftarrow{Z}(z_s) + \overrightarrow{Z}(z_s)}, \tag{6.19a}$$

$$I_i^p(\boldsymbol{\beta}_{m_q,n_q}, z_s^+, z_s) = \frac{V_i^p(\boldsymbol{\beta}_{m_q,n_q}, z_s, z_s)}{\overrightarrow{Z}(z_s)}, \tag{6.19b}$$

$$I_i^p(\boldsymbol{\beta}_{m_q,n_q}, z_s^-, z_s) = \frac{-V_i^p(\boldsymbol{\beta}_{m_q,n_q}, z_s, z_s)}{\overleftarrow{Z}(z_s)}. \tag{6.19c}$$

With the voltage and current known at z_s, one can apply (6.13) for $i = s - 1, s - 2, \ldots, 1$ and (6.5) for $i = s + 1, s + 2, \ldots, N - 1$ to determine Green's function voltages needed to evaluate Equations (6.18).

6.3   Magnetic Current Unknowns

6.3.1   Calculation of Incident Fields

In this case the incident field is the field that would exist in the structure in the absence of the unknown magnetic currents, but in the presence of the unperforated ground plane at $z = z_s$. That is, the incident field is the sum of the incoming and reflected (due to the ground plane) waves, with primary excitation from an incoming normalized Floquet mode with unit excitation coefficient.

There are two cases to consider. In the first case, the primary excitation is a Region 1 Floquet mode propagating in the $+z$ direction. In the second case, the exciting wave is a Region N Floquet mode propagating in the $-z$ direction.

Region 1 Incidence

The primary excitation is a plane wave incident from Region 1 with transverse magnetic field given by

$$\boldsymbol{h}_q^{(1)}(x, y)e^{-\gamma^{(1)}(z - z_1)} \tag{6.20}$$

where q is the modal triple index $q = (p_q, m_q, n_q)$. The transmission line equivalent circuit for determining the incident magnetic field present at any desired junction plane is shown in Figure 6.4. We choose the generator current $I_g = 2$ to supply a unit incoming current wave. The total incident (both incoming and reflected) magnetic field at $z = z_1$ is then

$$\bar{\boldsymbol{I}}_z \cdot \boldsymbol{H}^{\text{inc}}(x, y, z_1) = I(z_1)\boldsymbol{h}_q^{(1)}(x, y) = \frac{I_g}{2}(1 - S_{qq}^{11})\boldsymbol{h}_q^{(1)}(x, y) \tag{6.21}$$
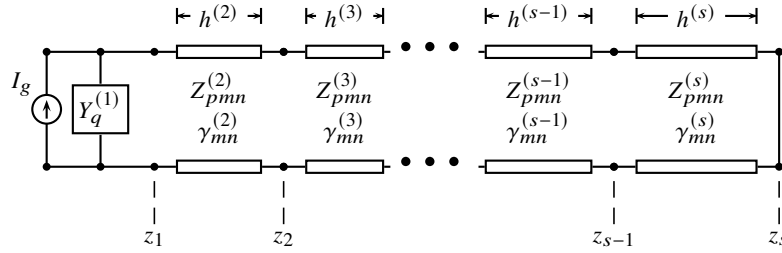
Figure 6.4: Equivalent transmission line circuit used to find incident magnetic field at $z = z_s$ for a plane wave incident from Region 1.

where S_{qq}^{11} is the partial GSM entry due to the incident fields. We can find $I(z_1)$ using the transmission line equivalent circuit. The current and voltage at the junction plane $z = z_1$ are

$$I(z_1) = \frac{I_g}{1 + \vec{Z}(z_1) Y_q^{(1)}}, \quad V(z_1) = \frac{I_g \vec{Z}(z_1)}{1 + \vec{Z}(z_1) Y_q^{(1)}}, \tag{6.22}$$

where $\vec{Z}(z_i)$ is the impedance seen looking to the right at $z = z_i$. The right-looking impedances seen at the junction planes are easily determined using the following recursive formulas derived from elementary transmission line theory:

$$\vec{Z}(z_{s-1}) = Z_q^{(s)} \tanh(\gamma_q^{(s)} h^{(s)}) \tag{6.23a}$$

$$\vec{Z}(z_i) = Z_q^{(i+1)} \frac{\vec{Z}(z_{i+1}) + Z_q^{(i+1)} \tanh(\gamma_q^{(i+1)} h^{(i+1)})}{Z_q^{(i+1)} + \vec{Z}(z_{i+1}) \tanh(\gamma_q^{(i+1)} h^{(i+1)})},$$
$$i = s - 2, s - 3, \ldots, 1. \tag{6.23b}$$

A similar recursive procedure can be used to calculate the equivalent circuit currents and voltages at each of the remaining junction planes:

$$I(z_i) = I(z_{i-1}) \cosh(\gamma_q^{(i)} h^{(i)}) - Y_q^{(i)} V(z_{i-1}) \sinh(\gamma_q^{(i)} h^{(i)}), \quad V(z_i) = I(z_i) \vec{Z}(z_i)$$
$$i = 2, 3, \ldots, s. \tag{6.24}$$

The total incident (both incoming and reflected) magnetic field at $z = z_s$ is then

$$\bar{I}_z \cdot \mathbf{H}^{\text{inc}}(x, y, z_s) = I(z_s) \mathbf{h}_q^{(1)}(x, y) = I(z_s) \frac{c_q^{(s)}}{c_q^{(1)}} \mathbf{h}_q^{(s)}(x, y), \tag{6.25}$$

where we used the fact that $c_q^{(1)} \mathbf{h}_q^{(1)} = c_q^{(s)} \mathbf{h}_q^{(s)}$.
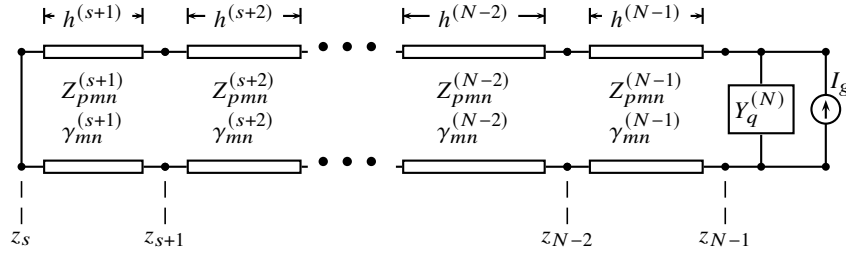
Figure 6.5: Equivalent transmission line circuit used to find incident electric field for a plane wave incident from Region N.

The partial reflection scattering parameter (due to the incident field) S_{qq}^{11} is obtained from the equivalent circuit current at $z = z_1$:

$$\bar{I} \cdot H^{\text{inc}}(x, y, z_1) = I(z_1) h_q^{(1)}(x, y) = (1 - S_{qq}^{11}) h_q^{(1)}(x, y), \tag{6.26}$$

so that

$$S_{qq}^{11} = 1 - I(z_1). \tag{6.27}$$

Region N Incidence

The primary excitation is a plane wave incident from Region N with transverse magnetic field given by

$$- h_q^{(N)}(x, y) e^{\gamma^{(1)}(z - z_{N-1})} \tag{6.28}$$

where q is the modal triple index $q = (p_q, m_q, n_q)$. The transmission line equivalent circuit for determining the incident field present at any desired junction plane is shown in Figure 6.5. We choose the generator current $I_g = 2$ to supply a unit incoming current wave. The total incident (both incoming and reflected) magnetic field at $z = z_{N-1}$ is

$$\bar{I}_z \cdot H^{\text{inc}}(x, y, z_{N-1}) = I(z_{N-1}) h_q^{(N)}(x, y) = (S_{qq}^{22} - 1) h_q^{(N)}(x, y) \tag{6.29}$$

where S_{qq}^{22} is the partial GSM entry due to the incident fields. We can find $V(z_{N-1})$ using the transmission line equivalent circuit. The current and voltage at the junction plane $z = z_{N-1}$ are

$$I(z_{N-1}) = \frac{-I_g}{1 + \overleftarrow{Z}(z_{N-1}) Y_q^{(N)}}, \quad V(z_{N-1}) = \frac{-I_g \overleftarrow{Z}(z_{N-1})}{1 + \overleftarrow{Z}(z_{N-1}) Y_q^{(N)}} \tag{6.30}$$

where $\overleftarrow{Z}(z_i)$ is the impedance seen looking to the left at $z = z_i$. The left-looking impedances seen at the junction planes are easily determined using the following recursive formulas derived from

elementary transmission line theory:

$$\overleftarrow{Z}(z_{s+1}) = Z_q^{(s+1)} \tanh(\gamma_q^{(s+1)} h^{(s+1)}) \tag{6.31a}$$

$$\overleftarrow{Z}(z_i) = Z_q^{(i)} \frac{\overleftarrow{Z}(z_{i-1}) + Z_q^{(i)} \tanh(\gamma_q^{(i)} h^{(i)})}{Z_q^{(i)} + \overleftarrow{Z}(z_{i-1}) \tanh(\gamma_q^{(i)} h^{(i)})}, \quad i = s+2, s+3, \ldots, N-1. \tag{6.31b}$$

A similar recursive procedure can be used to calculate the equivalent circuit currents and voltages at each of the remaining junction planes:

$$\begin{cases} I(z_i) = I(z_{i+1}) \cosh(\gamma_q^{(i+1)} h^{(i+1)}) + Y_q^{(i+1)} V(z_{i+1}) \sinh(\gamma_q^{(i+1)} h^{(i+1)}), \\ V(z_i) = -I(z_i) \overleftarrow{Z}(z_i) \end{cases}$$

$$i = N-2, N-3 \ldots, s. \tag{6.32}$$

The total incident (both incoming and reflected) magnetic field at $z = z_s$ is then

$$\bar{I}_z \cdot \boldsymbol{H}^{\mathrm{inc}}(x, y, z_s) = I(z_s) \boldsymbol{h}_q^{(N)}(x, y) = I(z_s) \frac{c_q^{(s+1)}}{c_q^{(N)}} \boldsymbol{h}_q^{(s+1)}(x, y), \tag{6.33}$$

where we used the fact that $c_q^{(N)} \boldsymbol{h}_q^{(N)} = c_q^{(s+1)} \boldsymbol{h}_q^{(s+1)}$.

The partial reflection scattering parameter (due to the incident field) S_{qq}^{22} is obtained from the equivalent circuit current at $z = z_{N-1}$:

$$\bar{I} \cdot \boldsymbol{H}^{\mathrm{inc}}(x, y, z_{N-1}) = I(z_{N-1}) \boldsymbol{h}_q^{(N)}(x, y) = (S_{qq}^{22} - 1) \boldsymbol{h}_q^{(N)}(x, y), \tag{6.34}$$

so that

$$S_{qq}^{22} = I(z_{N-1}) + 1. \tag{6.35}$$

6.3.2   Calculation of (scattered) GSM entries

We now assume that the magnetic surface currents $\sigma \boldsymbol{M}_{\mathrm{s}}$ at $z = z_s - 0$ and $-\sigma \boldsymbol{M}_{\mathrm{s}}$ at $z = z_s + 0$ have been numerically determined, where $\sigma = 1$ for a primary wave incident from Region 1 and $\sigma = -1$ for a primary wave incident from Region N. We seek expressions for the outgoing wave coefficients $\{b_q^{(1)}\}$ and $\{b_q^{(N)}\}$ in the scattered field expansions

$$\boldsymbol{H}^{\mathrm{sc}}(x, y, z) = \begin{cases} \displaystyle\sum_q -b_q^{(1)} \boldsymbol{h}_q^{(1)}(x, y) e^{j\gamma_q^{(1)}(z-z_1)} & (z < z_1) \\[2ex] \displaystyle\sum_q b_q^{(N)} \boldsymbol{h}_q^{(N)}(x, y) e^{-j\gamma_q^{(N)}(z-z_{N-1})} & (z > z_{N-1}). \end{cases} \tag{6.36}$$
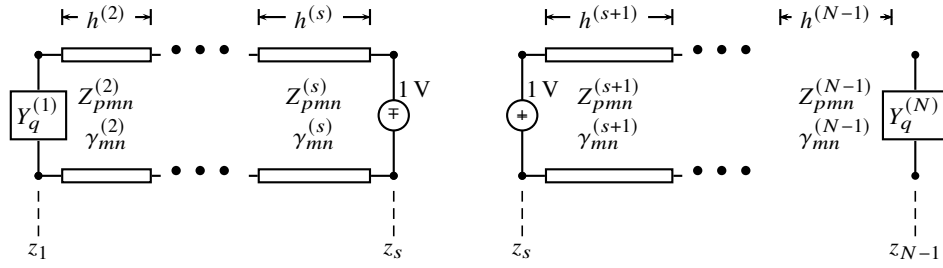
Figure 6.6: Equivalent transmission line circuits used to find scattered fields. We set $p = 1$ when evaluating I_v^{TE} and $p = 2$ for I_v^{TM}. Superscripted quantities in parentheses are region designators.

These coefficients are the partial GSM entries due to the scattered (radiated by the induced surface currents) fields. Using the results of [13] we find that they are

$$b_q^{(1)} = \hat{z} \times \hat{t}_q \cdot \tilde{M}_s(\beta_{m_q,n_q}) \frac{\sigma c_q^{(1)} I_v^{p_q}(\beta_{m_q,n_q}, z_1, z_s)}{P_0} \tag{6.37a}$$

$$b_q^{(N)} = \hat{z} \times \hat{t}_q \cdot \tilde{M}_s(\beta_{m_q,n_q}) \frac{\sigma c_q^{(N)} I_v^{p_q}(\beta_{m_q,n_q}, z_{N-1}, z_s)}{P_0} \tag{6.37b}$$

where $I_v^{p_q}$ is the transmission line Green's function for the current due to a unit voltage source for either the TE ($p_q = 1$) or TM ($p_q = 2$) equivalent circuit, as shown in Figure 6.6, and $P_0 \equiv 1$ W. For either the left-looking or right-looking equivalent circuit, we have a unit voltage source at $z = z_s$ so that the current there is equal to the admittance seen at that point:

$$V_v^p(\beta_{m_q,n_q}, z_s^-, z_s) = -1, \quad I_v^p(\beta_{m_q,n_q}, z_s^-, z_s) = \overleftarrow{Y}(z_s) = 1/\overleftarrow{Z}(z_s), \tag{6.38a}$$

$$V_v^p(\beta_{m_q,n_q}, z_s^+, z_s) = 1, \quad I_v^p(\beta_{m_q,n_q}, z_s^+, z_s) = \overrightarrow{Y}(z_s) = 1/\overrightarrow{Z}(z_s). \tag{6.38b}$$

With the voltage and current known at z_s, one can apply (6.32) for $i = s-1, s-2, \ldots, 1$ and (6.24) for $i = s+1, s+2, \ldots, N-1$ to determine Green's function currents needed to evaluate Equations (6.37).

Chapter 7

Moment Method Formulation

In this chapter we describe a procedure for determining the induced electric or magnetic surface currents on a single-sheet FSS (frequency selective surface) located at one of the junction planes in a multiply stratified medium, when excited by an incident plane wave. The analysis is performed using the method of moments, employing a space-domain formulation of the potential Green's functions, which are described in previous chapters. Once the equivalent induced surface currents have been determined, the single-sheet scattering parameters can be extracted using the formulas presented in Chapter 6. Scattering parameters of more complicated structures consisting of several cascaded FSS sheets interlaced with dielectric layers can be determined from the individual sheet scattering parameters using the results of Chapter 3. The following novel features are incorporated in this analysis:

- The use of a wide-band expansion of the stratified medium periodic Green's functions has been incorporated into the moment method procedure, greatly reducing the time needed to compute the elements of the interaction matrices. This technique was first reported in [15].

- Modifications have been introduced into the triangle subdomain basis functions of Rao, Wilton, and Glisson [2] to enable representation of currents that cross unit cell boundaries. This work was previously reported in [16].

The FSS is located in the interface plane $z = z_s$ of the multiple layered structure shown in Figure 7.1. The structure is laterally invariant, with each dielectric layer being homogeneous and isotropic. Each layer $i = 1, 2, \ldots, N$ is characterized by a complex permittivity ϵ_i and permeability μ_i, each of which lies either in the fourth quadrant of the complex plane, or on the real axis. The medium intrinsic wavenumbers are $k_i = \omega\sqrt{\mu_i\epsilon_i}$. We will assume that the single FSS sheet is located at interface number s, located between layers s and $s + 1$, where $1 \leq s < N$.

In general, we can model a zero-thickness, perfectly conducting FSS using either electric or magnetic currents as the unknowns. In the former case, the metalization is removed, and the support[1] of the unknown electric surface current consists of the region previously occupied by the

---

[1] The support of a function is defined as the closure of the set of points where the function takes nonzero values.
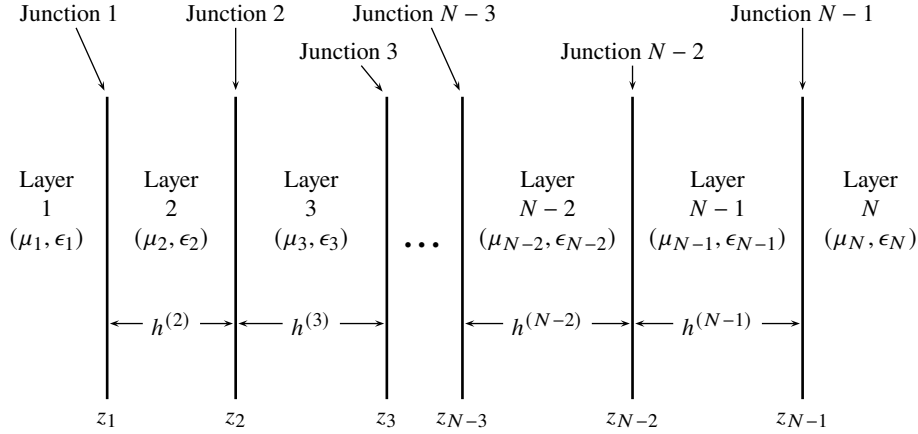
Figure 7.1: The structure under consideration is a stack of $N \geq 2$ dielectric layers. Layers 1 and N are semi-infinite in extent. For $2 \leq i \leq N - 1$, layer i lies in the region $z_{i-1} < z < z_i$, is of thickness $h^{(i)} = z_i - z_{i-1}$, and is characterized by permeability μ_i and permittivity ϵ_i.

metalization. In the latter case, the entire interface plane $z = 0$ is replaced with a zero-thickness PEC (perfect electric conductor) and the support of the magnetic current is the portion of the plane formerly *not* occupied by the PEC.

One generally chooses the type of equivalent currents employed in a given problem so as to minimize the area of the currents' support, and thus the number of unknowns to be solved for in the MoM problem. For aperture-type elements magnetic currents are usually selected; for wire-type elements electric currents are the natural choice. In the case where an FSS is constructed of lossy material, we are forced to use electric currents as the unknowns.

7.1 Electric Current Mixed Potential Integral Equation

In this section we consider an FSS that is modeled using equivalent electric surface current. This choice is convenient when less than half of the unit cell area is occupied by metal or when the FSS is etched onto a sheet of lossy material.

The boundary value problem to be solved is [17]

$$Z_s(\boldsymbol{\rho})\boldsymbol{J}_s(\boldsymbol{\rho}) - \bar{\boldsymbol{I}}_z \cdot \boldsymbol{E}^{\mathrm{sc}}(\boldsymbol{\rho}) = \bar{\boldsymbol{I}}_z \cdot \boldsymbol{E}^{\mathrm{inc}}(\boldsymbol{\rho}), \quad (\boldsymbol{\rho} \in S) \tag{7.1}$$

where $\boldsymbol{E}^{\mathrm{sc}}$ is the scattered electric field due to the equivalent currents flowing on the surface S of the FSS, $\boldsymbol{E}^{\mathrm{inc}}$ is the incident electric field (the plane wave, including incident, reflected, and transmitted components, that would exist in the absence of the FSS), Z_s is the surface resistance of the FSS sheet material, and $\bar{\boldsymbol{I}}_z = \hat{\boldsymbol{x}}\hat{\boldsymbol{x}} + \hat{\boldsymbol{y}}\hat{\boldsymbol{y}}$ is the unit surface dyadic. In terms of potentials this becomes

$$Z_s(\boldsymbol{\rho})\boldsymbol{J}_s(\boldsymbol{\rho}) + [j\omega\boldsymbol{A}(\boldsymbol{\rho}) + \boldsymbol{\nabla}\Phi(\boldsymbol{\rho})] \cdot \bar{\boldsymbol{I}}_z = \boldsymbol{E}^{\mathrm{inc}}(\boldsymbol{\rho}) \cdot \bar{\boldsymbol{I}}_z, \quad (\boldsymbol{\rho} \in S) \tag{7.2}$$

where the potentials can be expressed as superposition integrals using appropriately defined Green's functions (Chapter 5) G_{xx}^A and G^Φ:

$$\bar{I}_z \cdot A(\rho) = \iint G_{xx}^A(\rho - \rho') \cdot J_s(\rho') \, dS', \tag{7.3}$$

$$\Phi(\rho) = \iint G^\Phi(\rho - \rho') \cdot q_e(\rho') \, dS'. \tag{7.4}$$

In (7.3) and (7.4), J_s and q_e are the unknown induced electric surface current and surface charge densities, respectively, which will be determined by enforcing Equation (7.2) in an approximate manner using the method of moments. We use the triangle subdomain basis functions of Rao, Wilton and Glisson [2], suitably modified so as to accommodate the periodic boundary conditions encountered in the unit cell analysis.

7.1.1   Basis Functions

We now enunciate a few important definitions and and properties of the basis functions in order to establish notation. The support of J_s is first partitioned into a number of triangles. In [2] a basis function is defined over each pair of triangles which share a common edge. In this work, we include not only these adjacent pairs of triangles, but also those pairs of triangles which would be adjacent if one of the pair were translated by s_1 or s_2 from its actual position.

Consider first a typical pair of adjacent triangles; their common edge is not on the boundary of the unit cell. Figure 7.2 shows two such triangles, T_m^+ and T_m^-, which comprise the support of the mth basis function and which share an interior edge of the triangulated surface. Points in T_m^+ may be designated by either the position vector r which locates them with respect to the global origin, or by ρ_m^+, which is defined with respect to the free vertex of T_m^+. The vector ρ_m^- is defined similarly for points in T_m^-, except that it is directed *towards* the free vertex of T_m^-. Which of the two triangles is designated "plus" and which is "minus" depends on an arbitrary choice of positive current reference direction for the mth basis function. Positive reference current flows across the edge from T_m^+ to T_m^-. The basis function associated with the mth edge is then defined as

$$f_m(r) = \begin{cases} \dfrac{l_m e^{j\theta_m^+}}{2A_m^+} \rho_m^+ & \text{if } r \in T_m^+ \\[2ex] \dfrac{l_m e^{j\theta_m^-}}{2A_m^-} \rho_m^- & \text{if } r \in T_m^- \\[2ex] 0 & \text{otherwise,} \end{cases} \tag{7.5}$$

where l_m is the length of the common edge, $A_m^\pm$ is the area of triangle $T_m^\pm$, and $\theta_m^+ = \theta_m^- = 0$ in this case. A few facts about the basis functions should be kept in mind. First, the basis functions are unitless. Units are carried by the expansion coefficients associated with the basis functions. Second, the support of a single basis function is limited to two, typically adjacent triangles. Third, the total current density in any given triangle is the vector sum of contributions from up to three distinct
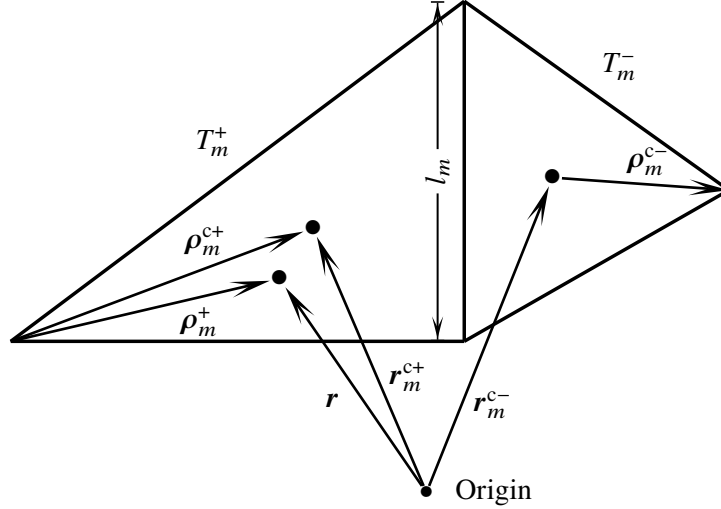
Figure 7.2: Triangular basis function geometry showing two triangles with a common edge. The superscript "c" denotes the centroid of the triangle.

basis functions whose common support includes that triangle. Fourth, any current flow normal to an edge is due entirely to the basis function associated with that edge. Finally, the basis functions are normalized so that the normal component of current density crossing the defining edge is unity[2] at any point of the edge. This means that the expansion coefficients $\{\mathcal{I}_m\}$ defined below can be interpreted as the total current crossing the associated edge(s) of the triangulated surface.

This definition is identical to that of [2] except for the introduction of the factors containing $\theta_n^\pm$. To see why these are necessary, consider the situation shown in Figure 7.3. Points within the unit cell are parameterized using

$$\boldsymbol{\rho} = \xi \boldsymbol{s}_1 + \eta \boldsymbol{s}_2, \quad 0 \leq \xi < 1, \ 0 \leq \eta < 1. \tag{7.6}$$

Unit cell boundaries are located at $\xi = 0$, $\xi = 1$, $\eta = 0$, and $\eta = 1$. In order to preserve the periodicity of the computed currents we agree to triangulate the unit cell in such a way that the number and location of the resulting edges along the $\xi = 0$ and $\xi = 1$ boundaries are identical, and similarly for the $\eta = 0$ and $\eta = 1$ boundaries. A pair of triangles T_m^+ and T_m^- with edges at the $\xi = 0$ and $\xi = 1$ boundaries, respectively, are shown in the figure. These edges both span the same range of η and so are parallel and congruent. A basis function is defined for each such pair of triangles on the $\xi = $ constant or $\eta = $ constant boundaries. We focus attention upon the basis function $\boldsymbol{f}_m$

---

[2]It is easy to see that the normal current density crossing an edge is constant by recalling that the equation of a plane in space is $\hat{\boldsymbol{n}} \cdot \boldsymbol{r} = $ constant. Similarly, the equation of the line containing the defining edge for the mth basis function is $\hat{\boldsymbol{n}} \cdot \boldsymbol{\rho}_m^\pm = $ constant. In fact, the normalization for the basis functions is selected so that this constant is unity in magnitude.
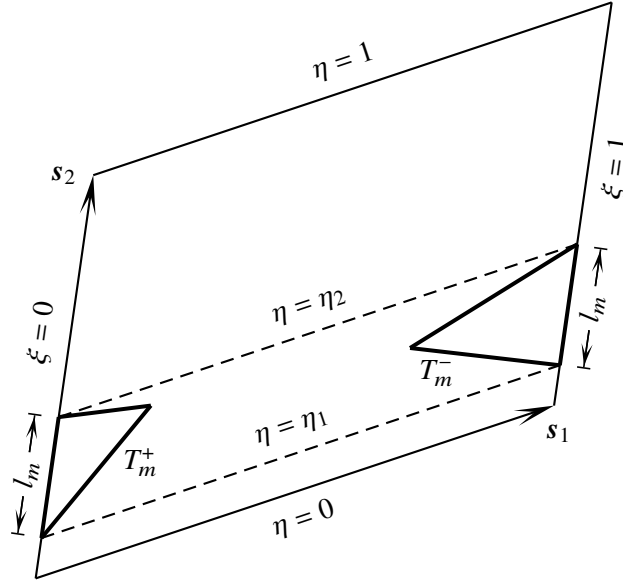
Figure 7.3: Triangular basis function geometry showing a pair of triangles located at the ξ = constant unit cell boundaries.

whose support is the union of the two triangle faces shown in the figure. Because of the boundary condition

$$V(\boldsymbol{r} + m\boldsymbol{s}_1 + n\boldsymbol{s}_2) = V(\boldsymbol{r})e^{-j(m\psi_1 + n\psi_2)}, \quad \forall m, n \in \mathbb{Z} \tag{7.7}$$

enforced on all currents and fields in the unit cell, it must be true that the normal current density crossing the edge at $\xi = 1$ is equal to that crossing the $\xi = 0$ edge multiplied by the factor $e^{-j\psi_1}$. Therefore, we must insist that

$$\theta_m^- = \theta_m^+ - \psi_1. \tag{7.8}$$

We will establish the convention that $\theta_m^{\pm} = 0$ for all edges except those along the $\xi = 1$ and $\eta = 1$ unit cell boundaries. Therefore, for the situation shown in Figure 7.3 we have $\theta_m^- = -\psi_1$ and similarly for all other triangles with one edge located on the $\xi = 1$ boundary. For triangles with an edge on the $\eta = 1$ boundary we set the corresponding phase to $-\psi_2$.

We now expand the unknown electric surface current density in a series of these basis functions:

$$\boldsymbol{J}_{\mathrm{s}}(\boldsymbol{\rho}) = \sum_{n=1}^{N_J} \frac{\mathcal{I}_n}{l_n} \boldsymbol{f}_n(\boldsymbol{\rho}). \tag{7.9}$$

The number of basis functions N_J is equal to the number of interior edges of the triangulated surface in the $z = 0$ plane of the unit cell plus the number of edges along the $\xi = 0$ and $\eta = 0$ borders of the unit cell. Note that $\mathcal{I}_n$ has units of A.

7.1.2   Impedance Matrix

Reduction to Matrix Equation

Having expanded the unknown current in a series of suitable basis functions, it is now desired to determine the coefficients in a way that satisfies Equation (7.2) as closely as possible. The method of moments transforms the functional Equation (7.2) to a matrix equation by enforcing it in an average manner. This is accomplished by first defining an inner product which maps a pair of functions to a single complex number, and then repeatedly *testing* the equation by taking the inner product of both sides with a number of *testing* or *weighting* functions.

The inner product used in testing Equation (7.2) is

$$\langle \boldsymbol{f}, \boldsymbol{g} \rangle = \iint \boldsymbol{f} \cdot \boldsymbol{g}^* \, \mathrm{d}S. \tag{7.10}$$

The asterisk denotes complex conjugation and the integration is performed over the portion of the $z = 0$ plane containing the common support of the two functions $\boldsymbol{f}$ and $\boldsymbol{g}$. We choose our testing functions to be the same as our basis functions (Galerkin's method). Then taking the inner product of (7.2) with each of the functions $\boldsymbol{f}_m/l_m$ for $m = 1, 2, \ldots, N_J$ yields

$$j\omega \left\langle \boldsymbol{A}, \boldsymbol{f}_m/l_m \right\rangle + \left\langle \boldsymbol{\nabla}\Phi, \boldsymbol{f}_m/l_m \right\rangle + \left\langle Z_s \boldsymbol{J}_\mathrm{s}, \boldsymbol{f}_m/l_m \right\rangle = \left\langle \boldsymbol{E}^\mathrm{inc}, \boldsymbol{f}_m/l_m \right\rangle,$$
$$m = 1, 2, \ldots, N_J. \tag{7.11}$$

Following [2] we can approximate the second term of (7.11) by

$$\left\langle \boldsymbol{\nabla}\Phi, \boldsymbol{f}_m/l_m \right\rangle \approx e^{-j\theta_m^-}\Phi(\boldsymbol{r}_m^{\mathrm{c}-}) - e^{-j\theta_m^+}\Phi(\boldsymbol{r}_m^{\mathrm{c}+}) \tag{7.12}$$

where $\boldsymbol{r}_m^{\mathrm{c}\pm}$ is the centroid of triangle $T_m^\pm$. The first term is also approximated as in the reference:

$$\left\langle \boldsymbol{A}, \boldsymbol{f}_m/l_m \right\rangle \approx \frac{1}{2} \left[\boldsymbol{A}(\boldsymbol{r}_m^{\mathrm{c}+}) \cdot \boldsymbol{\rho}_m^{\mathrm{c}+} e^{-j\theta_m^+} + \boldsymbol{A}(\boldsymbol{r}_m^{\mathrm{c}-}) \cdot \boldsymbol{\rho}_m^{\mathrm{c}-} e^{-j\theta_m^-} \right]. \tag{7.13}$$

$\boldsymbol{\rho}_m^{\mathrm{c}\pm}$ is the vector $\boldsymbol{\rho}_m^\pm$ evaluated at the centroid of the corresponding triangle.

Substituting the expansion of the current (7.9) into (7.11) yields the desired matrix equation.

$$\boldsymbol{\mathcal{Z}}\boldsymbol{\mathcal{I}} = \boldsymbol{\mathcal{V}}, \tag{7.14}$$

where $\boldsymbol{\mathcal{Z}} = [\mathcal{Z}_{mn}]$ is the so-called *generalized impedance matrix*, a square matrix of order N_J with units of Ω. $\boldsymbol{\mathcal{I}} = [\mathcal{I}_m]$ is the column matrix of unknown current coefficients with units of A. $\boldsymbol{\mathcal{V}} = [\mathcal{V}_m]$ is the excitation vector (or *generalized voltage vector*) with units of V. The elements of the generalized impedance matrix are

$$\mathcal{Z}_{mn} = \left\langle Z_s \boldsymbol{f}_n/l_n, \boldsymbol{f}_m/l_m \right\rangle$$
$$+ j\omega \left(\boldsymbol{A}_{mn}^+ \cdot \frac{\boldsymbol{\rho}_m^{\mathrm{c}+}}{2} e^{-j\theta_m^+} + \boldsymbol{A}_{mn}^- \cdot \frac{\boldsymbol{\rho}_m^{\mathrm{c}-}}{2} e^{-j\theta_m^-} \right) + \Phi_{mn}^- e^{-j\theta_m^-} - \Phi_{mn}^+ e^{-j\theta_m^+} \tag{7.15}$$

where

$$A_{mn}^{\pm} \equiv \frac{1}{l_n} \iint G_{xx}^A(r_m^{c\pm}; r') f_n(r') \, dS'$$

$$= \frac{e^{j\theta_n^+}}{2A_n^+} \iint_{T_n^+} G_{xx}^A(r_m^{c\pm}; r') \rho_n^+ \, dS' + \frac{e^{j\theta_n^-}}{2A_n^-} \iint_{T_n^-} G_{xx}^A(r_m^{c\pm}; r') \rho_n^- \, dS' \qquad (7.16)$$

and

$$\Phi_{mn}^{\pm} \equiv \frac{j}{\omega l_n} \iint G^{\Phi}(r_m^{c\pm}; r') \nabla'_s \cdot f_n(r') \, dS'$$

$$= \frac{j}{\omega} \left[\frac{e^{j\theta_n^+}}{A_n^+} \iint_{T_n^+} G^{\Phi}(r_m^{c\pm}; r') \, dS' - \frac{e^{j\theta_n^-}}{A_n^-} \iint_{T_n^-} G^{\Phi}(r_m^{c\pm}; r') \, dS' \right] \qquad (7.17)$$

and we have used the fact [2] that

$$\nabla_s \cdot f_n(r) = \begin{cases} \dfrac{l_n}{A_n^+} e^{j\theta_n^+} & \text{if } r \in T_n^+ \\ \dfrac{-l_n}{A_n^-} e^{j\theta_n^-} & \text{if } r \in T_n^- \\ 0 & \text{otherwise} \end{cases} \qquad (7.18)$$

which holds true for a basis function consisting of a pair of adjacent triangles. For basis functions defined on nonadjacent pairs, the expression for the surface divergence includes a pair of line singularities whose contributions to (7.17) can be shown to cancel.

Efficient Evaluation of the Generalized Impedance Matrix

The authors of [2] discuss the way in which redundant calculations can be avoided by considering face-pair contributions to $\mathcal{Z}$ rather than the edge-pair contributions used in the definitions of (7.16) and (7.17). Here we apply the same technique using our potential Green's functions specific to this problem. In addition, we individually track the contributions to the impedance matrix exhibiting distinct frequency dependence, thus allowing a wide-band implementation.

Vector Potential Contributions   Consider first a typical vector integral needed to evaluate $\mathcal{Z}_{mn}$. The quantity

$$A_i^{uv} = \frac{e^{j\theta_i^{\pm}}}{2A^v} \iint_{T^v} G_{xx}^A(r^{cu}; r') \rho_i \, dS' \qquad (7.19)$$

represents the magnetic vector potential at the centroid r^{cu} of triangle T^u due to the ith basis function defined on triangle T^v. In (7.19) we have temporarily assumed a local numbering scheme on the source triangle, with vertices at r_1, r_2, and r_3, and where

$$\rho_i = \pm(r' - r_i), \quad i = 1, 2, 3. \qquad (7.20)$$

The plus sign is selected in (7.19) and (7.20) if the associated basis function defines positive current to flow *out* through the ith edge of the triangle, which lies opposite the ith vertex. Using the expressions for the magnetic vector potential Green's function given in Chapter 5, Equation (7.19) can be written as the sum of a frequency dependent term arising from the modal difference series, added to several contributions arising from the spatial series:

$$A_i^{uv} = \frac{\tilde{\mu}}{4\pi} e^{j\theta_i^{\pm}} \left[4\pi I_{1i}^{uv} + \frac{1}{2A^v} \iint_{T^v} \frac{\rho_i}{\rho_{00}^{cu}} \, dS' + u J_i^{uv} + \frac{c_3(\mu_s, \epsilon_s, \mu_{s+1}, \epsilon_{s+1})}{u} K_i^{uv} \right] \tag{7.21}$$

where

$$I_{1i}^{uv} = \frac{1}{2A^v} \iint_{T^v} \Sigma_{M1}(r^{cu}; r') \rho_i \, dS', \tag{7.22a}$$

$$\Sigma_{M1}(r^{cu}; r') = \frac{1}{2A} \sum_{m,n} \left[\frac{2V_i^{\mathrm{TE}}(\beta_{mn}, z_s, z_s)}{j\omega\tilde{\mu}} - \frac{1}{\kappa_{mn}} - \frac{c_3(\mu_s, \epsilon_s, \mu_{s+1}, \epsilon_{s+1})}{\kappa_{mn}^3} \right] e^{-j\beta_{mn} \cdot (r^{cu} - r')}, \tag{7.22b}$$

$$J_i^{uv} = \frac{1}{2A^v} \iint_{T^v} \rho_i \sum_{m,n} \frac{e^{-u\rho_{mn}^{cu}} - \delta_{m0}\delta_{n0}}{u\rho_{mn}^{cu}} e^{-j(m\psi_1 + n\psi_2)} \, dS', \tag{7.22c}$$

$$K_i^{uv} = \frac{1}{2A^v} \iint_{T^v} \rho_i \sum_{m,n} e^{-u\rho_{mn}^{cu}} e^{-j(m\psi_1 + n\psi_2)} \, dS', \tag{7.22d}$$

and $\rho_{mn}^{cu} = \|r^{cu} - r' - ms_1 - ns_2\|$. Note that the only frequency dependence in (7.21) occurs in the terms I_{1i}^{uv} and c_3. Therefore, the contrubutions due to the singular integral, J_i^{uv} and K_i^{uv} can be computed once, stored, and combined appropriately at each new analysis frequency. Although I_{1i}^{uv} must be computed anew at each frequency, the modal difference series occurring in its integrand can be very rapidly evaluated by simple interpolation into a two-dimensional table obtained from the FFT (Section 5.4).

Calculation of the singular integral in (7.21) is discussed in Appendix B. Efficient evaluation of the remaining integrals is discussed next.

Each of the integrals I_{1i}^{uv}, J_i^{uv}, and K_i^{uv} is of the form

$$L_i = \hat{x} L_{ix} + \hat{y} L_{iy} = \frac{1}{2A^v} \iint_{T^v} \rho_i \, f(r; r') \, dS'. \tag{7.23}$$

Each involves a bounded, well-behaved integrand which can be integrated numerically using a low-order Gaussian scheme designed especially for surface integration (cubature) over triangular domains [18]. However, it is advantageous to first express them in terms of integrals which do not depend on the particular basis function index i. To accomplish this, we employ the so-called *normalized area coordinates* (ξ, η, ζ).[3] The source point can be written in terms of area coordinates as

$$r' = \xi r_1 + \eta r_2 + \zeta r_3 \tag{7.24}$$

---

[3]In this section "η" is used to mean one of the normalized area coordinates. Elsewhere in these notes the same symbol may be used to represent the intrinsic impedance of a dielectric medium.

so that

$$\boldsymbol{\rho}_i = \pm(\boldsymbol{r}' - \boldsymbol{r}_i) = \pm(\xi\boldsymbol{r}_1 + \eta\boldsymbol{r}_2 + \zeta\boldsymbol{r}_3 - \boldsymbol{r}_i) . \tag{7.25}$$

where the $\{\boldsymbol{r}_i\}$ are the vertices of the source triangle T^v having area A^v. Only two of the three (nonnegative) coordinates can be independently specified since $\xi + \eta + \zeta = 1$ for points in the triangle. The area element in normalized area coordinates is $\mathrm{d}S' = 2A^v\,\mathrm{d}\xi\,\mathrm{d}\eta$.

The desired integral $\boldsymbol{L}_i$ can be expressed in terms of scalar integrals over normalized area coordinates which are independent of i in the following way.

$$\boldsymbol{L}_i = \pm\left[\boldsymbol{r}_1 L_\xi + \boldsymbol{r}_2 L_\eta + \boldsymbol{r}_3 L_\zeta - \boldsymbol{r}_i L\right] \tag{7.26}$$

where

$$L_\xi = \int_0^1 \int_0^{1-\eta} \xi\, f(\boldsymbol{r}^{cu}; \xi\boldsymbol{r}_1 + \eta\boldsymbol{r}_2 + \zeta\boldsymbol{r}_3)\,\mathrm{d}\xi\,\mathrm{d}\eta \tag{7.27a}$$

$$L_\eta = \int_0^1 \int_0^{1-\eta} \eta\, f(\boldsymbol{r}^{cu}; \xi\boldsymbol{r}_1 + \eta\boldsymbol{r}_2 + \zeta\boldsymbol{r}_3)\,\mathrm{d}\xi\,\mathrm{d}\eta \tag{7.27b}$$

$$L_\zeta = \int_0^1 \int_0^{1-\eta} \zeta\, f(\boldsymbol{r}^{cu}; \xi\boldsymbol{r}_1 + \eta\boldsymbol{r}_2 + \zeta\boldsymbol{r}_3)\,\mathrm{d}\xi\,\mathrm{d}\eta \tag{7.27c}$$

$$L = \int_0^1 \int_0^{1-\eta} f(\boldsymbol{r}^{cu}; \xi\boldsymbol{r}_1 + \eta\boldsymbol{r}_2 + \zeta\boldsymbol{r}_3)\,\mathrm{d}\xi\,\mathrm{d}\eta. \tag{7.27d}$$

It is important to note that the above integrals are not all independent. We also have that

$$L = L_\xi + L_\eta + L_\zeta \tag{7.28}$$

so that in general there are three integrals to be numerically evaluated for each observation point / source triangle pair. These integrals, when weighted according to Equation (7.26) contribute to as many as nine entries of $\mathfrak{Z}$, depending on the number of basis functions defined in each triangle. They are computed using the seven-point cubature formula from [18],

$$\int_0^1 \int_0^{1-\eta} f(\xi, \eta)\,\mathrm{d}\xi\,\mathrm{d}\eta \approx \sum_{k=1}^7 w_k f(\xi_k, \eta_k). \tag{7.29}$$

The sample points and weights are given in Table 7.1.

Scalar Potential Contributions   In addition to the vector integrals just discussed, it is also necessary to calculate scalar integrals of the form

$$\Phi_i^{uv} = \pm\frac{j e^{j\theta_i^\pm}}{\omega A^v} \iint_{T^v} G^\Phi(\boldsymbol{r}^{cu}; \boldsymbol{r}')\,\mathrm{d}S'. \tag{7.30}$$

Φ_i^{uv} is the electric scalar potential at the centroid of triangle T^u due to the surface electric charge density associated with the ith basis function defined on triangle T^v. As before, the sign is taken

k	ξ_k	η_k	w_k
1	0.33333333	0.33333333	0.112500000
2	0.05971587	0.47014206	0.066197075
3	0.47014206	0.05971587	0.066197075
4	0.47014206	0.47014206	0.066197075
5	0.79742699	0.10128651	0.062969590
6	0.10128651	0.79742699	0.062969590
7	0.10128651	0.10128651	0.062969590

Table 7.1: Sample points and weights for seven point triangular cubature.

to be positive if the basis function in question defines positive reference current to flow *out* of T^v through the ith edge. We proceed as before, using the results in Chapter 5 for the electric scalar potential Green's function to write the above integral as

$$\Phi_i^{uv} = \frac{\pm j e^{j\theta_i^\pm}}{2\pi\omega\bar{\epsilon}} \left[4\pi I_2^{uv} + \frac{1}{2A^v} \iint_{T^v} \frac{\mathrm{d}S'}{\rho_{00}^{cu}} + uJ^{uv} + \frac{d_3(\mu_s,\epsilon_s,\mu_{s+1},\epsilon_{s+1})}{u} K^{uv} \right] \qquad (7.31)$$

where

$$I_2^{uv} = \frac{1}{2A^v} \iint_{T^v} \Sigma_{M2}(r^{cu};r') \, \mathrm{d}S', \qquad (7.32a)$$

$$\Sigma_{M2}(r^{cu};r') = \frac{1}{2A} \sum_{m,n} \left[\frac{2j\omega\bar{\epsilon}(V_i^{\mathrm{TM}} - V_i^{\mathrm{TE}})}{\beta_{mn}^2} - \frac{1}{\kappa_{mn}} - \frac{d_3(\mu_s,\epsilon_s,\mu_{s+1},\epsilon_{s+1})}{\kappa_{mn}^3} \right] e^{-j\beta_{mn}\cdot(r^{cu}-r')}, \quad (7.32b)$$

$$J^{uv} = \frac{1}{2A^v} \iint_{T^v} \sum_{m,n} \frac{e^{-u\rho_{mn}^{cu}} - \delta_{m0}\delta_{n0}}{u\rho_{mn}^{cu}} e^{-j(m\psi_1+n\psi_2)} \, \mathrm{d}S', \qquad (7.32c)$$

$$K^{uv} = \frac{1}{2A^v} \iint_{T^v} \sum_{m,n} e^{-u\rho_{mn}^{cu}} e^{-j(m\psi_1+n\psi_2)} \, \mathrm{d}S'. \qquad (7.32d)$$

Note that J^{uv} and K^{uv} have already been computed as scalar portions of the corresponding vector integrals $\boldsymbol{J}_i^{uv}$ and $\boldsymbol{K}_i^{uv}$, respectively (see Equation 7.27d). The only new quantities to be computed are I_2^{uv} and the singular integral. The integral I_2^{uv} can be computed in exactly the same manner as I_1^{uv} using the FFT. Evaluation of the singular integral is discussed in Appendix B. Note that the only frequency dependence in (7.31) occurs in the factor ω and the terms I_2^{uv} and d_3.

Surface Impedance Contributions   The contribution to the generalized impedance matrix due to finite surface impedance of the conducting layer is given by the inner product

$$\langle Z_s \boldsymbol{f}_n/l_n, \boldsymbol{f}_m/l_m \rangle. \qquad (7.33)$$

Note that in most cases basis functions m and n do share any common support and the inner product yields zero. Otherwise, two cases remain. Either $n = m$, or $n \neq m$ with edges n and m common to a single triangle. The formulas for the inner product in these cases, assuming that the surface impedance is constant on each triangle face, are derived in Appendix B.1. For $n = m$ the result is

$$\left\langle Z_s \boldsymbol{f}_n / l_n, \boldsymbol{f}_n / l_m \right\rangle = \frac{Z_s^+}{48 A_n^+} (3 l_a^{+2} + 3 l_b^{+2} - l_n^2) + \frac{Z_s^-}{48 A_n^-} (3 l_a^{-2} + 3 l_b^{-2} - l_n^2) \qquad (7.34)$$

where the plus and minus signs refer to triangles T_n^+ and T_n^-, respectively, and $l_a^\pm$ and $l_b^\pm$ are the lengths of the two other edges on these triangles. For $n \neq m$ the result is

$$\left\langle Z_s \boldsymbol{f}_n / l_n, \boldsymbol{f}_m / l_m \right\rangle = \pm e^{j(\theta_n - \theta_m)} \frac{Z_s^{mn}}{48 A^{mn}} (l_m^2 + l_n^2 - 3 l_p^2) \qquad (7.35)$$

where the double superscript mn refers to the triangle common to basis functions m and n and l_p is the length of the third edge. The minus sign is taken if one of the basis functions $\boldsymbol{f}_m$ and $\boldsymbol{f}_n$ define positive current flow out of the triangle while the other basis function defines positive current flow into the triangle. If the two basis functions agree in this respect the plus sign is used.

7.1.3   Generalized Voltage Vector

The elements of the generalized voltage vector are defined as

$$\mathcal{V}_m = \left\langle \boldsymbol{E}^{\text{inc}}, \boldsymbol{f}_m / l_m \right\rangle = \frac{1}{l_m} \iint \boldsymbol{E}^{\text{inc}} \cdot \boldsymbol{f}_m^* \, dS, \quad m = 1, 2, \dots, N_J. \qquad (7.36)$$

The incident field $\boldsymbol{E}^{\text{inc}}$ is the field that would exist in the absence of the FSS metalization due to an incoming, normalized Floquet mode from Region 1 or N with unit amplitude coefficient. This scenario was treated in Chapter 6 and we use the results derived there. Let $i \in \{1, N\}$ be the region index designating the source of the incoming Floquet mode. The mode index is $q = (p_q, m_q, n_q)$ where $p_q = 1$ for TE modes and $p_q = 2$ for TM modes. The transverse portion of the incident electric field evaluated in the $z = z_s$ plane is:

$$\bar{\boldsymbol{I}}_z \cdot \boldsymbol{E}^{\text{inc}}(\boldsymbol{\rho}) = V(z_s) \boldsymbol{e}_q^{(i)}(\boldsymbol{\rho}) = V(z_s) c_q^{(i)} \hat{\boldsymbol{t}}_q e^{-j \boldsymbol{\beta}_{m_q n_q} \cdot \boldsymbol{\rho}} \qquad (7.37)$$

where the modal polarization vector $\hat{\boldsymbol{t}}_q$ is defined as

$$\hat{\boldsymbol{t}}_q = \begin{cases} \hat{\boldsymbol{z}} \times \hat{\boldsymbol{\beta}}_{mn} & p_q = 1 \text{ (TE modes)}, \\ \hat{\boldsymbol{\beta}}_{mn} & p_q = 2 \text{ (TM modes)}, \end{cases} \qquad (7.38)$$

and $V(z_s)$ is the equivalent transmission line voltage evaluated at $z = z_s$ using the formulas presented in Chapter 6.

Upon substituting the incident field of (7.37) into (7.36) we find that

$$
\begin{aligned}
\mathcal{V}_m &= \frac{V(z_s)c_q^{(i)}}{l_m}\hat{\boldsymbol{t}}_q \cdot \iint f_m^*(\boldsymbol{\rho})e^{-j\boldsymbol{\beta}_{m_q n_q}\cdot\boldsymbol{\rho}}\,\mathrm{d}S \\
&= \frac{V(z_s)c_q^{(i)}}{l_m}\hat{\boldsymbol{t}}_q \cdot \tilde{\boldsymbol{f}}_m^*(\boldsymbol{\beta}_{m_q n_q}), \quad m = 1, 2, \dots, N_J,
\end{aligned}
\tag{7.39}
$$

where

$$
\tilde{\boldsymbol{f}}_m(\boldsymbol{k}) = \iint \boldsymbol{f}_m(\boldsymbol{\rho})\, e^{j\boldsymbol{k}\cdot\boldsymbol{\rho}}\,\mathrm{d}S
\tag{7.40}
$$

is the Fourier transform of the mth basis function evaluated at $\boldsymbol{k} = \hat{\boldsymbol{x}}k_x + \hat{\boldsymbol{y}}k_y$. The Fourier transform is numerically evaluated using the formulas of [19].

7.2   Magnetic Current Mixed Potential Integral Equation

In this section we consider an FSS that is modeled using equivalent magnetic surface current. This choice is convenient when more than half of the unit cell area is occupied by perfectly conducting metal.

We assume that the primary excitation is an incoming Floquet mode with unit amplitude, incident upon the multilayered structure from either Region 1 or N.

Using the equivalence principle, the FSS aperture S is filled in with PEC and an unknown magnetic surface current ($\boldsymbol{M}$ on the incident side, and $-\boldsymbol{M}$ on the far side) is impressed just outside the metal surface, so as to reproduce the scattered field exactly in all regions. The incident field is thus the field that would exist in the structure with an unperforated ground plane at $z = z_s$. It includes reflections from the ground plane on the incident side of z_s and is zero on the far or transmitted side.

In the case where the incoming wave is incident from Region 1, the boundary value problem to be solved is

$$
\bar{\boldsymbol{I}}_z \cdot [\boldsymbol{H}^{\mathrm{inc}}(x, y, z_s) + \boldsymbol{H}^{(s)}\{\boldsymbol{M}\}(x, y, z_s)] = \bar{\boldsymbol{I}}_z \cdot \boldsymbol{H}^{(s+1)}\{-\boldsymbol{M}\}(x, y, z_s), \quad (\boldsymbol{\rho} \in S)
\tag{7.41}
$$

where $\boldsymbol{H}^{\mathrm{inc}}$ is the total "incident" magnetic field in the presence of the unperforated PEC plane at $z = 0$, $\boldsymbol{H}^{(s)}\{\boldsymbol{M}\}(\boldsymbol{r})$ is the magnetic field evaluated at point $\boldsymbol{r} \in \{z < z_s\}$ that would be radiated by the periodic magnetic surface current $\boldsymbol{M}$ impressed on the groundplane at $z = z_s - 0$, and $\boldsymbol{H}^{(s+1)}\{\boldsymbol{M}\}(\boldsymbol{r})$ is the magnetic field evaluated at point $\boldsymbol{r} \in \{z > z_s\}$ that would be radiated by the periodic magnetic surface current $\boldsymbol{M}$ impressed on the groundplane at $z = z_s + 0$. In the case where the incoming wave is incident from Region N, the boundary value problem to be solved is

$$
\bar{\boldsymbol{I}}_z \cdot \boldsymbol{H}^{(s)}\{-\boldsymbol{M}\}(x, y, z_s) = \bar{\boldsymbol{I}}_z \cdot [\boldsymbol{H}^{\mathrm{inc}}(x, y, z_s) + \boldsymbol{H}^{(s+1)}\{\boldsymbol{M}\}(x, y, z_s)], \quad (\boldsymbol{\rho} \in S)
\tag{7.42}
$$

Using the linearity of the magnetic field operator allows us to rewrite the both integral equations in a unified form:

$$
-\bar{\boldsymbol{I}}_z \cdot [\boldsymbol{H}^{(s)}\{\boldsymbol{M}\}(\boldsymbol{\rho}) + \boldsymbol{H}^{(s+1)}\{\boldsymbol{M}\}(\boldsymbol{\rho})] = \bar{\boldsymbol{I}}_z \cdot \boldsymbol{H}^{\mathrm{inc}}(\boldsymbol{\rho}), \quad (\boldsymbol{\rho} \in S)
\tag{7.43}
$$

where it is to be understood that ρ represents a point in the plane $z = z_s$. In terms of potentials the boundary value problem becomes

$$[-j\omega \boldsymbol{F}(\rho) + \boldsymbol{\nabla}\Psi(\rho)] \cdot \bar{\boldsymbol{I}}_z = \boldsymbol{H}^{\mathrm{inc}}(\rho) \cdot \bar{\boldsymbol{I}}_z, \quad (\rho \in S) \tag{7.44}$$

where the potentials can be expressed as superposition integrals

$$\bar{\boldsymbol{I}}_z \cdot \boldsymbol{F}(\rho) = \iint G_{xx}^F(\rho - \rho') \cdot \boldsymbol{M}(\rho')\,\mathrm{d}S', \tag{7.45}$$

$$\Psi(\rho) = \iint G^\Psi(\rho - \rho') \cdot q_{\mathrm{m}}(\rho')\,\mathrm{d}S'. \tag{7.46}$$

In (7.45) and (7.46), $\boldsymbol{M}$ and q_{m} are the unknown induced magnetic surface current and surface charge densities, respectively, which will be determined by enforcing Equation (7.44) in an approximate manner using the method of moments. The functions G_{xx}^F and G^Ψ are the sum of the left-looking and right-looking Green's functions as defined in Chapter 5:

$$G_{xx}^F(\rho - \rho') = \overleftarrow{G}_{xx}^F(\rho - \rho', z_s, z_s) + \overrightarrow{G}_{xx}^F(\rho - \rho', z_s, z_s) \tag{7.47a}$$

$$G^\Psi(\rho - \rho') = \overleftarrow{G}^\Psi(\rho - \rho', z_s, z_s) + \overrightarrow{G}^\Psi(\rho - \rho', z_s, z_s). \tag{7.47b}$$

We again employ the triangle subdomain basis functions that were described in Section 7.1.1.

We now expand the unknown magnetic surface current density in a series of triangle-pair basis functions:

$$\boldsymbol{M}(\rho) = \sum_{n=1}^{N_M} \frac{\mathcal{V}_n}{l_n} \boldsymbol{f}_n(\rho). \tag{7.48}$$

The number of basis functions N_M is equal to the number of interior edges of the triangulated aperture in the $z = 0$ plane of the unit cell plus the number of edges along the $\xi = 0$ and $\eta = 0$ borders of the unit cell. Note that $\mathcal{V}_n$ has units of V.

7.2.1   Admittance Matrix

Reduction to Matrix Equation

Having expanded the unknown magnetic surface current in a series of suitable basis functions, it is now desired to determine the coefficients in a way that satisfies Equation (7.44) as closely as possible.

We choose our testing functions to be the same as our basis functions (Galerkin's method). Then taking the inner product of (7.44) with each of the functions $\boldsymbol{f}_m/l_m$ for $m = 1, 2, \ldots, N_M$ yields

$$-j\omega \left\langle \boldsymbol{F}, \boldsymbol{f}_m/l_m \right\rangle + \left\langle \boldsymbol{\nabla}\Psi, \boldsymbol{f}_m/l_m \right\rangle = \left\langle \boldsymbol{H}^{\mathrm{inc}}, \boldsymbol{f}_m/l_m \right\rangle,$$

$$m = 1, 2, \ldots, N_M. \tag{7.49}$$

We approximate the inner products in the same manner as was done for the case of electric sources:

$$\left\langle \nabla \Psi, f_m/l_m \right\rangle \approx e^{-j\theta_m^-}\Psi(r_m^{\mathrm{c}-}) - e^{-j\theta_m^+}\Psi(r_m^{\mathrm{c}+}) \tag{7.50}$$

where $r_m^{\mathrm{c}\pm}$ is the centroid of triangle $T_m^{\pm}$. Also, we use

$$\left\langle F, f_m/l_m \right\rangle \approx \frac{1}{2}\left[F(r_m^{\mathrm{c}+}) \cdot \rho_m^{\mathrm{c}+} e^{-j\theta_m^+} + F(r_m^{\mathrm{c}-}) \cdot \rho_m^{\mathrm{c}-} e^{-j\theta_m^-} \right]. \tag{7.51}$$

$\rho_m^{\mathrm{c}\pm}$ is the vector $\rho_m^{\pm}$ evaluated at the centroid of the corresponding triangle.

Substituting the expansion of the current (7.48) into (7.49) yields the desired matrix equation.

$$\mathcal{Y}\mathcal{V} = \mathcal{I}, \tag{7.52}$$

where $\mathcal{Y} = [\mathcal{Y}_{mn}]$ is the so-called *generalized admittance matrix*, a square matrix of order N_M with units of S. $\mathcal{V} = [\mathcal{V}_m]$ is the column matrix of unknown magnetic current coefficients with units of V. $\mathcal{I} = [\mathcal{I}_m]$ is the excitation vector (or *generalized current vector*) with units of A. The elements of the generalized admittance matrix are

$$\mathcal{Y}_{mn} = -j\omega\left(F_{mn}^+ \cdot \frac{\rho_m^{\mathrm{c}+}}{2}e^{-j\theta_m^+} + F_{mn}^- \cdot \frac{\rho_m^{\mathrm{c}-}}{2}e^{-j\theta_m^-} \right) + \Psi_{mn}^- e^{-j\theta_m^-} - \Psi_{mn}^+ e^{-j\theta_m^+} \tag{7.53}$$

where

$$
\begin{aligned}
F_{mn}^{\pm} &\equiv \frac{1}{l_n} \iint G_{xx}^F(r_m^{\mathrm{c}\pm}; r') f_n(r')\, \mathrm{d}S' \\
&= \frac{e^{j\theta_n^+}}{2A_n^+}\iint_{T_n^+} G_{xx}^F(r_m^{\mathrm{c}\pm}; r')\,\rho_n^+\, \mathrm{d}S' + \frac{e^{j\theta_n^-}}{2A_n^-}\iint_{T_n^-} G_{xx}^F(r_m^{\mathrm{c}\pm}; r')\,\rho_n^-\, \mathrm{d}S'
\end{aligned}
\tag{7.54}
$$

and

$$
\begin{aligned}
\Psi_{mn}^{\pm} &\equiv \frac{j}{\omega l_n} \iint G^{\Psi}(r_m^{\mathrm{c}\pm}; r')\nabla_s' \cdot f_n(r')\, \mathrm{d}S' \\
&= \frac{j}{\omega}\left[\frac{e^{j\theta_n^+}}{A_n^+}\iint_{T_n^+} G^{\Psi}(r_m^{\mathrm{c}\pm}; r')\, \mathrm{d}S' - \frac{e^{j\theta_n^-}}{A_n^-}\iint_{T_n^-} G^{\Psi}(r_m^{\mathrm{c}\pm}; r')\, \mathrm{d}S' \right]
\end{aligned}
\tag{7.55}
$$

Efficient Evaluation of the Generalized Admittance Matrix

Vector Potential Contributions   Consider first a typical vector integral needed to evaluate $\mathcal{Y}_{mn}$. The quantity

$$F_i^{uv} = \frac{e^{j\theta_i^{\pm}}}{2A^v} \iint_{T^v} G_{xx}^F(r^{\mathrm{c}u}; r')\,\rho_i\, \mathrm{d}S' \tag{7.56}$$

represents the electric vector potential at the centroid $r^{\mathrm{c}u}$ of triangle T^u due to the ith basis function defined on triangle T^v. In (7.56) we have temporarily assumed a local numbering scheme on the

source triangle, with vertices at r_1, r_2, and r_3, and where ρ_i is defined in Equation (7.20). Using the expressions for the electric vector potential Green's function given in Chapter 5, Equation (7.56) can be written as the sum of a frequency dependent term arising from the modal difference series, added to several contributions arising from the spatial series:

$$F_i^{uv} = -\frac{\bar{\epsilon}}{\pi} e^{j\theta_i^{\pm}} \left[\frac{\pi \epsilon_0}{\bar{\epsilon}} I_{1i}^{'uv} + \frac{1}{2A^v} \iint_{T^v} \frac{\rho_i}{\rho_{00}^{cu}} \, \mathrm{d}S' + u J_i^{uv} + \frac{c_3^{(s)} \epsilon_s + c_3^{(s+1)} \epsilon_{s+1}}{2\bar{\epsilon}u} K_i^{uv} \right] \qquad (7.57)$$

where

$$I_{1i}^{'uv} = \frac{1}{2A^v} \iint_{T^v} \Sigma'_{M1}(r^{cu}; r') \, \rho_i \, \mathrm{d}S' \qquad (7.58)$$

and Σ'_{M1} is defined in Equation (5.26). Note that the only frequency dependence in (7.57) occurs in the terms I_{1i}^{uv} and c_3. Therefore, the contrubutions due to the singular integral, J_i^{uv} and K_i^{uv} can be computed once, stored, and combined appropriately at each new analysis frequency. Although the value of $I_{1i}^{'uv}$ must be computed anew at each frequency, the modal difference series occurring in its integrand can be very rapidly evaluated by simple interpolation into a two-dimensional table obtained from the FFT (Section 5.4).

Scalar Potential Contributions   In addition to the vector integrals just discussed, it is also necessary to calculate scalar integrals of the form

$$\Psi_i^{uv} = \pm \frac{j e^{j\theta_i^{\pm}}}{\omega A^v} \iint_{T^v} G^{\Psi}(r^{cu}; r') \, \mathrm{d}S'. \qquad (7.59)$$

Ψ_i^{uv} is the magnetic scalar potential evaluated at the centroid of triangle T^u due to the surface magnetic charge density associated with the ith basis function defined on triangle T^v. As before, the sign is taken to be positive if the basis function in question defines positive reference current to flow *out* of T^v through the ith edge. We proceed as before, using the results of Chapter 5 for the magnetic scalar potential Green's function to write the above integral as

$$\Psi_i^{uv} = \frac{\pm 2 j e^{j\theta_i^{\pm}}}{\pi \omega \tilde{\mu}} \left[\frac{\pi \tilde{\mu}}{\mu_0} I_{2i}^{'uv} + \frac{1}{2A^v} \iint_{T^v} \frac{\mathrm{d}S'}{\rho_{00}^{cu}} + u J_i^{uv} + \frac{\tilde{\mu}}{2u} \left(\frac{d_3^{(s)}}{\mu_s} + \frac{d_3^{(s+1)}}{\mu_{s+1}} \right) K_i^{uv} \right] \qquad (7.60)$$

where

$$I_{2i}^{'uv} = \frac{1}{2A^v} \iint_{T^v} \Sigma'_{M2}(r^{cu}; r') \, \rho_i \, \mathrm{d}S' \qquad (7.61)$$

and Σ'_{M2} is defined in Equation (5.26).

All of the integrals in (7.60) have been previously discussed. Note that the only frequency dependence occurs in the terms $I_{2i}^{'uv}$ and d_3.

7.2.2 Generalized Current Vector

The elements of the generalized current vector are defined as

$$\mathcal{I}_m = \langle \boldsymbol{H}^{\text{inc}}, \boldsymbol{f}_m/l_m \rangle = \frac{1}{l_m} \iint \boldsymbol{H}^{\text{inc}} \cdot \boldsymbol{f}_m^* \, dS, \quad m = 1, 2, \ldots, N_J. \tag{7.62}$$

The incident field $\boldsymbol{H}^{\text{inc}}$ is the field that would exist in the presence of the unperforated FSS metalization due to an incoming, normalized Floquet mode from Region 1 or N with unit amplitude coefficient. This scenario was treated in Chapter 6 and we use the results derived there. Let $i \in \{1, N\}$ be the region index designating the source of the incoming Floquet mode. The mode index is $q = (p_q, m_q, n_q)$ where $p_q = 1$ for TE modes and $p_q = 2$ for TM modes. The transverse portion of the incident magnetic field evaluated in the $z = z_s$ plane is:

$$\bar{\boldsymbol{I}}_z \cdot \boldsymbol{H}^{\text{inc}}(\boldsymbol{\rho}) = I(z_s)\boldsymbol{h}_q^{(i)}(\boldsymbol{\rho}) = I(z_s)Y_q^{(i)} c_q^{(i)} \hat{\boldsymbol{z}} \times \hat{\boldsymbol{t}}_q e^{-j\boldsymbol{\beta}_{m_q n_q} \cdot \boldsymbol{\rho}} \tag{7.63}$$

where the modal polarization vector $\hat{\boldsymbol{t}}_q$ was defined in (7.38) and $I(z_s)$ is the equivalent transmission line current evaluated at $z = z_s$ using the formulas presented in Chapter 6.

Upon substituting the incident field of (7.63) into (7.62) we find that

$$\begin{aligned}
\mathcal{I}_m &= \frac{I(z_s)Y_q^{(i)} c_q^{(i)}}{l_m} \hat{\boldsymbol{z}} \times \hat{\boldsymbol{t}}_q \cdot \iint \boldsymbol{f}_m^*(\boldsymbol{\rho}) e^{-j\boldsymbol{\beta}_{m_q n_q} \cdot \boldsymbol{\rho}} \, dS \\
&= \frac{I(z_s)Y_q^{(i)} c_q^{(i)}}{l_m} \hat{\boldsymbol{z}} \times \hat{\boldsymbol{t}}_q \cdot \tilde{\boldsymbol{f}}_m^*(\boldsymbol{\beta}_{m_q n_q}), \quad m = 1, 2, \ldots, N_M,
\end{aligned} \tag{7.64}$$

where

$$\tilde{\boldsymbol{f}}_m(\boldsymbol{k}) = \iint \boldsymbol{f}_m(\boldsymbol{\rho}) \, e^{j\boldsymbol{k} \cdot \boldsymbol{\rho}} \, dS \tag{7.65}$$

is the Fourier transform of the mth basis function evaluated at $\boldsymbol{k} = \hat{\boldsymbol{x}}k_x + \hat{\boldsymbol{y}}k_y$. The Fourier transform is numerically evaluated using the formulas of [19].

Appendix A

Orthogonality of Floquet Modes

We wish to show that the Floquet modes are orthogonal in the following sense:

$$\iint_{U'} \boldsymbol{e}_{pmn} \times \boldsymbol{h}^*_{p'm'n'} \cdot \hat{z} \, \mathrm{d}A = \delta_{pp'} \delta_{mm'} \delta_{nn'} P_{pmn} \tag{1.1}$$

where U' is the restriction of the unit cell to the plane $z = 0$, $\boldsymbol{e}_{pmn}$ and $\boldsymbol{h}_{p'm'n'}$ are defined in Equations (2.19), δ_{kl} is the Kronecker delta, and P_{pmn} is given in Equation (2.22). Verification of Equation (1.1) is treated in two cases:

A.1 Both Modes Share Common Wave Vector

We consider here the case with $\boldsymbol{\beta}_{mn} = \boldsymbol{\beta}_{m'n'}$ which implies that

$$m\boldsymbol{\beta}_1 + n\boldsymbol{\beta}_2 = m'\boldsymbol{\beta}_1 + n'\boldsymbol{\beta}_2. \tag{1.2}$$

Taking the cross product of each side of (1.2) with $\boldsymbol{\beta}_1$ shows that $n = n'$, and similarly, crossing both sides with $\boldsymbol{\beta}_2$ shows that $m = m'$. It remains to show orthogonality when $p \neq p'$ and also that the normalization given in Equation (1.1) is correct when $p = p'$. These both follow immediately from examining Equations (2.19), after noting that

- The cross product $\boldsymbol{e}_{pmn} \times \boldsymbol{h}^*_{p'mn}$ is identically zero for $p \neq p'$ at all points in the unit cell due to colinearity of the two vectors, and

- The phase variation of the two factors in the cross product perfectly cancel.

A.2 Distinct Wave Vectors

Here we assume that the two wave vectors $\boldsymbol{\beta}_{mn}$ and $\boldsymbol{\beta}_{m'n'}$ are distinct. Orthogonality then depends on the value of the integral

$$I_{mnm'n'} \equiv \iint_{U'} e^{-j(\boldsymbol{\beta}_{mn} - \boldsymbol{\beta}_{m'n'}) \cdot \boldsymbol{\rho}} \, \mathrm{d}A = \iint_{U'} e^{-j[(m-m')\boldsymbol{\beta}_1 + (n-n')\boldsymbol{\beta}_2] \cdot \boldsymbol{\rho}} \, \mathrm{d}A. \tag{1.3}$$

We introduce the change of variables $\boldsymbol{\rho} = \xi_1 \boldsymbol{s}_1 + \xi_2 \boldsymbol{s}_2$ so that the area element is $\mathrm{d}A = A\,\mathrm{d}\xi_1\,\mathrm{d}\xi_2$, where $A = \hat{\boldsymbol{z}} \cdot \boldsymbol{s}_1 \times \boldsymbol{s}_2$ is the transverse area of the unit cell. The integral in (1.3) then becomes

$$I_{mnm'n'} = A \int_{\xi_1=0}^{1} \int_{\xi_2=0}^{1} e^{-j[(m-m')\boldsymbol{\beta}_1 + (n-n')\boldsymbol{\beta}_2] \cdot (\xi_1 \boldsymbol{s}_1 + \xi_2 \boldsymbol{s}_2)} \,\mathrm{d}\xi_1\,\mathrm{d}\xi_2 \tag{1.4}$$

We now employ the properties of the direct and reciprocal lattice vectors:

$$\boldsymbol{\beta}_1 \cdot \boldsymbol{s}_1 = 2\pi, \quad \boldsymbol{\beta}_1 \cdot \boldsymbol{s}_2 = 0 \tag{1.5a}$$

$$\boldsymbol{\beta}_2 \cdot \boldsymbol{s}_2 = 2\pi, \quad \boldsymbol{\beta}_2 \cdot \boldsymbol{s}_1 = 0. \tag{1.5b}$$

The integral then becomes

$$\begin{aligned}
I_{mnm'n'} &= A \int_{\xi_1=0}^{1} \int_{\xi_2=0}^{1} e^{-j2\pi[(m-m')\xi_1 + (n-n')\xi_2]} \,\mathrm{d}\xi_1\,\mathrm{d}\xi_2 \\
&= A e^{-j(m-m')\pi} e^{-j(n-n')\pi} j_0[(m-m')\pi] j_0[(n-n')\pi] \\
&= A e^{-j(m-m')\pi} e^{-j(n-n')\pi} \delta_{mm'} \delta_{nn'} \\
&= A \delta_{mm'} \delta_{nn'},
\end{aligned} \tag{1.6}$$

where we have used the identity

$$\int_0^1 e^{-j2\pi\alpha x} \mathrm{d}x = e^{-j\alpha\pi} j_0(\alpha\pi), \tag{1.7}$$

j_0 being the spherical Bessel function of the first kind of order zero:

$$j_0(x) = \begin{cases} \frac{\sin x}{x} & \text{if } x \neq 0 \\ 1 & \text{if } x = 0. \end{cases} \tag{1.8}$$

This completes the orthogonality proof.

Appendix B

Evaluation of Singular Integrals

This Appendix is concerned with evaluating the singular integrals that occur in Equations (7.21) and (7.31). Since we are concerned only with strictly planar structures, both integrals can be simply evaluated by specializing the formulas of [9] to the case where the observation point is in the plane of the source triangle.

The two integrals of interest are

$$\iint_{T^v} \frac{dS'}{\|\boldsymbol{r}' - \boldsymbol{r}^{cu}\|} \quad \text{and} \quad \iint_{T^v} \frac{\boldsymbol{r}' - \boldsymbol{r}_i}{\|\boldsymbol{r}' - \boldsymbol{r}^{cu}\|} \, dS' \tag{2.1}$$

where T^v is the source triangle, and $\boldsymbol{r}^{cu}$ is the centroid of the observation triangle. For the purposes of this Appendix we adopt a local numbering scheme $\boldsymbol{r}_i \in \{\boldsymbol{r}_1, \boldsymbol{r}_2, \boldsymbol{r}_3\}$ for the source triangle vertices. For convenience in the formulas presented below, we also define $\boldsymbol{r}_4 \equiv \boldsymbol{r}_1$.

The second, vector, integral in (2.1) can be written

$$\iint_{T^v} \frac{\boldsymbol{r}' - \boldsymbol{r}_i}{\|\boldsymbol{r}' - \boldsymbol{r}^{cu}\|} \, dS' = \iint_{T^v} \frac{\boldsymbol{r}' - \boldsymbol{r}^{cu}}{\|\boldsymbol{r}' - \boldsymbol{r}^{cu}\|} \, dS' + (\boldsymbol{r}^{cu} - \boldsymbol{r}_i) \iint_{T^v} \frac{dS'}{\|\boldsymbol{r}' - \boldsymbol{r}^{cu}\|} \tag{2.2}$$

which is a more convenient representation, because it is now expressed in terms of the two integrals directly treated in [9]. We thus have the two formulas

$$\iint_{T^v} \frac{dS'}{\|\boldsymbol{r}' - \boldsymbol{r}^{cu}\|} = \sum_{i=1}^{3} \boldsymbol{P}_i^0 \cdot \hat{\boldsymbol{u}}_i \ln \frac{P_i^+ + l_i^+}{P_i^- + l_i^-} \tag{2.3a}$$

$$\iint_{T^v} \frac{\boldsymbol{r}' - \boldsymbol{r}^{cu}}{\|\boldsymbol{r}' - \boldsymbol{r}^{cu}\|} \, dS' = \frac{1}{2} \sum_{i=1}^{3} \hat{\boldsymbol{u}}_i \left[\left(P_i^0 \right)^2 \ln \frac{P_i^+ + l_i^+}{P_i^- + l_i^-} + l_i^+ P_i^+ - l_i^- P_i^- \right] \tag{2.3b}$$

which are the specializations of Equations (5) and (6), respectively, of [9] to the case when the

variable d defined in [9] is zero. The additional variables needed to evaluate (2.3) are

$$l_i = r_{i+1} - r_i, \qquad\qquad l_i = \|l_i\|, \qquad\qquad \hat{l}_i = l_i / l_i, \qquad (2.4a)$$

$$l_i^+ = (r_{i+1} - r^{cu}) \cdot \hat{l}_i, \qquad l_i^- = (r_i - r^{cu}) \cdot \hat{l}_i, \qquad \hat{u}_i = \hat{l}_i \times \hat{n}, \qquad (2.4b)$$

$$\hat{n} = \frac{(r_3 - r_2) \times (r_1 - r_2)}{2A^v}, \qquad P_i^0 = (r_i - r^{cu}) - l_i^- \hat{l}, \qquad P_i^0 = \|P_i^0\|, \qquad (2.4c)$$

$$P_i^+ = \|r_{i+1} - r^{cu}\|, \qquad\qquad P_i^- = \|r_i - r^{cu}\| \qquad\qquad (2.4d)$$

B.1   Basis Function Inner Products

This appendix is concerned with computing the inner product of two basis functions $\langle f_n, f_m \rangle$. Clearly, the inner product is nonzero only when the support of basis functions m and n are common to at least a single triangle. The two cases to be treated are when $m = n$, or $m \neq n$.

B.1.1   Basis Function Self Inner Product

Using the definition of Equation (7.5) we have

$$\langle f_n, f_n \rangle = B^+ + B^- \qquad\qquad (2.5)$$

where

$$B^\pm = \frac{l_n^2}{4A_n^{\pm 2}} \iint_{T_n^\pm} \rho_n^\pm \cdot \rho_n^\pm \, dS. \qquad\qquad (2.6)$$

As shown in Figure B.1 let l_a^+ and l_b^+ be vectors drawn from the free vertex (i.e. the vertex which
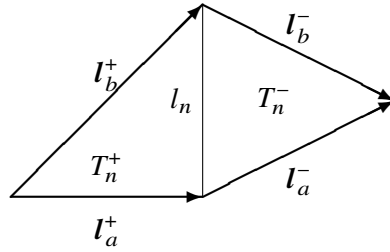

Figure B.1: Geometry for calculating self-term inner product.

is not incident upon edge l_n) of triangle T_n^+ to the nodes of edge n. Vectors l_a^- and l_b^- are defined similarly for triangle T_n^- except that they are directed towards the free vertex. Using normalized area coordinates we can then write $\rho_n^\pm$ as

$$\rho_n^\pm = \xi l_a^\pm + \eta l_b^\pm. \qquad\qquad (2.7)$$

Equation (2.6) can now be evaluated as

$$
\begin{aligned}
B^{\pm} &= \frac{l_n^2}{4A_n^{\pm 2}} \int_0^1 \int_0^{1-\eta} (\xi \boldsymbol{l}_a^{\pm} + \eta \boldsymbol{l}_b^{\pm}) \cdot (\xi \boldsymbol{l}_a^{\pm} + \eta \boldsymbol{l}_b^{\pm}) \, (2A_n^{\pm} \, \mathrm{d}\xi \, \mathrm{d}\eta) \\
&= \frac{l_n^2}{2A_n^{\pm}} \int_0^1 \int_0^{1-\eta} (\xi^2 l_a^{\pm 2} + \eta^2 l_b^{\pm 2} + 2\xi \eta \boldsymbol{l}_a^{\pm} \cdot \boldsymbol{l}_b^{\pm}) \, \mathrm{d}\xi \, \mathrm{d}\eta \\
&= \frac{l_n^2}{24 A_n^{\pm}} (l_a^{\pm 2} + l_b^{\pm 2} + \boldsymbol{l}_a^{\pm} \cdot \boldsymbol{l}_b^{\pm}) \\
&= \frac{l_n^2}{48 A_n^{\pm}} (3l_a^{\pm 2} + 3l_b^{\pm 2} - l_n^2).
\end{aligned}
\tag{2.8}
$$

The final equality above follows from the Law of Cosines:

$$
\boldsymbol{l}_a^{\pm} \cdot \boldsymbol{l}_b^{\pm} = \frac{1}{2}(l_a^{\pm 2} + l_b^{\pm 2} - l_n^2).
\tag{2.9}
$$

Although the above result assumed that the two triangles comprising the support of $\boldsymbol{f}_n$ are adjacent, the derivation is identical in the case where they are separated.

B.1.2   Inner Product of Distinct Basis Functions

We denote the triangle common to basis functions m and n as T^{mn}. The vertices are denoted by $\boldsymbol{r}_a$, $\boldsymbol{r}_b$, and $\boldsymbol{r}_c$, where without loss of generality we assume, as shown in Figure B.2, that $\boldsymbol{r}_a$ is opposite the center edge of basis function m and $\boldsymbol{r}_b$ is opposite the center edge of basis function n. We also

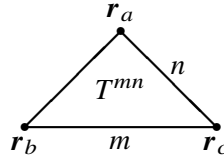**Figure B.2:** Geometry for calculating inner product of distinct basis functions.

define $\boldsymbol{l}_{ij} = \boldsymbol{r}_i - \boldsymbol{r}_j$, for $i, j \in \{a, b, c\}$. Then

$$
\langle \boldsymbol{f}_n, \boldsymbol{f}_m \rangle = \pm \frac{l_{ac} l_{bc}}{4(A^{mn})^2} e^{j(\theta_n - \theta_m)} \iint_{T^{mn}} (\boldsymbol{r} - \boldsymbol{r}_b) \cdot (\boldsymbol{r} - \boldsymbol{r}_a) \, \mathrm{d}S.
\tag{2.10}
$$

The negative sign above is used if one of the basis functions $\boldsymbol{f}_n$ or $\boldsymbol{f}_m$ defines positive current to flow out of the triangle while the other basis function defines positive current to flow into the

triangle. If the two basis functions agree in this respect the positive sign is used. Using normalized area coordinates the factors in the integral can be written

$$\boldsymbol{r} - \boldsymbol{r}_a = \xi \boldsymbol{l}_{ba} + \eta \boldsymbol{l}_{ca} \tag{2.11}$$

$$\boldsymbol{r} - \boldsymbol{r}_b = (\boldsymbol{r} - \boldsymbol{r}_a) + (\boldsymbol{r}_a - \boldsymbol{r}_b) = \xi \boldsymbol{l}_{ba} + \eta \boldsymbol{l}_{ca} + \boldsymbol{l}_{ab}. \tag{2.12}$$

The inner product can now be written as the phase factor times the sum of two terms

$$\langle \boldsymbol{f}_n, \boldsymbol{f}_m \rangle = \pm (C_1 + C_2) e^{j(\theta_n - \theta_m)} \tag{2.13}$$

where

$$C_1 = \frac{l_{ac} l_{bc}}{2A^{mn}} \int_0^1 \int_0^{1-\eta} (\xi \boldsymbol{l}_{ba} + \eta \boldsymbol{l}_{ca}) \cdot (\xi \boldsymbol{l}_{ba} + \eta \boldsymbol{l}_{ca}) \, \mathrm{d}\xi \, \mathrm{d}\eta \tag{2.14}$$

and

$$C_2 = \frac{l_{ac} l_{bc}}{2A^{mn}} \int_0^1 \int_0^{1-\eta} \boldsymbol{l}_{ab} \cdot (\xi \boldsymbol{l}_{ba} + \eta \boldsymbol{l}_{ca}) \, \mathrm{d}\xi \, \mathrm{d}\eta \tag{2.15}$$

C_1 is easily found using the results of Section B.1.1:

$$C_1 = \frac{l_{ac} l_{bc}}{48 A^{mn}} (3 l_{ab}^2 + 3 l_{ac}^2 - l_{bc}^2). \tag{2.16}$$

An expression for C_2 is also obtained with a bit of algebra:

$$\begin{aligned} C_2 &= \frac{l_{ac} l_{bc}}{2A^{mn}} \int_0^1 \int_0^{1-\eta} (-\xi l_{ab}^2 + \eta \boldsymbol{l}_{ab} \cdot \boldsymbol{l}_{ca}) \, \mathrm{d}\xi \, \mathrm{d}\eta \\ &= \frac{l_{ac} l_{bc}}{12 A^{mn}} (\boldsymbol{l}_{ab} \cdot \boldsymbol{l}_{ca} - l_{ab}^2) \\ &= \frac{l_{ac} l_{bc}}{24 A^{mn}} (l_{bc}^2 - 3 l_{ab}^2 - l_{ac}^2) \end{aligned} \tag{2.17}$$

where the last equality follows from the Law of Cosines.

Combining the expressions for C_1 and C_2 yields

$$\langle \boldsymbol{f}_n, \boldsymbol{f}_m \rangle = \pm e^{j(\theta_n - \theta_m)} \frac{l_{ac} l_{bc}}{48 A^{mn}} (l_{ac}^2 + l_{bc}^2 - 3 l_{ab}^2) \tag{2.18}$$

which is the desired formula.

References

[1] J. Bezanson, A. Edelman, S. Karpinski, and V. B. Shah, "Julia: A fresh approach to numerical computing," *SIAM review*, vol. 59, no. 1, pp. 65–98, 2017.

[2] S. M. Rao, D. R. Wilton, and A. W. Glisson, "Electromagnetic scattering by surfaces of arbitrary shape," *IEEE Trans. Antennas Propagat.*, vol. AP-30, pp. 409–418, May 1982.

[3] R. E. Collin, *Field Theory of Guided Waves*. IEEE Press, 2nd ed., 1991.

[4] E. C. Dufort, "Finite scattering matrix for an infinite antenna array," *Radio Science*, vol. 2, pp. 19–27, Jan. 1967.

[5] C. Kittel, *Introduction to Solid State Physics*. John Wiley and Sons, 3rd ed., 1966.

[6] N. Balabanian, T. A. Bickart, and S. Seshu, *Electrical Network Theory*. John Wiley & Sons, Inc., 1969.

[7] R. Mittra, C. H. Chan, and T. Cwik, "Techniques for analyzing frequency selective surfaces," *Proc. IEEE*, vol. 76, pp. 1593–1615, Dec. 1988.

[8] J. M. Ortega, *Matrix Theory—A Second Course*. Plenum Press, 1987.

[9] D. R. Wilton, S. M. Rao, A. W. Glisson, D. H. Schaubert, O. M. Al-Bundak, and C. M. Butler, "Potential integrals for uniform and linear source distributions on polygonal and polyhedral domains," *IEEE Trans. Antennas Propagat.*, vol. AP-32, pp. 276–281, Mar. 1984.

[10] I. Stakgold, *Green's Functions and Boundary Value Problems*. New York: John Wiley & Sons, 1979.

[11] A. Papoulis, *The Fourier Integral and its Applications*. New York: McGraw-Hill, 1962.

[12] N. N. Lebedev, *Special Functions and their Applications*. Dover Publications, Inc., 1972.

[13] K. A. Michalski and J. R. Mosig, "Multilayered media Green's functions in integral equation formulations," *IEEE Trans. Antennas Propagat.*, vol. 45, pp. 508–519, Mar. 1997.

[14] M. Abramowitz and I. A. Stegun, eds., *Handbook of Mathematical Functions*. Dover Publications, Inc., 1972.

[15] P. S. Simon, "Efficient Green's function formulation for analysis of frequency selective surfaces in stratified media," in *Dig. 2001 IEEE AP-S Int. Symp.*, vol. 4, (Boston, MA), pp. 374–377, July 2001.

[16] P. S. Simon, "Modified RWG basis functions for analysis of periodic structures," in *2002 IEEE MTT-S International Microwave Symposium Digest*, vol. 3, (Seattle, WA), pp. 2029–2032, June 2002.

[17] K. M. Mitzner, "Effective boundary conditions for reflection and transmission by an absorbing shell of arbitrary shape," *IEEE Trans. Antennas Propagat.*, vol. AP-16, pp. 706–712, Nov. 1968.

[18] P. C. Zienkiewitz, *The Finite Element Method in Engineering Science*. McGraw-Hill, 1971.

[19] K. McInturff and P. S. Simon, "The Fourier transform of linearly varying functions with polygonal support," *IEEE Trans. Antennas Propagat.*, vol. AP-39, pp. 1441–1443, Sept. 1991.